Evaluating techno-economic scenarios for low-temperature district heating and cooling networks and conventional solutions

Selva Calixto

B.S., University of Concepción, Chile, 2014
M.S., Columbia University, USA, 2016

Supervisor:	Giampaolo Manzolini
Advisors:	Marco Cozzini
	Roberto Fedrizzi

POLITECNICO DI MILANO

DEPARTMENT OF ENERGY

September 2022

Submitted in partial fulfilment of the requirements for the Ph.D. degree in Energy and Nuclear Science and Technology of Politecnico di Milano

Abstract

Neutral temperature district heating and cooling (NT-DHC) is a relatively new concept in the district heating (DH) sector. A missing aspect in current literature is the ability to model the performance of NT-DHC systems and draw master plans (even for traditional DH systems). Experimental data are scarce, preventing the development of validated models. The energy modeling for systems of this kind is also more complex than for conventional systems due to the multiple energy sources and the higher complexity of decentralized heat pumps (HPs) compared to heat exchanger substations.

A tool is developed for the analysis of techno-economic scenarios in DHC systems. In Ospitaletto, Italy, the monitoring data from a NT-DHC network is employed to improve the model's reliability. A knapsack algorithm is used to find transition pathways for the network expansion.

The model can be applied to any city if the necessary heat density data is available. However, the approach was applied to the case study mentioned previously for simplicity. It goes beyond the State of the Art in that it models decentralized HPs' substations, accounts for economic aspects that DH physical models do not possess and incorporates optimization for selecting the best system extension. A sensitivity analysis is also conducted to find out to what extent, under which energy price conditions and subsidies, the NT-DHC concept is competitive over individual heating and cooling (H&C) solutions.

The model's results are in alignment with qualitative expectations. The optimization algorithm determines which combination of potential extensions maximizes the overall economic value. The NT-DHC solution is more convenient for dense urban zones, while air-to-water heat pumps (A/W HPs) are better suited to zones with low-heat density. By selecting waste heat sources at temperatures between 30-40°C, the SCOP of the NT-DHC solution can be enhanced compared to reversible A/W HPs. In the case of Ospitaletto, despite having low building heat density compared to larger cities, it is still possible to identify feasible scenarios. This opens the opportunity to many other cases.

This tool has the potential impact in the DHC sector of reducing the energy demand risks, providing

more certainty as to which zones a network can expand to be competitive. It is targeted at energy planners, utilities, energy engineers, and DHC specialists since they require decision-making support and recommendations for replicating a new type of DHC system. This tool will enable pre-feasibility studies and preliminary designs to determine the opportunities and limitations of a system of this kind from an economic and technological perspective.

Keywords:
Neutral temperature district heating and cooling, knapsack algorithm, transition pathways, network expansion scenarios, energy planning

Abstract (IT)

Il teleriscaldamento e teleraffreddamento a temperatura neutra (NT-DHC) è un concetto relativamente nuovo nel settore del teleriscaldamento (DH). Un aspetto mancante nella letteratura attuale è la capacità di modellare le prestazioni dei sistemi NT-DHC e di definire piani generali (anche per i sistemi DH tradizionali). I dati sperimentali sono scarsi e ciò impedisce lo sviluppo di modelli convalidati. La modellazione energetica per sistemi di questo tipo è inoltre più complessa rispetto ai sistemi convenzionali. Questo è dovuto alle molteplici fonti di energia e alla maggiore complessità delle pompe di calore decentralizzate (HP) rispetto alle sottostazioni di scambio termico.

È stato sviluppato uno strumento per l'analisi degli scenari tecno-economici dei sistemi DHC. I dati di monitoraggio di una rete NT-DHC di Ospitaletto, in Italia, sono utilizzati per migliorare l'affidabilità del modello. Viene utilizzato un algoritmo knapsack per trovare percorsi di transizione per l'espansione della rete.

Il modello può essere applicato a qualsiasi città se sono disponibili i dati necessari sulla densità di calore. Tuttavia, l'approccio è stato applicato al caso di studio citato in precedenza per semplicità. Il modello va oltre lo stato dell'arte in quanto modella le sottostazioni di HP decentralizzate, tiene conto di aspetti economici che i modelli fisici DH non possiedono e prevede l'ottimizzazione per identificare lo sviluppo migliore del sistema. È stata inoltre condotta un'analisi di sensibilità per scoprire in che misura, a quali condizioni di prezzo dell'energia e con quali sussidi, il concetto di NT-DHC è competitivo rispetto alle soluzioni individuali di riscaldamento e raffreddamento (H&C).

I risultati del modello sono in linea con quanto qualitativamente atteso. L'algoritmo di ottimizzazione determina quale combinazione di potenziali sviluppi massimizza il valore economico complessivo. La soluzione NT-DHC è più conveniente per le zone urbane dense, mentre le pompe di calore aria-acqua (A/W HP) sono più adatte alle zone a bassa densità termica. Selezionando fonti di calore di scarto a temperature comprese tra 30 e 40°C, lo SCOP della soluzione NT-DHC può essere migliorato rispetto alle pompe di calore aria/acqua reversibili. Nel caso di Ospitaletto, nonostante la bassa densità termica

degli edifici rispetto a città più grandi, è ancora possibile identificare scenari fattibili. Questo apre l'opportunità a molti altri casi.

Il potenziale di questo strumento nel settore DHC consiste nel ridurre i rischi legati alla domanda di energia, fornendo maggiori certezze su quali zone una rete può espandersi per essere competitiva. Si rivolge a pianificatori energetici, utility, ingegneri energetici e specialisti di DHC, che necessitano di un supporto decisionale e di raccomandazioni per replicare un nuovo tipo di sistema di DHC. Questo strumento consentirà di realizzare studi di prefattibilità e progetti preliminari per determinare le opportunità e i limiti di un sistema di questo tipo da un punto di vista economico e tecnologico.

Parole chiave:

Teleriscaldamento e teleraffrescamento a temperatura neutra, algoritmo knapsack, percorsi di transizione, scenari di sviluppo della rete, pianificazione energetica

To my family

"Have the courage to follow your heart and intuition. They somehow already know what you truly want to become. Everything else is secondary."

S.Jobs

Acknowledgments

During my first bachelor's thesis submission, the assistant in charge of the submissions gave me a sermon about thanking the people who helped us during our long career in higher education. Clearly, he was right. The rush to turn it in and time constraints caused me to overlook this gesture. I hope to redeem myself this time. My first thanks go to him.

I would like to extend my sincere thanks to those who supervised my doctoral work, Marco Cozzini and Giampaolo Manzolini. For always keeping expectations high and pushing me to do my best. A special thanks to Marco for his regular collaboration, patience, and guidance over the years. I hope I have captured in this work the many hours of brainstorming. Also, thank you for reading each of the articles I wrote and giving honest and constructively critical feedback. Thanks should also go to Roberto Fedrizzi, for sharing his expertise in this innovative area of study and the intensive discussions that shaped the objectives and results of this study. Thank you for allowing me to be part of the Sustainable Heating and Cooling group and to share in a highly competent and qualified environment. Additionally, this endeavor would not have been possible without the financial support of the Institute for Renewable Energy at EURAC Research and the National Commission for Scientific and Technological Research in Chile (ANID).

I am also grateful to my EURAC colleagues Paolo and Mauro, for welcoming me into the group and being patient with my Italian learning. Riccardo, Amir, Federico, for being excellent colleagues and providing moral support. Tim for sharing his expertise in programming and optimization algorithms. My female colleagues, who unfortunately most of them had to leave the group. Chiara di P., Chiara U., Elena, and Rosanna are examples for me of strength in the face of a system that fails to adapt to the needs that characterize us. I hope one day working conditions will be fairer for us. Finally, to my colleagues and fellow PhD students, Elisa and Valeria, with whom I was fortunate to share the challenges of this program together.

Finally, I would be remiss in not mentioning my friends and family. First of all, my parents, for giving me the values and tools that have been fundamental to face life's challenges. My siblings, Mauro for being my mentor and example of success and Valentina, who has given me the honor of being her supporting arm. David and Antonella, my closest Chilean-Italian friends, for making my stay in Milan more enjoyable. My friends from Chile and the United States who were present despite the distance, especially during the pandemic: Juan, Gaby, Harry, Mike and Paul. My Renon neighbors Vera and Magda. Finally, my husband, for his great belief in my abilities that kept my spirits up in the most complex moments.

As the great Gustavo Cerati said, "Gracias totales".

Contents

List of Figures

List of Tables

Abbreviations

TDH	Traditional District Heating
4GDH	Fourth-generation District Heating
5GDH	Fifth-generation District Heating
A/W	Air to Water
CDD	Cooling degree days
COP	Coefficient of Performance
DH	District Heating
DHC	District Heating and Cooling
DHN	District Heating networks
DHW	Domestic Hot Water
EER	Energy Efficiency Ratio
FU	Functional Unit (a generic area of 1 km^2)
SFH	Single-family House
GM	Gaussian Mixture
GSHP	Ground Source Heat Pump
H&C	Heating and Cooling
HDD	Heating degree days
HP	Heat pump
IRR	Internal Rate of Return
KM	K-Means
LT	Low temperature
LCOH	Levelized Cost of Heat
NPV	Net Present Value
NT-DHC	Neutral-temperature district heating and cooling
NTS	Neutral-temperature sources

PBT	Payback Time
RES	Renewable Energy Sources
ROI	Return on Investment
SB	Special Building
SC	Spectral Clustering
SCOP	Seasonal Coefficient of Performance
SH	Space Heating
SHW	Sanitary Hot Water
SPF	Seasonal Performance Factor
TEA	Techno-economic assessment
VSP	Virtual Source Point
WH	Waste Heat
W/W	Water to Water

Nomenclature

A_B	Building space area, m^2
A_L	Land area, m^2
CO_2	Carbon emissions, t CO_2/y
c_{tax}	Carbon tax, €/t CO_{2eq}
C_{fix}	Fixed operation and maintenance fee, €
C_{NT-DHC}	Total annual costs of NT-DHC operation, €
D_{avg}	Average pipe diameter, mm
E_s	Waste heat availability, MW
E_{cap_s}	Source thermal capacity, MW
$E_{th,sh}$	Space heating demand, MWh
$E_{\%sh}$	Space heating share with respect to total demand, %
$E_{th,h}$	Total heating demand, MWh/y
$E_{th,c}$	Total cooling demand, MWh/y
$E_{loss,s}$	Total thermal losses on the supply pipe, MWh
$E_{loss,r}$	Total thermal losses on the return pipe, MWh
$E_{th,HP,c}$	Annual thermal energy supplied at the condenser side of the heat pumps, MWh/y
$E_{th,HP,e}$	Annual thermal energy carried from the network to the heat pumps evaporator, MWh/y
$E_{el,HP}$	Annual electric energy consumed by the heat pumps, MWh/y
$E_{th,loss}$	Annual thermal losses, MWh/y
$E_{th,\mathrm{WH}}$	WH supplied to the network, MWh
$E_{el,pump}$	Annual electric energy consumed by the network pump, MWh/y
f_h	Daily heating profile
$f_{em,fuel}$	Fuel emission factor, tCO_{2eq}/MWh
$f_{em,el}$	Electricity emission factor, tCO_{2eq}/MWh

I_{NT-DHC}	Investment in the NT-DHC solution, €
I_{net}	Network investment, €
I_{srcs}	Investment in heat recovery on the production sites, €
I_{HPs}	Investment in HPs substations, €
$L_{pipe_{i,j}}$	Overall lengths of pipes with diameter i and material j, m
OM	Fixed operating and maintenance costs, €
$OPEX$	Operational expenses, €
p_{heat}	Price of heating service sold through the NT-DHC network, €/MWh
p_{cool}	Price of cooling service sold through the NT-DHC network, €/MWh
$p_{el,\mathrm{ind}}$	Industrial electricity price, €/MWh
$p_{el,\mathrm{res}}$	Residential electricity price, €/MWh
$p_{fuel,j}$	Fuel price used by auxiliary system j, €/MWh
p_{WH}	WH price, €/MWh
Δp	Pressure losses
r	Rate of return, %
R	Earth's radius, km
t_{min}	Day of minimum surface temperature
t_{cyc}	Cycle period
T_{amb}	Ambient temperature, °C
T_{b-heat}	Base indoor temperature setpoint, °C
T_{DHW}	Domestic hot water temperature, °C
T_{SH}	Space heating temperature, °C
T_c	Condenser temperature of the heat pump refrigerant, K
T_e	Evaporator temperature of the heat pump refrigerant, K
$T_{c,o}$	External fluid temperature on the heat pump condenser, °C
$T_{e,o}$	External fluid temperature on the heat pump evaporator, °C

ΔT_{HEX}	Heat exchanger lift, K
T_{gs}	Ground temperature, °C
T_{avg}	Average ground temperature, °C
ΔT_{amp}	Amplitude of the temperature variation at the ground surface, °C
$T_{net,s}$	Network supply temperature, °C
$T_{net,r}$	Network return temperature, °C
T_f	Fluid temperature, °C
U_{avg}	Overall thermal conductivity, kW/K
$U_{pipe_{i,j}}$	Pipe thermal conductivity of diameter i and material j, W/(m·K)
v	Value, €
$\dot{V}$	Volume flow rate, m^3/s
W	Maximum waste heat potential, MW
z	Depth, m
z_{net}	Network pipes depth, m
z_{aq}	Aquifer wells depth, m
α	Ground thermal diffusivity, m^2/s
c_p	Water specific heat capacity, J/(kg·K)
e	Plot ratio
η_m	Compressor efficiency, %
v	Fluid velocity, m/s
τ	Time constant
ρ	Water density, kg/m^3
w	Effective width
ϕ	Latitude
Ψ	Longitude

1

Introduction

Climate change is one of the international community's most significant challenges, and experts claim to act worldwide to mitigate its effects. Anthropogenic greenhouse gas emissions (GHG) have increased since the pre-industrial era with more substantial increases between 2000 and 2010, despite a rising number of mitigation policies[1]. Electricity and heat were the largest sources of CO_2 emissions in 2019, accounting for 42% of the global total[2]. When allocating emissions from electricity to consuming sectors, the industry was the more significant emitter followed by buildings. The global energy demand for heating is expected to increase until 2030 and stabilize. In contrast, it is projected that the cooling demand worldwide will overtake that used in heating [3]. The awareness of global warming in the 1990s, creating the United Nations Framework Convention on Climate Change (UNFCCC) and the Kyoto protocol, created a renewed interest in district heating systems to replace fossil fuels with renewables and several low-temperature heat sources[4].

1.1 Background

1.1.1 State of the art of the research field

District Heating (DH) is an energy service that moves heat from available heat sources to customers via a piping network. A fundamental principle of DH today is to use local sources that would otherwise be wasted to satisfy the customers' heating needs [5]. DH technology has proven its advantages over individual heating and cooling (H&C) systems. There is growing recognition that it is a promising solution for reducing local and global emissions and lowering the primary energy consumption associated with H&C building demands. DHC systems, if properly managed, can contribute to reducing greenhouse gas emissions and, therefore, mitigating the effects of climate change.

Traditional DH systems (TDH) operate typically at high temperatures (more than 80°C), giving rise to

high thermal losses and the need for costly piping insulation. Examples of traditional DH sources are co-generation plants, industrial waste heat, and incinerators, where heat is a by-product of other industrial processes [6]. The first three generations in the DH sector are characterized by the constant trend of lowering the network distribution temperature, using lean material components, and prefabrication to reduce human resources requirements. The fourth-generation DH (4GDH) concept and the definition of smart thermal grids were first introduced in [7]. This generation is defined as a technological and institutional concept that must fulfill several challenges to reach a future non-fossil heating and cooling supply: the ability to supply low-temperature (LT) DH for space heating (SH) and domestic hot water (DHW) to existing and new low-energy buildings; lowering the grid losses; introduce renewable energy sources (RES) and heat recycling from LT sources; and the strategic planning and motivation structures for the investments related to the transformation into a sustainable energy system.

Neutral temperature district heating and cooling (NT-DHC) is a recent concept in the DH sector, which further lowers operating temperatures to a level equivalent to ambient and ground temperatures. The advantages are the thermal losses reduction in the distribution system, the direct exploitation of available ground sources (e.g., aquifer wells), urban low-temperature waste heat sources, and the possibility of providing heating and cooling using reversible heat pumps. This concept is aligned with the electrification trend in the energy sector. As of today, there is no consensus within the scientific community about labeling NT-DHC as part of the family of 4GDH technology or consider it as 5GDH[4][8][9][10]. The concept does not seek to validate itself as the best available system, but rather to share the common strategy for decarbonizing the H&C energy system by replacing existing fossil-based technologies.

The European Commission has funded several research projects in the DH sector within the H2020 framework. The FLEXYNETS project [6] was the first to investigate the strengths and weaknesses of this technology through numerical simulation activities and laboratory tests. These systems are currently being deployed in several real demonstrators within the ongoing projects D2grids [11], Life4HeatRecovery [4], and REWARDHeat [13]. Additional ongoing projects that highlight the effort of the EU in boosting the DHC sector are ReUseHeat [14], WEDISTRICT [15], Upgrade DH [16], COOL DH [17], among others.

NT-DHC systems are new, and therefore models and tools are needed to study their applications. A missing aspect in current literature is the ability to model the performance of NT-DHC systems and draw master plans (even for traditional DH). Experimental data are scarce, preventing the development of validated models. Moreover, the energy modeling of systems of this kind is more complex than a conventional one, considering multiple energy sources and the higher complexity of HPs compared to

the heat exchangers used in conventional DH substations.

1.1.2 Models and tools

Several tools and models support the decision-makers in choosing H&C solutions for the built environment. The level of detail and focus varies according to their purpose (see Figure 1). They are typically used for energy planning or network design, with functions including demand forecasting, the integration of renewables, feasibility studies, etc. According to their geographical application, time resolution, and purpose, these simulation tools can be categorized into two main groups: detailed analyses at the building/district level and city/national energy planning [18].

The first category of tools focuses on load forecasting and simulation of a given system for a single-building, local community, or single-project. They have a high temporal resolution and are more suitable for design purposes. Examples of this kind of tools are TRNSYS, HOMER, and ESP-r [19][20][21]. There are also detailed tools for DH modeling, called physical models, suitable for network design. They provide high accuracy but solving a very complex system can be computationally expensive due to the required number of variables. In addition, these models do not include decentralized heat pumps or economic data for planning. Therefore, they are not suitable for a comprehensive techno-economic comparison between energy scenarios. Some notable examples of these commercial tools are TERMIS, energyPRO, and COMSOF Heat[22][23][24].

The second category of tools has the property to simulate the operation and performance of energy supply and demand systems at a high level, including heating, cooling, electricity, transport, and water. These long-term energy planning models typically have a low time resolution and miss the details related to the modeling of DH aspects such as thermal losses along pipes, network pumping consumptions, and the performance of HPs on an hourly basis. Tools that fit in this category are EnergyPLAN [25], LEAP [26], Crystal City [27], and METIS [28].

Purpose	Design		Energy planning
Geographical application	Single-building	District	City/national
Temporal resolution	Seconds - minutes	Hourly	Daily - years
Pros	High accuracy		High sector-coupling resolution: heating, cooling, electricity, transport, water, etc.
Cons	• Computationally expensive • Not suitable for comprehensive economic scenario analyses • Lack of heat pumps substations modeling • Lack of long-term planning		• Not suitable for DH specific analyses (network thermal losses, pumping consumptions). • Lack of heat pumps substations modeling
Examples	TRNSYS, HOMER, ESP-r	TERMIS, energyPRO, and COMSOF Heat	EnergyPLAN and LEAP

Figure 1. Models and tools characterization

1.2 Neutral temperature networks

1.2.1 Sources

A general classification of DH sources is presented in Figure 2. It shows the variety of sources suitable for direct exploitation in a DH network (70°C or more), as well as low and ultra-low sources that can be exploited through HPs. An estimation of the HPs COP is presented on the left when lifting the temperature to 60°C and 80°C. The neutral-temperature sources (NTS) that can be exploited in NT-DHC networks (also classified as low-temperature sources in the literature [29][30][31]) based on their origin are presented in Table 1 and highlighted in the green box.

Table 1. Neutral temperature sources classification by origin

Environment	**Industrial/Service**	**Commercial**
Water basins: rivers, lakes, sea (5-18°C)	Industries and production companies	Supermarkets
		Shopping malls
Park areas suitable for aquifer wells or boreholes (10-15°C)	Metal sector (e.g., foundries, metal product manufacturing)	Service sector buildings (25-40 °C):
	Plastic sector	Hospitals
	Food & beverage sector (e.g., large bakeries, wineries, dairies)	Hotels
		Large public buildings (municipality, schools)
	Data centers and server rooms (15-35°C)	Large offices
	Sewage/wastewater (8-15°C)	Restaurants
	Subways (5-35°C)	Large laundries
		Swimming pools
		Gyms

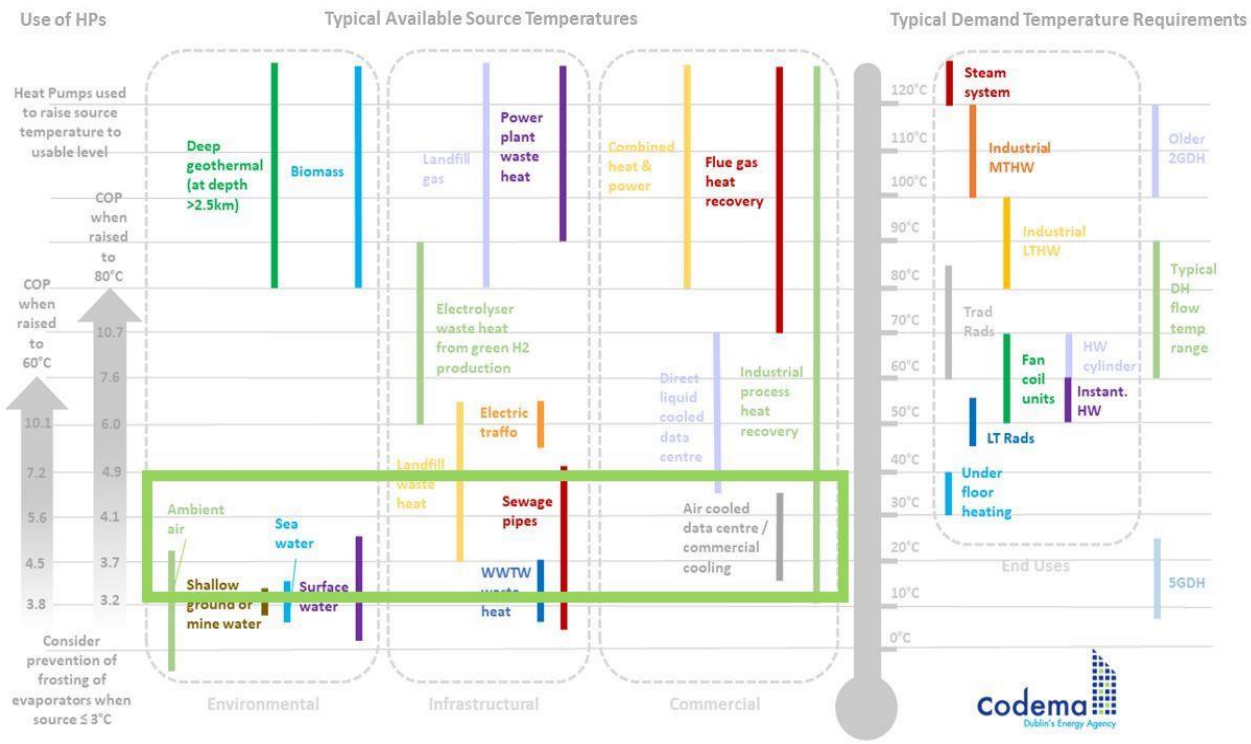

Figure 2. Sources temperature levels classified in environmental, infrastructural, and commercial origin. It is important to note that any hydraulic break will typically add 5°C to the required temperature increase. Temperatures in sewage pipes are usually below 25°C but can exceed 40°C when carrying wastewater from industrial sites. The temperature of direct liquid cooling in data centers varies depending on which components of the data center are being cooled (CPUs have the highest temperature if cooled directly, other elements have lower temperatures). Source: Codema [32]. Adapted with permission.

The author in [8] surveyed 40 neutral-temperature DH case studies (in the range of 10-35°C, they are cited in this paper as 5GDHC systems) located in Italy, Germany, Switzerland, The Netherlands, Belgium, UK, and Norway. Figure 3 shows their classification by source and temperature levels. In the survey, 62.5% of the systems were supplied by a single source, and half of these, were quasi-infinite thermal sources (groundwater, seawater, and river). In the remaining cases, there are sources with a fixed capacity but constant throughout the year (excess heat, geo structure) or natural-based sources with a storage regeneration medium such as horizontal or vertical ground heat exchangers. The following subsections will discuss the two main NTS of interest in this study: ground source heat and waste heat.

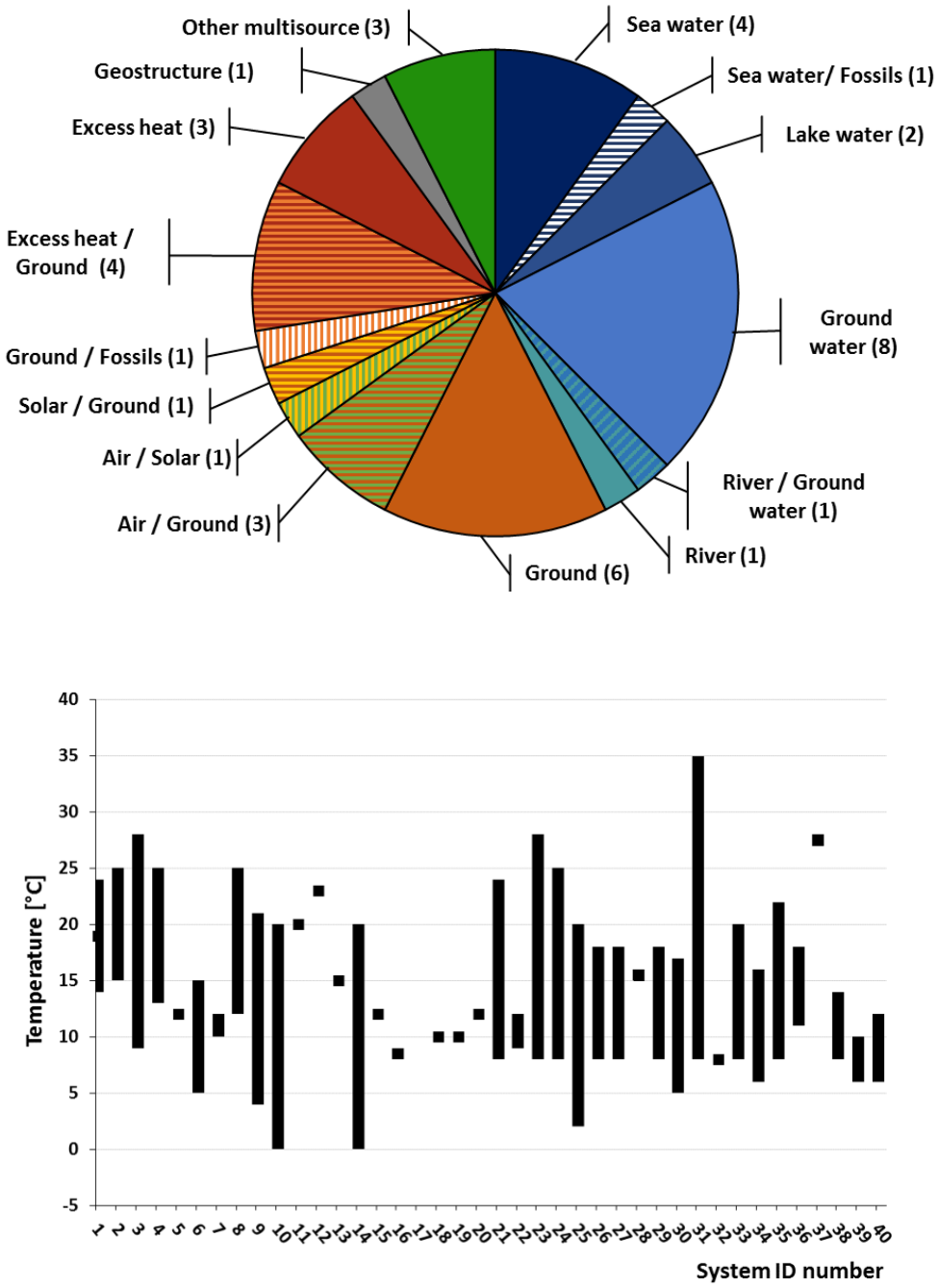

Figure 3. Neutral-temperature DH case studies surveyed in [8] classified by source and temperature levels.

1.2.2 Ground source

Figure 4 illustrates how geothermal energy systems can be classified by depth operation: shallow (less than 300 m) or deep (more than 300 m) fields, as well as by temperature operation: low enthalpy (horizontal and vertical ground source heat pumps (GSHPs)), medium enthalpy (district heating), and high enthalpy (power production fields). Medium and high enthalpy systems can be exploited in conventional DH. A NT-DHC system can be treated as a GSHP system on a district level, which utilizes other thermal energy sources.

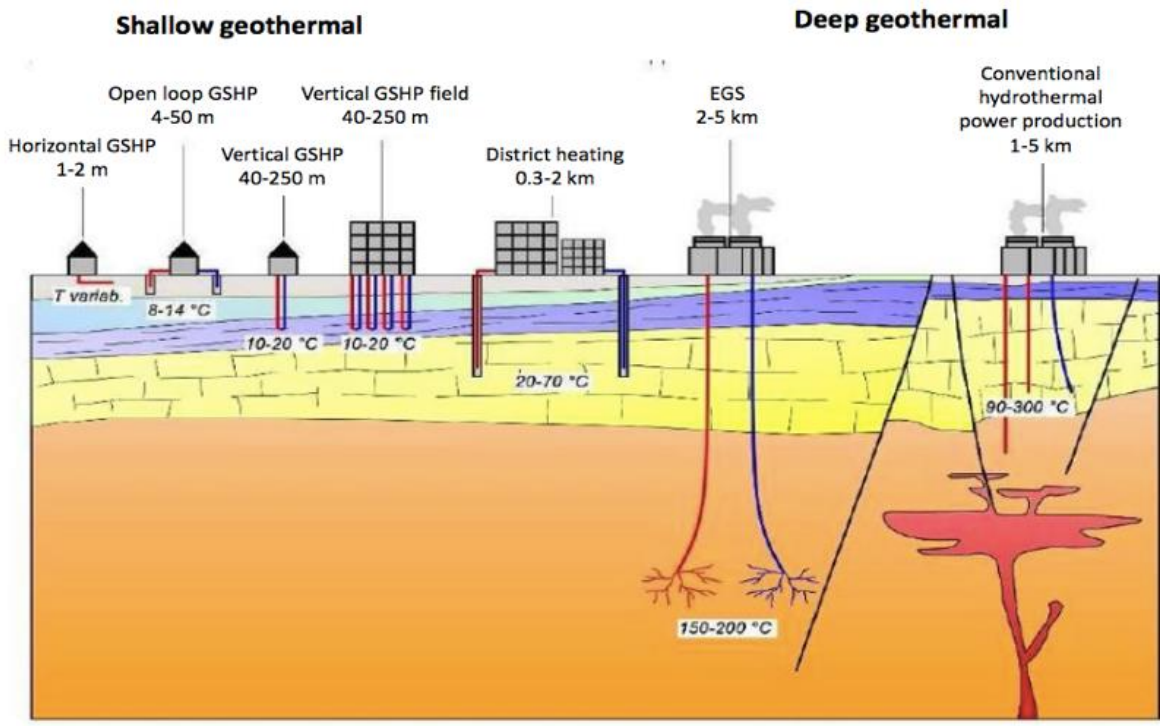

Figure 4. Geothermal energy systems classification according to depth operation[33].

A general classification of GSHPs systems is open and closed loop (horizontal and vertical circuit)[34][35][36]:

- Open systems: The heat pump uses groundwater as a heat carrier. In an open system, groundwater wells extract or inject water from/to water layers underground ("aquifers"). It usually requires two wells to remove groundwater from an aquifer and reinject it in the same one where it was produced.
- Closed systems: Heat exchangers are located underground (either horizontally or vertically). A heat carrier is circulated within the heat exchangers, transporting heat from the ground to the heat pump (or vice versa). Horizontal systems suit well in places with land availability. The

most common configurations in Europe are in series or parallel, while spiral boreholes are the most popular in the US. The optimal trench depth is of about 1.2 – 2 m[37]. In contrast, vertical systems are better suited in places with scarce land availability. Vertical ground heat exchangers are widely favored because the temperature below 15 to 20 m remains constant throughout the year.

1.2.3 Waste heat sources

Heat recycling refers to the general term for recovery of heat to be reused before released to the ambient temperature[4]. Excess heat, waste heat (WH), surplus heat are synonyms for the produced heat of a process but not utilized [38]. It is expected that DH in a renewable energy society will require less excess heat from CHP plants since traditional power plants will be less dominant in the electricity market. In contrast, the DH technology must be redesigned to allow the utilization of local, almost free ambient and low-temperature sources.

The integration of WH into DH networks (DHN) is intended to increase energy efficiency, save energy, reduce carbon footprints, and decarbonize the energy sector[30][39]. WH complements other renewable energy sources (RES) such as solar thermal, geothermal, and biomass for the transition to more sustainable energy systems. As outlined in [39], each of these sources have advantages and disadvantages. As in the case of solar thermal, RES technologies are mature, highly efficient, and reliable, but they could also be intermittent and present a mismatch between supply and demand. Other technologies, such as geothermal and biomass, are safe and modular, but highly dependent on geographical conditions. Low-enthalpy WH sources are found in urban areas near end-users and provide consistent production year-round. Even so, there are still many urban sources in the literature that have yet to be explored[29][40].

WH utilization encounters several non-technical limitations. The lack of legal frameworks for stakeholders to be involved in WH recovery projects is a barrier, so policy upgrades are needed. In this sense, long-term contracts could lower the risks involved in this kind of project. WH projects are also adversely affected by the fact that, currently, there are monetary incentives that favor other RES and the efficiency of CHP solutions, making it very challenging to attract investment[4]. According to [41], the authors assessed the potential for WH recovery from data centers in Northern European countries and found that lack of transparency on the business models and getting economic benefits from the heat sales are among the main barriers to its adoption. Furthermore, the bureaucracy involved is also a limitation to advancing and replicating these projects, so easing the permitting process would be beneficial.

Heat can be integrated directly in a DHN when the process that produces the heat falls within the range

of the supply temperature via heat exchangers (as occurs in the thermal power generation and high-temperature industrial processes)[29]. For the integration of lower-temperature sources, however, HPs are required either in the production site or in the users' substations to raise the source temperature to levels proper for consumers. The model focuses on the latter case.

Several research studies have been conducted in the context of mapping and quantifying WH and RES that are suitable for DH systems, such as in Denmark [42][43], UK [44][45], Sweden [46], Germany [47], Spain [48], and Italy [49][50]. In addition, the MEMPHIS project [51]developed an international applicable methodology to assess WH potential. The developed platform promotes the exploration of spatially distributed WH sources. In summary, WH potential in the urban context can be quantified using a variety of methods, maps, tools, and studies, though this field is still developing.

1.2.4 Environmental impact and opportunities

According to Frederiksen and Werner [52], in the context of climate change and local emissions reduction, DH systems are an environmental opportunity for seven reasons:

1. WH recycling reduces the need for primary fuels, which will often lead to lower emissions. An industry can recycle WH into a DH system to replace individual boilers at buildings that are connected to the grid.
2. DH can introduce RES such as biomass and geothermal energy. This and the previous argument may contribute to the mitigation of climate change.
3. In large scale combustion boilers, pollution equipment become more efficient and affordable. In contrast, small boilers do not have the proper equipment for the capture of particulates.
4. DH utilities can monitor the fuel quality, something that is not necessarily of concern to individual homeowners. For example, in some countries, it is common practice to burn any type of material, including old railroad ties, timber treated with pesticides, tires, and even municipal solid waste. Burning such materials might harm residents. Even biomass that could be mistakenly considered an environmentally friendly source, if improperly combusted, can result in significant harmful emissions, such as polyaromatic hydrocarbons, which are known carcinogens. Wood and coal emissions have been linked to serious health problems such as respiratory and cardiovascular diseases, as well as cancer. The World Health Organization numbers report that indoor air pollution from fuel use for household energy in 2012 led to 4.3 million deaths worldwide, with six out of ten deaths occurring among women and girls.[53].

5. DH operators can sell the byproducts of large-scale thermal plants in secondary markets, such as the gypsum produced in sulphuric scrubbers utilized for cement production.
6. Due to the previous arguments, legislators can implement more strict emissions standards.
7. A DH operator can continuously monitor the emissions to meet the legal standards. Legal demands for non-compliant large-scale equipment can be realistically enforced by addressing the responsibility to a professional plant manager, while this would not be possible for small-scale equipment owners.

As stated in the first two arguments, NT-DHC networks share the same environmental benefits as DH systems generally, with the additional advantage that no combustion process is required, alleviating much of the local pollution problem. In contrast, the relevant environmental impact of the NT-DHC system can be attributed to its electricity use. As a result, from a life cycle perspective, the quality of electricity becomes crucial.

This study used emission factors derived from the latest dataset (2017) from the Covenant of Mayors for Climate and Energy initiative [54]. In this database, the emission factors for local inventories vary depending on the country, calculation method used (standard or LCA approach), and the reference year. The default value for gas emissions is assumed 0.202 $tCO_{2\text{-eq}}$/MWh according to the standard IPCC values from 2006. Electricity emission factors are updated until 2013, so it is recommended that users of the model check country-specific reports for more updated values.

The impact of carbon emissions is assessed in all competing scenarios by introducing a carbon tax. The consensus among experts is that a uniform global carbon price should be higher than the current global average carbon price of $3 per ton of CO_2 (for European rates see Figure 5). Global experts on carbon pricing compiled recommendations from 400 publications across 40 countries and found that, on average, they do not support the notion of freeriding; the introduction of border carbon adjustment (BCA) facilitates higher unilateral carbon price recommendations, and BCA facilitates higher levels of agreement on carbon prices[55].

The European Commission in July 2021 exposed its plans to make importers and non-EU manufacturers pay for the carbon emissions associated with the materials and goods they sell in the EU[56]. This tax is an integral part of a broader reset of the EU's climate change policy. The significant impact will be on the cost of high-carbon inputs such as steel, cement, aluminium, chemicals, and electricity, after its complete implementation in January 2026. EU importers and non-EU producers of these inputs will be required to pay an estimated €75/ton of CO_2 emissions[57].

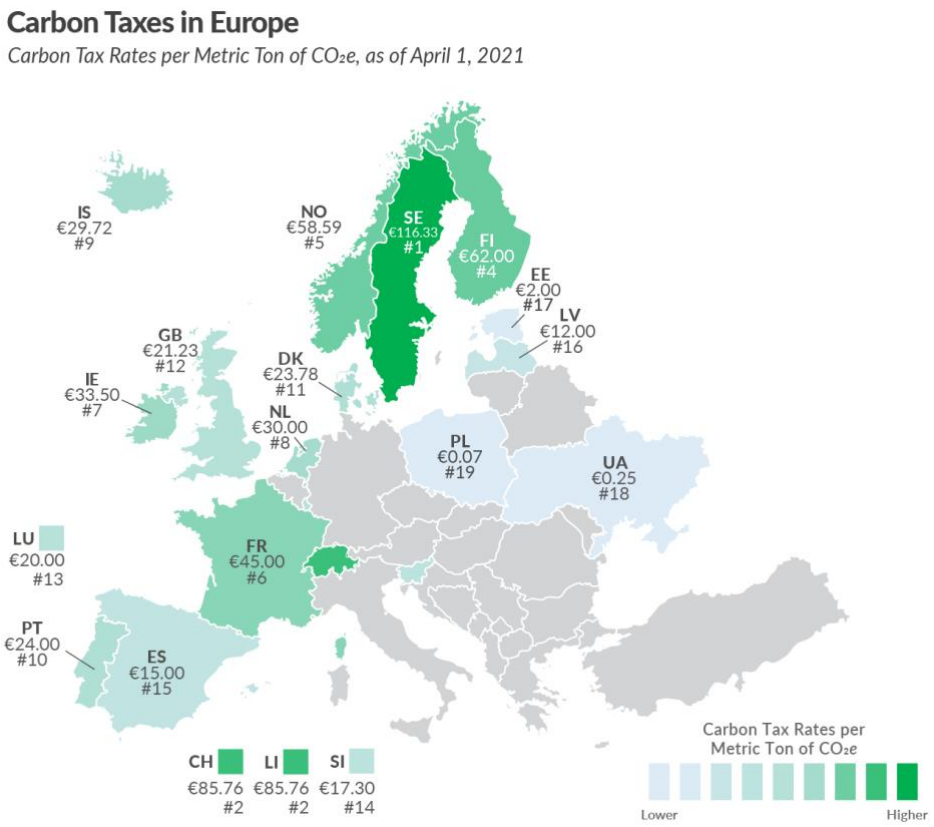

Figure 5. Carbon taxes in Europe per metric ton of CO_2 as of April 2021[56].

1.3 Objectives and Scope of thesis work

The project scope is to develop an innovative and reliable model for the technical, economic, and environmental performance of NT-DHC systems. In this context, the present work aims to achieve the following specific objectives:

- To develop a new methodology for the techno-economic scenario analysis of NT-DHC systems and validate it on a case study.
- To apply an optimization model to identify transition pathways for the network extension and its application to the case study.

The findings from this research are intended to contribute to the planning of potential network expansions by identifying the transition pathways from an initial phase to a final stage. Energy planners, utilities, energy engineers, and DH specialists are the intended audience since they require decision-making support and recommendations for replicating the NT-DHC system. In Ospitaletto, Italy, the operation of a real network will provide valuable data to improve the model's reliability and verify the main energy outputs.

1.4 Motivations and research questions

In the DHC sector, techno-economic assessments (TEA) are typically centered around optimal operation solutions to enhance existing systems. Instead, this project provides an approach for the TEA of developing areas where DH is not present. In addition to optimal investment allocation, this project will investigate the cost-effective operation of NT-DHC networks. The development of a tool for scenario analysis of NT-DHC based on reversible HP substations will aid in the energy planning of future energy systems, allowing for the identification of robust solutions. The outcome is expected to be used for pre-feasibility studies and preliminary design of a new type of DHC network. These findings will contribute to a deeper understanding of the opportunities and constraints of a system of this kind from a techno-economic standpoint.

A key advantage of the proposed model is its ability to simultaneously analyze techno-economic energy scenarios at high temporal resolution, including HP's modeling. This feature has become increasingly important, given the attention towards the sector coupling potential of NT-DHC networks (a feature that is presently missing from current DHC tools).

The research questions that drive this work are:

- RQ1. Is it feasible to expand a NT-DHC network efficiently using available waste heat sources?
- RQ2. Which conditions (technical, economic, environmental) make the NT-DHC solution more competitive than individual solutions?
- RQ3. Is it possible to identify optimal expansion strategies, minimizing the overall costs and emissions (through carbon taxes)?

1.5 Methodology

The research questions and primary objective of this work are addressed through the development of a tool that follows the methodology presented in the following Figure:

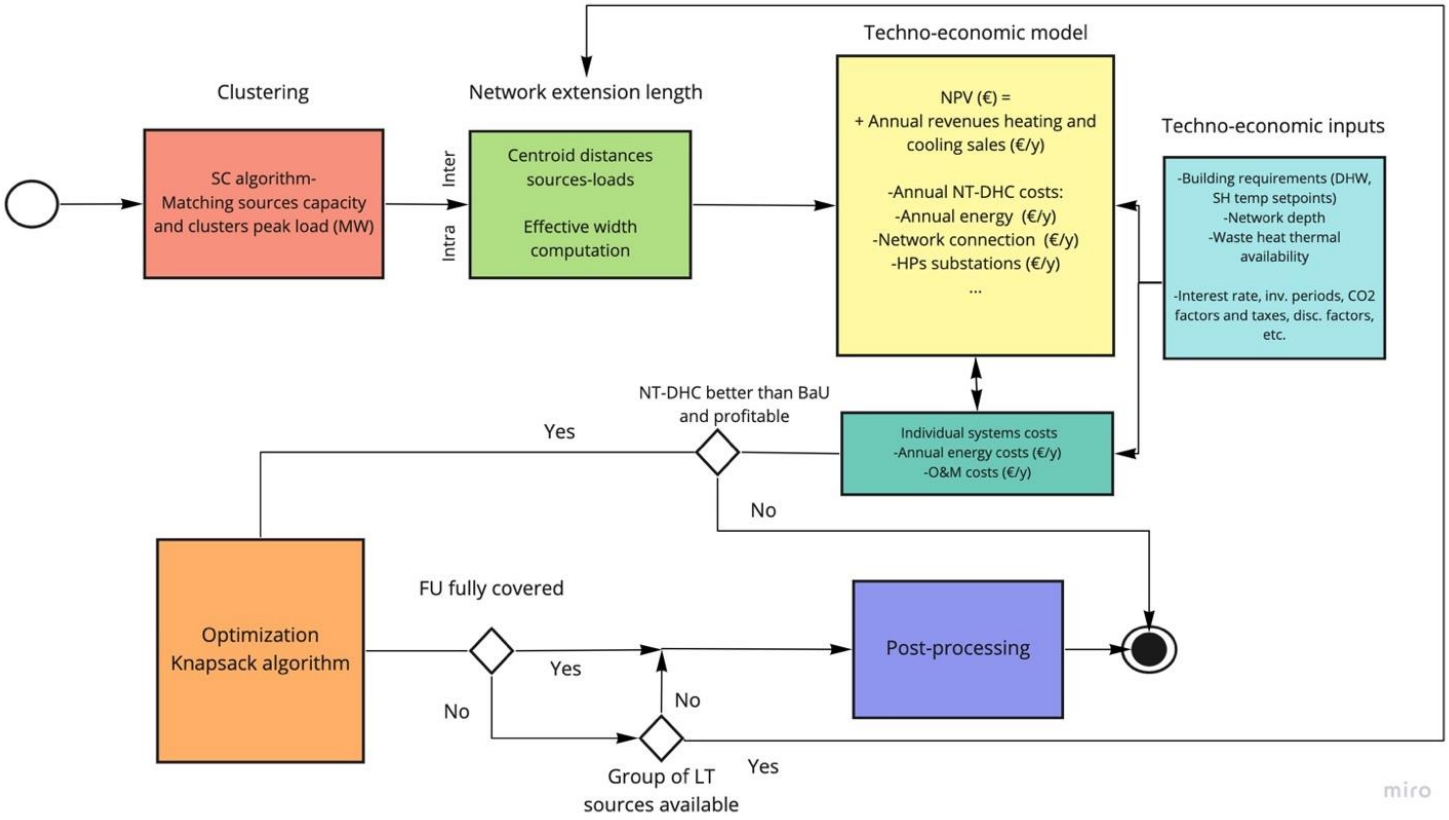

Figure 6. Model methodology. The colors represent separate calculation blocks. The yellow box represents the base DHC techno-economic model. This calculation block is called iteratively in every extension scenario as part of the new extension and optimization model.

The entire methodology is meant to be simple and approximate. It preserves the detail level of the original techno-economic tool that is comprised within this approach.

The first part of the methodology outlines the possible areas where the network can expand, and the potential neutral-temperature sources (NTS) utilized. The spatial resolution used to analyze the NT-DHC network scenarios corresponds to the urban scale. A Functional Unit (FU) of 1 km^2 of residential areas was established. This choice was motivated by previous publications in which a reference area of this size has already been investigated [58][59]. The required input data comes from the mapping tool Hotmaps [60]. This tool uses a top-down statistical method to estimate the H&C demands of any European city zone with a spatial resolution from the hectare to the national level.

In the absence of information on how the built environment is organized, the model divides the FU into clusters with a peak thermal power not larger than the capacity of the available sources. Cluster analysis corresponds to an unsupervised machine learning task involving natural data grouping. Many clustering methods are available, and no single best clustering algorithm for all cases exists. Therefore, a test was carried out to find the method that provides the optimal number of clusters given a limited available thermal power to exploit. It was found that the Spectral Clustering method from the scikit-learn library [61] can perform this task. This method was applied to the case of Ospitaletto, selecting a FU of interest from the city center (see Figure 7).

In addition to the aggregation of residential areas into clusters, special buildings (commercial, public, schools, etc.) are also candidates to be connected to the network. The main distinction concerning residential buildings is that special buildings (SBs) exhibit different H&C profiles, both daily and seasonal.

Estimating the length of a network involves both distribution and service pipes installations. The first category corresponds to the main backbone to connect the sources with the potential loads (inter-distance). Through the geometrical centroid of a number of sources points (latitude and longitude coordinates), a Virtual Source Point (VSP) can be identified and connected to any potential candidate through their respective centroid. The pipe diameter corresponds to the largest pipe size, facilitating the network flow in peak conditions. The second network length category incorporates all the service pipes within the cluster's area for the heat delivery to the buildings in the cluster (intra-distance). This length is estimated through the theoretical framework introduced by Persson in [62]. The authors expressed the network length as a function of two parameters: the effective width, which is the ratio of the land area served by a network and its length, and the gross floor area of the buildings. These parameters are available in the open-source database from Hotmaps. Through the VSP, SBs are grouped similarly to sources, and the total network length required to connect them is the same as for clusters, except for the effective width approach.

The algorithm calculates the extension feasibility to each potential candidate (clusters and SBs). This iterative process involves the hourly calculation of the NT-DHC performance: it considers the energy balance between sources and loads, and accounts for both heating and cooling supply.

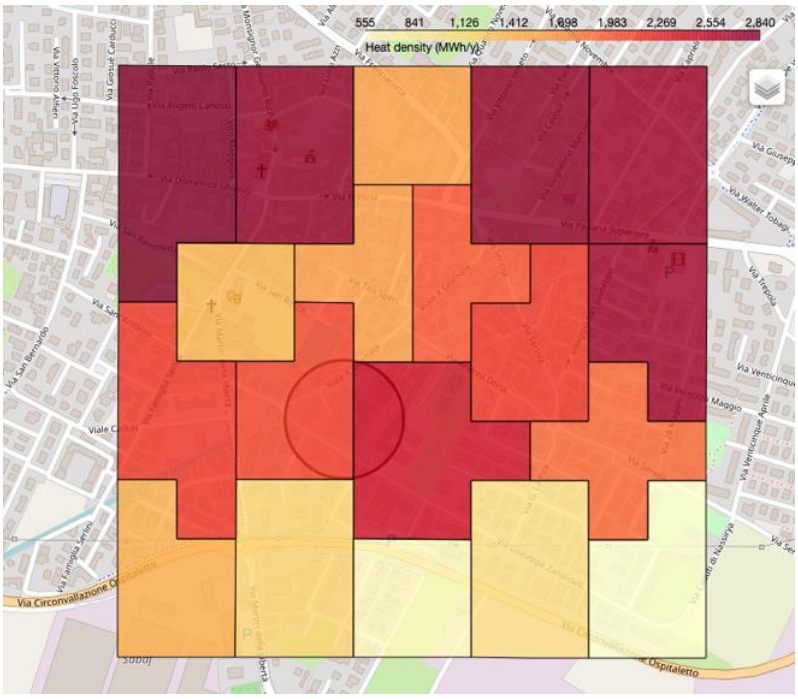

(a)

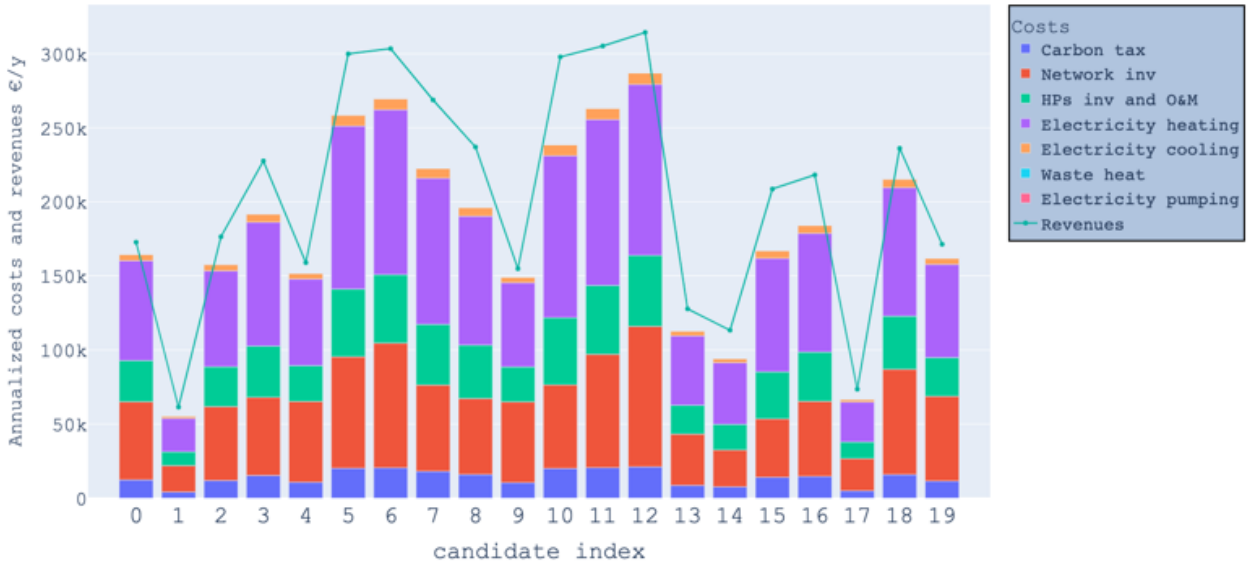

(b)

Figure 7. (a) Spectral Clustering method applied to the case study. Inputs are latitude, longitude, and heat density of each city hectare. (b) Annual costs and revenues per candidate. The difference between the green line and the bars represents the net economic margin per year [€/y].

In addition to the network extension costs, the operational costs include electricity consumptions of the HPs, use of WH and other NTS, network pumping consumptions, etc. The TEA of the best extension scenarios will depend on a value function that considers the economic margin (revenues from the H&C sales minus implementation costs, including CO_2 emissions' taxes) and the maximum available capacity from NTS. The right panel of Figure 7 shows the breakdown of expenses assessed in each extension scenario (in this process, the techno-economic model shown in Figure 6 is called iteratively).

In each extension scenario, the TEA of the NT-DHC solution is compared with the Business as Usual (BaU) cases. Benchmark technologies are reversible air-to-water HPs (A/W HPs) and individual gas boilers with split cooling units (individual H&C scenario). The feasibility of the system depends on the boundary conditions set by the model user, who will define the available and potential H&C sources, network operating conditions, energy prices, etc.

An optimization algorithm selects the combination of extension choices that maximize the overall value of the portfolio after filtering out the choices that are more competitive compared to the BaU scenario. Investment allocation of potential extensions is a problem that can be framed as the 0-1 knapsack problem, which restricts the number of candidates that can be included to zero or one. Given a set of n candidates numbered from 1 to n, each with a weight of w_i(peak capacity) and a value v_i (economic benefit of providing energy to candidate i) along with maximum sources capacity W, the constraint$\sum_i w_i \leq W$ must be respected. Dynamic programming is the technique used to solve this problem, which reduces the complexity and, therefore, the running time in comparison to a brute force approach (O(nW) vs. O(2^n)). In this way, the model will prioritize the clusters or buildings that provide a higher value to the overall extension plan assuming a H&C service price equal to competing individual technologies.

1.6 Novelty

The methodology can be applied to any city zone with the proper heat density and geographical data. This approach goes beyond the State of the art because it includes modeling decentralized HPs' substations, accounts for economic aspects that DH physical models do not possess and comprises optimization for selecting the best system extension.

In the literature, the knapsack approach has been used in the past, but never for the allocation of investments in NT-DHC network extensions. The authors in [63] examined the preferences of consumers using residential smart meters. This mathematical formulation was applied to optimize the appliances costs to identify optimal consumption scenarios and support end-users in their decision making during peak hours. A model was built in [64] to optimize the DHN sources investment. In a

previous study [65], the authors used this framework to optimize DH delivery from high-temperature sources such as municipal solid waste and industrial WH.

In contrast, in this model, the NT-DHC sources are considered a user's choice. This is due to the difficulty in automatization because of the lack of information and the social aspects involved in such a decision process, including risks associated with the expected duration of a source, the industry type and age, and theoretical vs. practical energy potential. Consequently, this tool can be used to determine the transition pathways from an initial to a final network development and so plan long-term extensions.

Table 2. Characteristics of the developed model

Characteristics	
Scope	Simulation and investment optimization of H&C scenarios
Time resolution	Hourly (8760 h)
Spatial resolution	City level. From building groups to hectare cells to clusters of hectares.
Urban sources type	Multi-sources: integration of ground-based with waste heat sources
Sources availability	Multi-source thermal availability profiles
Loads typologies	Special buildings (schools, commercial, offices, etc.) and residential zones are aggregated in clusters.
Load profiles	Specific heat load profiles in special buildings and climate-dependent profiles for clusters
Network temperature	Variable
Network control	Allows the implementation of specific operation strategies (sources' merit order).
Economic database	Yes (annualized energy and investment costs)
Energy balance calculations	Yes (thermal losses, pumping consumptions included)
Network length methodology	Effective width approach + network backbone based on the spatial distance between sources and loads
Long-term energy planning	Yes
Storage modeling	Yes
Network extension optimization	Yes

1.7 Thesis organization

Chapter 2: Model methodology.

The components of the optimization tool are described in detail in this chapter. This chapter describes the modelling of neutral-temperature sources, the data collection for loads, and clustering in the pre-processing phase. The network model and techno-economic assessment are presented in sections 2.3 and 2.4. Lastly, the optimization method is explained in subsection 2.4 and its application to the allocation of investments problem in the NT-DHC context is discussed.

Chapter 3: Verification and validation.

The base techno-economic tool for NT-DHC network scenario analysis is described, along with its first application to a FU in a Mediterranean climate. Even if the study is not extensively reported, its main findings have been published in the AiCARR journal [58]. The following steps focused on verifying the base model approach with a physical model and monitored data from a real NT-DHC network located in Ospitaletto, Italy, as stated in the first specific objective of this project. During this period, the upgrades described in Table 2 were implemented. The results were presented in the 15th Conference on Sustainable Development of Energy, Water and Environment Systems – SDEWES 2020[66] and then published in [67]. The validation with experimental data was presented at the 17th International Symposium on District Heating and Cooling in Nottingham Trent University[68], and then published in[69].

Chapter 4: Model application.

For simplicity, in this chapter, the model is applied to the Ospitaletto case study to explore potential spatial extensions when considering a selected number of sources. Identification of potential ground and WH sources, technical and economic inputs, assumptions relating to energy prices, emission factors, and sensitivity analyses are discussed.

Chapter 5: Results.

This chapter investigates the technical and economic conditions under which NT-DHC can be competitive. Based on this work's second specific objective, scenario analyses are conducted by comparing the former system with benchmark solutions and exploring its advantages and limitations.

Chapter 6: Conclusions and further work.

To conclude, this chapter highlights the contribution of this thesis and prospective benefits of the proposed approach. An overview of the research questions, main findings, and conclusions, as well as future perspectives, are presented in this chapter.

2

Model methodology

This chapter has been partially presented in:

S. Calixto, M. Cozzini, and G. Manzolini, “Techno-economic tool for the evaluation of neutral-temperature district heating and cooling networks and individual solutions”. Euroheat & Power conference, Hilton Brussels Grand Place, Brussels, Belgium, June 2022.

2.1 Neutral temperature sources and control

In traditional DH systems with one central plant supplying heat, typically the supply and return temperatures are constant. In contrast, NT-DHC networks are designed to operate with multiple sources. A merit order is therefore needed to prioritize the sources with the goal of maximizing the efficiency of the HPs substations. This can be achieved by prioritizing the sources with the highest temperature available. Therefore, WH sources have always a higher priority with respect to ground sources. It is assumed that when WH is not available, a ground source satisfies the total load.

The geothermal system can be designed to operate with an auxiliary heater to supply a peak load (bivalent system), such as a gas or biomass boiler[37]. An alternative arrangement is a monovalent system in which the ground source heat pump is oversized to meet the peak load and no back-up is necessary. It was assumed the second configuration, since in section 2.2.2 is explained that the system is designed to support the peak loads using the total WH thermal capacity.

The ground heat is controllable, can be used as an auxiliary heater or cooler, and provides a fairly constant profile throughout the year (balancing systems). The auxiliary heaters, cooling towers, and the chiller have controllable schedules and thus can operate in the event of a surge in heating or cooling demand which cannot be met by the non-balancing systems or the ground source (Figure 8).

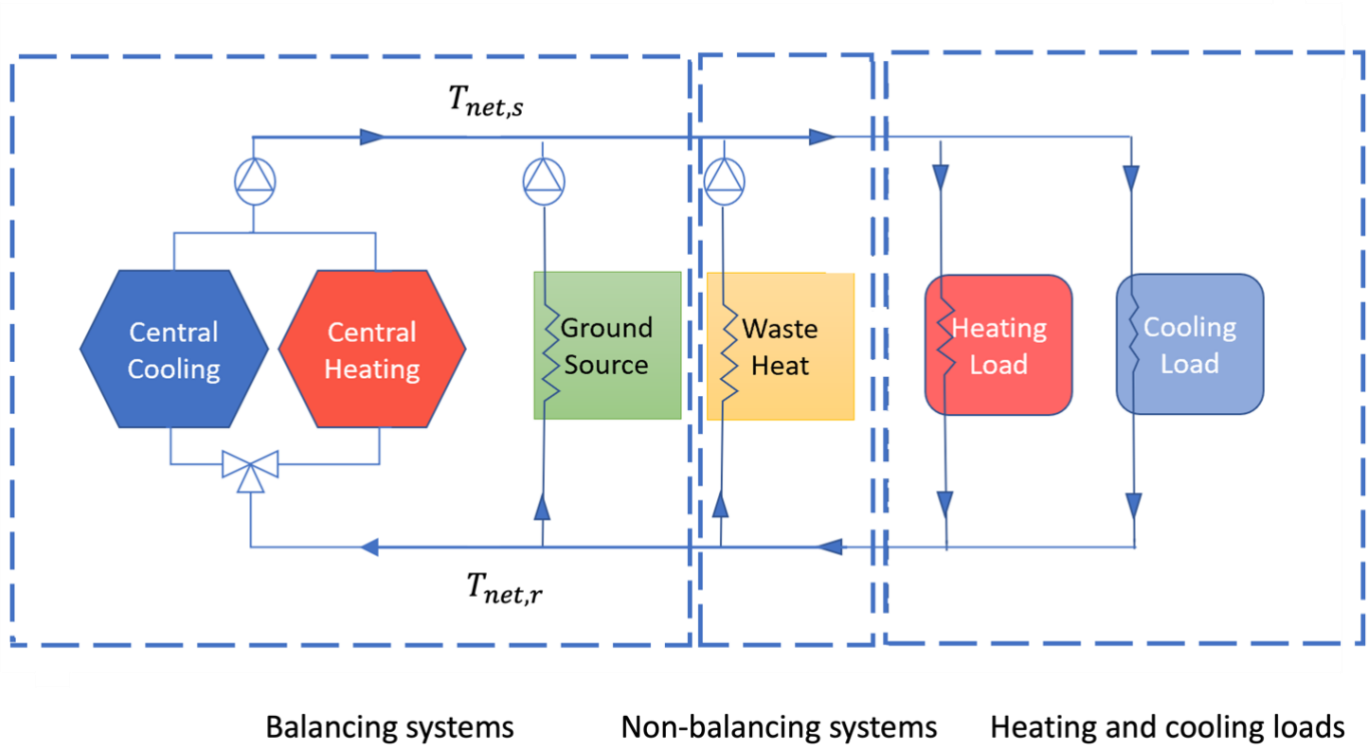

Figure 8. Scheme of a NT-DHC network including WH and ground sources for heating and cooling applications

The modeling of sources is done as follows. The WH availability (E_s) profiles are obtained from the input of the user in the form of a binary matrix (A_s) that represents the hours ($n = 1, \dots, 24$) in a week ($p = 1, \dots, 7$) when a source is ready to deliver heat to the network. This method is appropriate for WH sources whose availability is constant throughout the year (refrigeration units in supermarkets, shopping malls, data centers, industrial waste heat, wastewater) and their thermal capacity (E_{cap_s}) is known. The model accepts the input of maximum three sources.

In contrast, sources that present a seasonal availability (service sector, metro stations) were not in the scope of this model, nevertheless, the model could be potentially expanded to accept hourly profiles of WH availability if this information is present.

$$E_s = E_{cap_s} \times A_s \; ; \;\; s = 1,2,3 \tag{2.1}$$

$$A_s = \begin{bmatrix} a_{11} & \cdots & a_{1j} & \cdots & a_{1p} \\ \vdots & \ddots & & & \vdots \\ a_{i1} & & a_{ij} & & a_{ip} \\ \vdots & & & \ddots & \vdots \\ a_{n1} & \cdots & a_{nj} & \cdots & a_{np} \end{bmatrix} \tag{2.2}$$

After that the WH availability is set, and the sources temperatures are known, the model prioritizes the sources according to their temperature level as follows:

$$T_{net,s} = \begin{cases} T_{gs} & if\ T_{s_1} = T_{s_2} = T_{s_3} = 0°C \\ max\left(T_{s_1}, T_{s_2}, T_{s_3}\right) & otherwise \end{cases} \tag{2.3}$$

Figures below illustrate a fictitious example of a NT-DHC network operating in London, UK, served by two WH sources and a ground source. It is assumed that source 1 has priority over source 2 over the course of the entire year. The yellow area represents the electricity contribution characteristic from this kind of network. The weekly pattern is assumed to be constant throughout the year, regardless of the season's thermal demand.

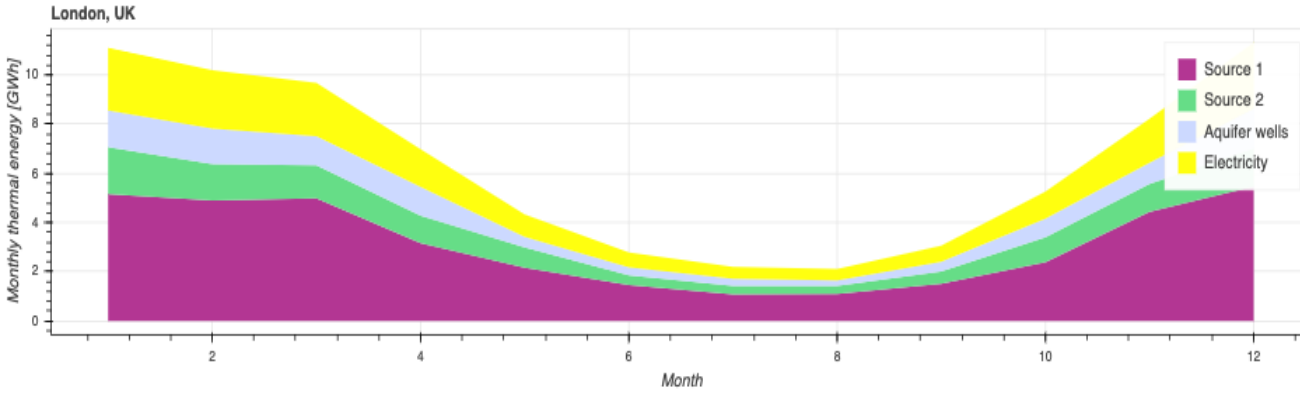

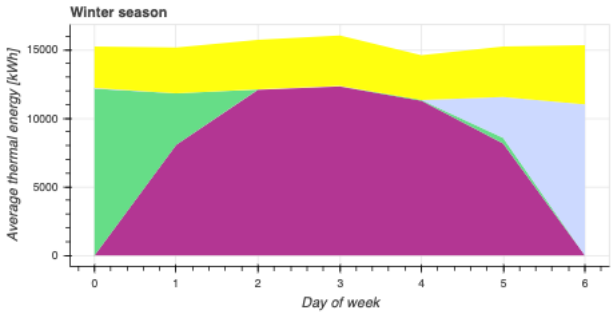

(a) Winter

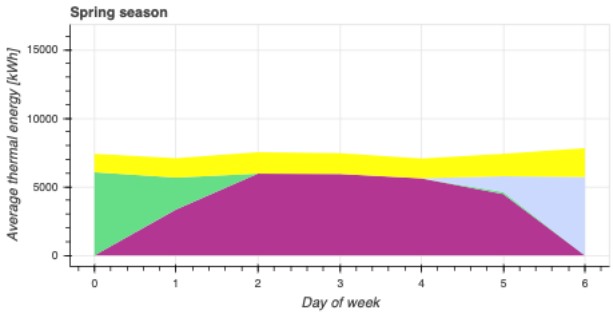

(b) Spring

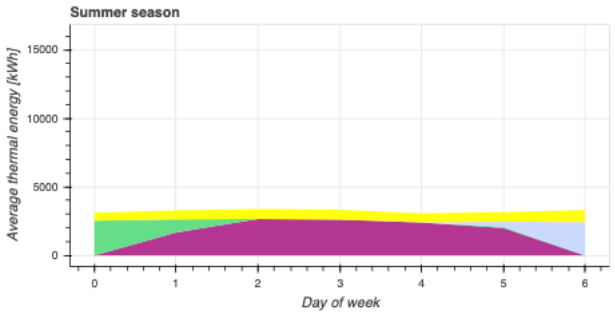

(c) Summer

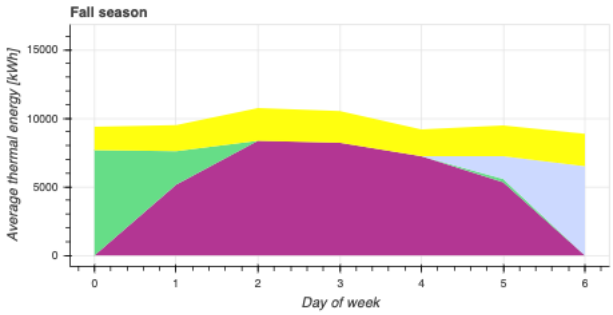

(d) Fall

Figure 9. Thermal energy delivery by source type

2.2 Loads analysis and clustering

2.2.1 Heat density data and spatial resolution

As the developed tool is intended to provide a broad methodology, it must use an open, accessible database. The Hotmaps project developed a free online database for the planning and mapping of heating and cooling systems for EU28 countries at national and local level[70]. Its small spatial resolution of 100 x 100 m sets the granularity level for this type of analysis. This toolbox's versatility allows to analyze H&C scenarios in any of the covered countries. Obtaining a more realistic representation at a more granular level (at the building level) would require more information than is currently available. Even then, retrieving or managing large amounts of data can be difficult and time-consuming.

Hotmaps generates raster maps with typical building stock indicators (H&C heat density, gross floor area, buildings volume, etc.) covering the entire EU28 building stock. The map was derived from aggregated values including data from the 2011 Eurostat census, land use data, the European Settlement Map layer, data from the Global Human Settlement project, and data from OpenStreetMap[71]. Online data tools were used to extrapolate and assemble data during the data collection process. Data was obtained from the TABULA web-tool [72] for the residential sector, and from the EU building database for the commercial sector. In the process of generating the Hotmaps default datasets, quality, completeness, accuracy, and reliability are critical factors. In this context, a questionnaire containing all features included in the database for the residential sector was sent to two experts from each country.

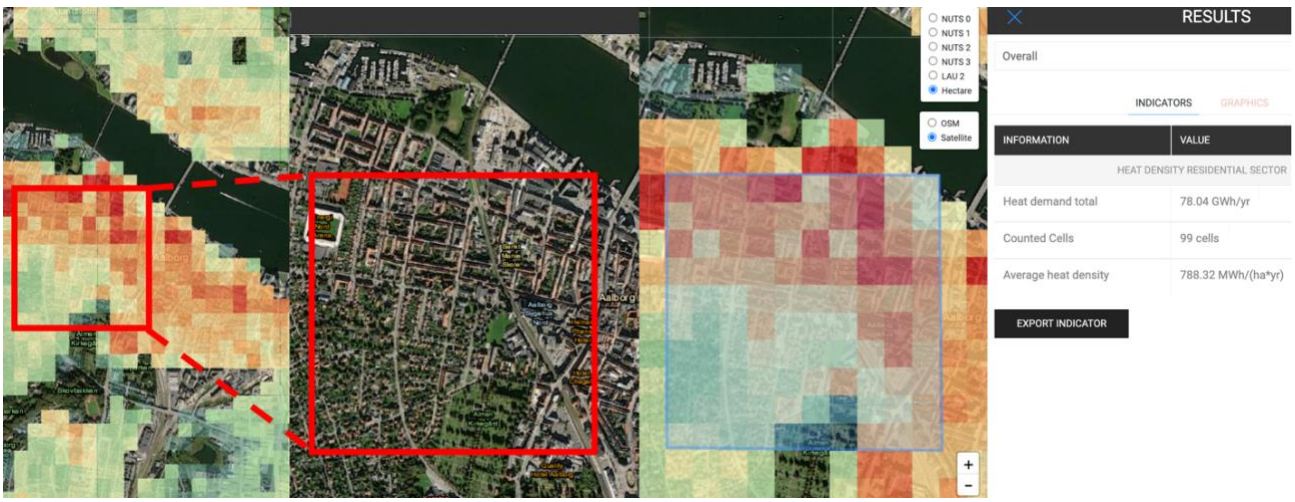

Figure 10. Spatial view of a residential city quarter in Aalborg, Denmark. In the Hotmaps tool, 1 km^2 of FU was selected, and the total heat density was displayed. Each cell equals a hectare.

2.2.2 Clustering

From a network manager perspective, there are at least three important aspects of interest when planning an expansion:

- Exploiting cheap sources that are geographically identified, quantified the thermal potential, and assessed their level of priority when more than one source exists.
- Procuring a stable H&C supply to secure the highest amount of energy sold. Long-term contracts with the thermal providers would allow to reduce the risks of shortage.
- Minimizing the network length needed to connect sources with loads to reduce costs.

In contrast to conventional DH thermal plants, NT-DHC systems rely on sources with limited capacity, sometimes less than 1 MW as in the case of supermarkets [73][30]. As a result, it is assumed that it is very unlikely to evaluate scenarios where a source can satisfy the H&C demands of an entire city or even the FU defined in this approach. Therefore, identifying the communities to be served must be identified such that technically these sources could provide thermal energy in peak conditions. The following assumptions were accounted for in this process:

- The loads must be aggregated in an adjacent form: this requirement would minimize the distribution network piping, and therefore the costs.
- The loads (or the aggregation of loads) thermal peak power cannot exceed the sources capacity.
- The aggregation method should give the flexibility to modify the number of clusters and their size to match the source capacity constraint. As a result, the method can be adapted to as many contexts as possible.
- The loads aggregation method must be computationally manageable. A test should be necessary to recognize whether the execution time escalates with the number of partitions.
- Reducing the discretization level would allow to reduce the computational effort when managing large datasets.
- It is not foreseen to embed a streets' map where a network can be potentially installed. In contrast, the calculations of the distribution network length would follow the aggregate approach developed by Persson for traditional DHN[62]. Therefore, the spatial and heat density limitations of this method should be aligned with the selected discretization.

The aggregation process can be addressed by applying a clustering algorithm: a machine learning

process that aggregates similar data points into the same cluster and assigns less similar points to other clusters. Scikit-learn [61] proposes several clustering algorithms; the following table lists the required parameters for the most common clustering techniques.

A proper number or size of clusters (n, epsilon, or any other clustering parameter) depends on the capacity restrictions mentioned previously. A test was therefore conducted in which, iteratively, the number of clusters was provided to a clustering algorithm. As a result, the size of the clusters is reduced so that the largest cluster size does not exceed the capacity restriction.

According to Table 3, the methods that accept the number of clusters as input are K-Means (KM) and Spectral Clustering (SC). Ideally, the outputs will present even cluster sizes, not necessary a flat geometry, and the number of clusters should be minimal to preserve the aggregate approach and speed up the a posteriori techno-economic evaluation. The Gaussian mixture (GM) method was also tested since it also allows to vary the number of elements in the cluster.

The case of Aalborg University in Denmark, which belongs to the Life4HeatRecovery project[12], is used for testing purposes. A polygon of about 2 km^2 was selected from the immediate vicinity, as shown in Figure 11. This corresponds to 86 data cells with 21.43 GWh/year total heat demand. Based on this example, four NT-DHC sources were identified through a spatial search and selected. It is assumed that a source with capacity 1.6 MW sets the cluster-size threshold.

This preliminary comparison (see) exhibits that even if initially the algorithms provide a similar solution, the GM method creates uneven clusters sizes when increasing the granularity. The comparison between KM and SC is less straightforward, but their differences can be explained by:

- KM has the limitation of assuming spherical clusters that are separable so that the mean converges towards the cluster center. The clusters are expected to be of similar size, so that the assignment to the nearest cluster center is the correct assignment. This strong assumption might lead to inaccurate cluster splitting.
- SC does not make assumptions with regards to the statistics of the clusters.
- SC methods are easy to implement and fast for sparse datasets up to several thousand[74].
- KM assumes a flat geometry while SC algorithms do not make assumptions about the clusters' shape/form.

Table 3. A comparison of clustering methods [61]

Method	**Parameters**	**Use case**	**Flat geometry**	**Metric used**
K-Means	Number of clusters	General-purpose, even cluster size, few clusters	Yes	Distances between points
Spectral clustering	Number of clusters	Few clusters, even cluster size	No	Graph distance (nearest neighbor)
Gaussian mixtures	Many	Good for density estimation	Yes	Mahalanobis distances to centers
Affinity propagation	Sample preference	Many clusters, uneven cluster size	No	Graph distance (nearest neighbor)
Mean-shift	Bandwidth	Many clusters, uneven cluster size	No	Distances between points
Ward hierarchical clustering	Number of clusters or distance threshold	Many clusters, possibly connectivity constraints	N/A	Distances between points
Agglomerative clustering	Number of clusters or distance threshold	Many clusters, possibly connectivity constraints	N/A	Any pairwise distance
DBSCAN	Neighborhood size	Uneven cluster sizes, outlier removal	No	Distances between points
OPTICS	Minimum cluster membership	Uneven cluster sizes, variable cluster density	No	Distances between points
BIRCH	Branching factor, threshold	Large dataset, outlier removal	N/A	Euclidean distance between points

(a) (b)

Figure 11. Application of clustering methods to a test case. (a) Selection of the bounding box for Aalborg University, Denmark from the Hotmaps database. (b) Train data, each cell representing a heat demand point. Sources nearby are displayed.

Figure 12. Application of three clustering algorithms iteratively to identify the optimal configuration

.

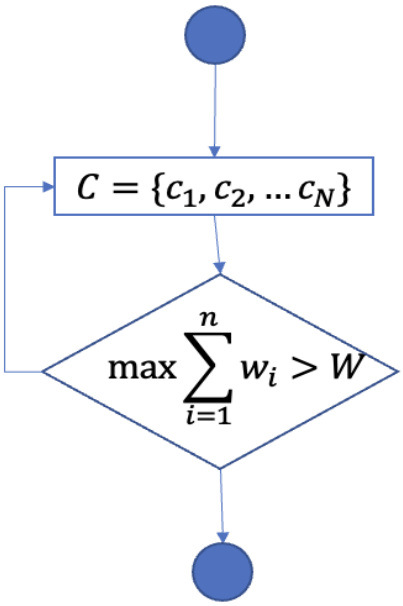

Figure 13. Iterative process varying the number of clusters N to find the optimal configuration.

The methods were tested iteratively varying N to find the optimal configuration that leads to a maximum cluster size not larger than the capacity of sources W (Figure 13). The problem was formulated such that given a set of thermal power data points $w_1, w_2, \ldots, w_N$ and sources capacity W, a clustering method was applied to find the N subsets. The outputs of this process are presented in Figure 14.

Due to the advantages mentioned previously, the SC method was selected as the default algorithm as opposed to the KM method. Figure 14 shows that both approaches result in the same solution for this case. Finally, it is noteworthy that the chosen clustering method finds the optimal configuration in a short period of time. The iterative clustering process of the 86 cells covering about 2 km^2 in this example was completed in only 40 seconds.

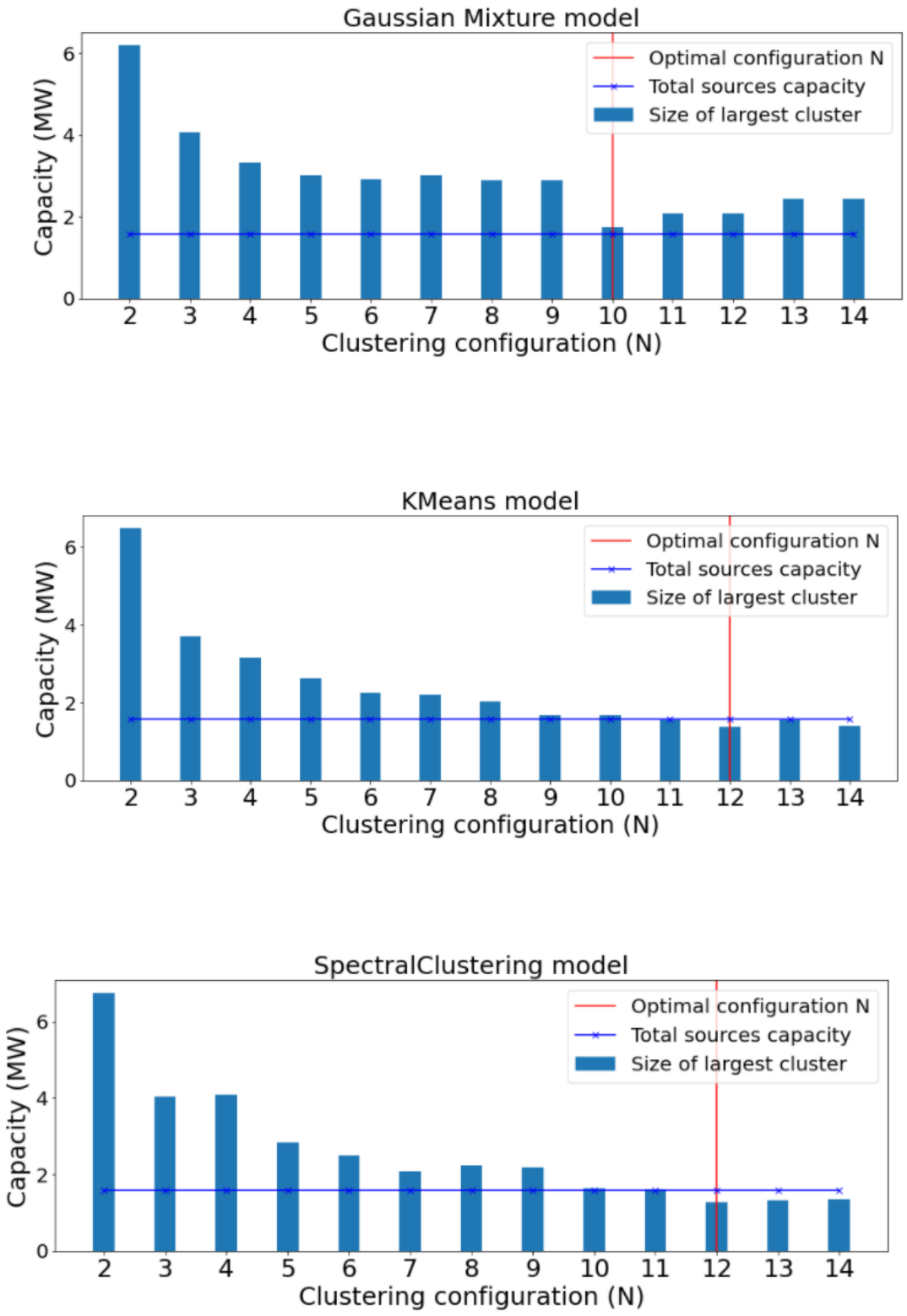

Figure 14. Clustering methods comparison and its relationship with the capacity restriction

2.2.3 Space heating and domestic hot water

The space heating profile is obtained with a time dependency according to the heating degree days (HDD) method. This method is commonly used in the energy literature, accounts the amount (in degrees) and for how long (in hours) thermal heat is required, for a given building and climate, with regards to the average daily outdoor temperature (T_{amb})[75].

The space heating hourly profile ($E_{th,sh}$) is obtained setting a base temperature (T_{b-heat}). The default value is 15°C, in line with the average European base temperature[76], however, it can be modified by the tool's user. How to choose the optimal base temperature and hourly H&C profiles (f_h) are discussed in the following subsection. The calculation is performed daily and distributed hourly. Then, for day j and hour h:

$$E_{th,sh}(j,h) = E_{\%sh} \times \frac{(T_{b-heat} - T_{amb,j})}{\sum_{i=1}^{365}(T_{b-heat} - T_{amb,i})} \times f_h,\ T_{amb,j} < T_{b-heat} \qquad 2.4$$

Building energy requirements and the European climatic zone determine the energy share required for space heating ($E_{\%sh}$). The model allows customization of this value based on the data presented in Table 4. The reported data is based on the results of reference single-family housing (SFH) building typologies built between 1945 and 1970 [77]. Building renovations affect the energy levels and therefore the space heating and cooling consumption, while DHW production is constant regardless of climate. The entire range of building typologies can be found on the iNSPiRe project [78] website.

Unless there is a specific ambient temperature dataset available, there are four default climatic datasets, representative of the following European climates:

- Stuttgart, Germany, Continental climate
- London, United Kingdom, Oceanic climate
- Madrid, Spain, Southern-dry climate
- Rome, Italy, Mediterranean climate

Domestic hot water consumption (DHW) is not weather-dependent, and its variation is almost constant throughout the year. Table 4 shows the annual share of consumption of DHW. The demand in each day is evenly spread across the year, and the hourly distribution is obtained by multiplying the daily needs by a random hourly profile.

The model contains the profiles used in [67], however, the DHW profile can be customized using free software that uses statistical means based on user-specific requirements[79].

Table 4. Heating, cooling, and domestic hot water consumption of SFHs in different European climates

Climate	Energy Level [kWh/m²y]	Space Heating [kWh/m²y]	Space Cooling [kWh/m²y]	DHW [kWh/m²y]	Ventilation [kWh/m²y]
Northern Continental	15	23,3	9,4	21,7	5,0
	45	45,50	6,0	21,70	5,0
	70	73,70	5,5	21,70	0,0
Oceanic	15	10,5	9,1	21,7	4,2
	45	42,90	5,9	21,80	0,0
	70	74,80	2,7	21,80	0,0
Southern dry	15	11,8	34,3	21,8	4,2
	45	53,30	35,9	21,80	0,0
	70	85,60	26,6	21,80	0,0
Mediterranean	15	16,2	33,1	21,8	4,2
	25	28,1	33,1	21,8	4,2
	70	75,90	28,4	21,70	0,0
Nordic	15	21,5	11,8	21,7	5,2
	45	51,30	7,4	21,70	5,2
	70	76,40	8,0	21,70	0,0
Continental	15	26,3	10,9	21,7	4,5
	45	56,30	10,1	21,70	0,0
	70	68,90	10,4	21,70	0,0

2.2.4 Cooling

Cooling demand data in Europe is very scarce. Indeed, the only project with reliable information on this regard is the EcoHeatCool project [80] which created a cooling index based on the cooling degree days method (CDD) to estimate the specific demands in European countries. The CDD method follows the same procedure as heating degree days. The calculation aims at estimating how much (in degrees), and for how long in days the outdoor temperature was above a certain level.

Base temperature estimation is not a straightforward procedure due to the multitude of factors that affect the selection. In the literature, [29] reports that HDD and CDD have been used at a wide range of temperatures. In some studies, the base temperature is defined as the "basic indoor comfort" level[81][82][83], others define it as the outdoor balance-point temperature [84][85][86]. Additionally, the HDD base temperatures vary according to country-specific conditions: in Turkey, [84] assumed 14-22 °C, in Russia, [81] assumed 18°C, in Greece, [87] assumed 10-20°C and in Europe, [76] assumed 15.5°C. CDD, on the other hand, varies from 10°C to 28°C [75]. Though acceptable for a preliminary estimate, the degree day approach is less accurate for cooling, since cooling is more influenced by sun irradiance and other disturbances not related to outdoor temperatures.

The iNSPiRe project provided a more detailed methodology for estimating the specific cooling consumptions in seven European climates (Southern dry, Mediterranean, Southern continental, Oceanic, Continental, Northern continental, and Nordic).

The results of this study show that the cooling consumption in the residential sector ranges from 4-8 kWh/m^{2}y in the Nordic countries, Southern dry regions present a specific consumption of 16 kWh/m^{2}y, and Mediterranean zones present the highest values up to 22 kWh/m^{2}y (assuming a base temperature equal to 24-25°C) [88]. However, it was found that only a fraction of the residential building stock was cooled, from 50% of the floor area in the Southern dry climate, 20% in the Mediterranean to 7% in the Southern continental climate.

Using a cooling factor, this model calculates the total cooling demand based on the cooling/heating ratio for each floor square meter. According to a study simulating a three-floor residential building in Bolzano, Italy, specific cooling and heating loads were calculated at 12 and 128 kWh/m^{2}y. Based on Ospitaletto's southern location relative to Bolzano, this ratio was adjusted according to their HDD, yielding a cooling factor of 10.7%[89]. The factor means that for every square meter that is heated and cooled, 10.7% of the total heating load corresponds to cooling. The default simulation assumes that all the customers connected to the network receive the H&C service. The cooling factor can then be extrapolated to other applications with the specific heating and cooling consumption data.

The cooling temporal distribution is obtained similarly to the heating distribution. Figure 16 displays the daily profiles retrieved from [89], but they can be customized if more information is available.

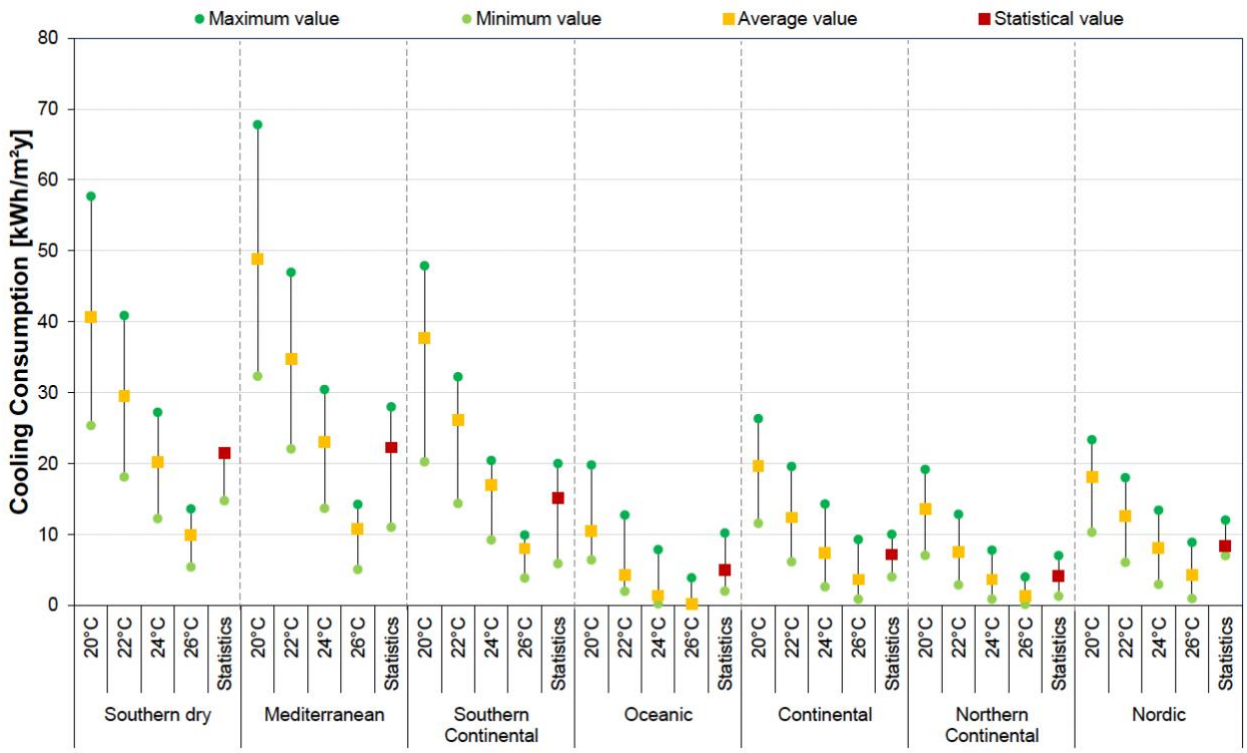

Figure 15. Annual cooling consumption of residential buildings-simulation results and statistical values[78].

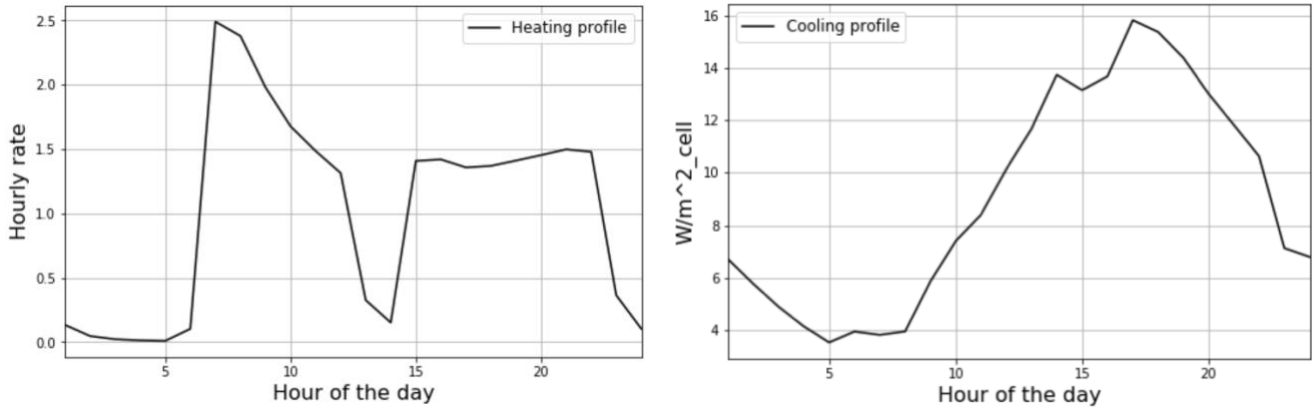

Figure 16. Heating and cooling daily default profiles for residential buildings[89].

2.3 Network model

The network required to connect each potential zone is calculated based on the type of sink (clusters or SBs). It is divided into two components: the intra-cluster distance, corresponding to the service pipes required to connect buildings within a cluster/group of SBs; and the inter-distance, the primary network backbone that connects the sources with the loads. Rather than representing the real network faithfully, this structure represents a reasonable simplification of the network's length. The following subsections provide an overview of the methods chosen for estimating the total network costs in each scenario.

2.3.1 Inter-distance

Identified the sources and their geographical coordinates, the model estimates the required network length to connect them. A Virtual Source Point (VSP) is found through the geometrical centroid of a set of *s* finite points. The latitude ϕ and longitude Ψ are found as follow:

$$VSP(\phi, \Psi) = \left(\frac{\sum_{i=1}^{s} \phi_i}{s}, \frac{\sum_{i=1}^{s} \Psi_i}{s} \right) \quad 2.5$$

Thus, the total length required to connect the sources is estimated as the total sum of Euclidean distances between each of the sources and the VSP. This investment is considered a fixed cost equal in all extension scenarios, it does not depend on how distant the sources are from the sinks.

On the contrary, the inter-distance accounts for the differences among sources and sinks. It can be interpreted as the main pipe that constitutes the backbone of the network. It is estimated as the haversine distance between the VSP and the centroid of a cluster. This method calculates the shortest distance between two points on a sphere using their latitudes and longitudes measured along the surface, it can be expressed as follows[90]:

$$d = 2R\ sin^{-1} \sqrt{sin^2\left(\frac{\phi_2 - \phi_1}{2}\right) + \cos(\phi_1)\cos(\phi_2) sin^2\left(\frac{\Psi_2 - \Psi_1}{2}\right)} \quad 2.6$$

Here, d is the distance between two points, with latitude and longitude (ϕ, Ψ) and R is the Earth's radius. As the Earth is nearly spherical, the haversine formula provides a good approximation of the distance between two points of the Earth surface, with a less than 1% error on average.

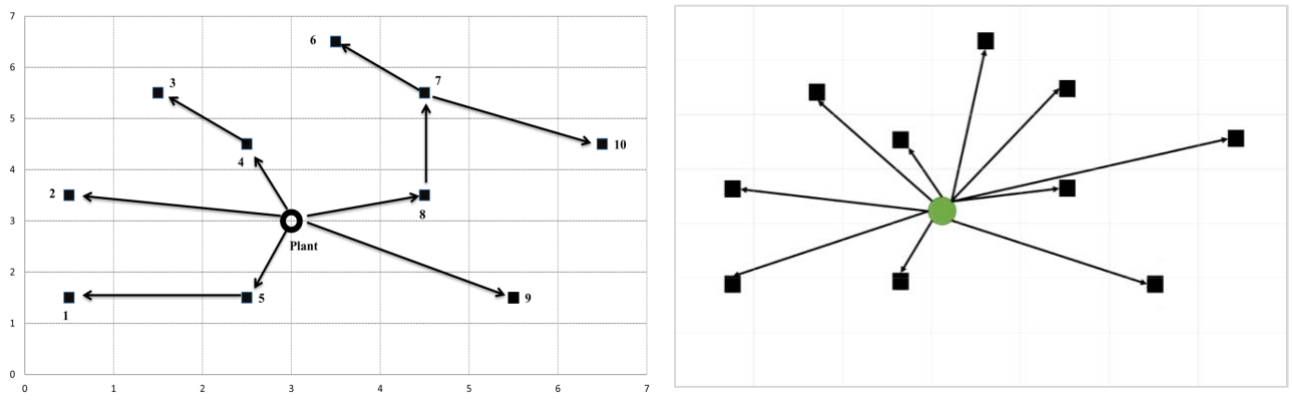

(a) (b)

Figure 17. Optimal district heating network configurations. (a) Connections between a centralized heating plant and its consumers. (b) Star-like connection method.

This method likely underestimates the real backbone since it overlooks the presence of streets or paths in which it is not possible to lay down a network due to technical or administrative limitations. A better approach would be to account for the streets using the Manhattan distance, or to overlap a layer that contains the streets data. However, this can be compensated when considering multiple extensions. When the optimal extension is found, the model proposes several backbones starting from the same origin (the sources centroid), resulting in a star-like shape. A visual representation of this approach can be observed in Figure 17. On the left, the authors in [91] presented a method for optimizing the network connection between a central plant and end-users. In the alternative on the right, the loads are directly linked to the VSP. A limitation of this approach is that the techno-economic evaluation is made individually, and therefore, does not reflect synergies among clusters that could lead to an optimal solution with a minimal total network length.

In view of the recent development of NT-DHC networks, it is challenging to forecast how the system will expand in space, but if one examines the evolution of conventional networks, they tend to evolve based on a more complex structure (as presented in Figure 18, a typical evolution in order of increasing complexity). However, a more accurate representation of a real network expansion in space is beyond the scope of this study.

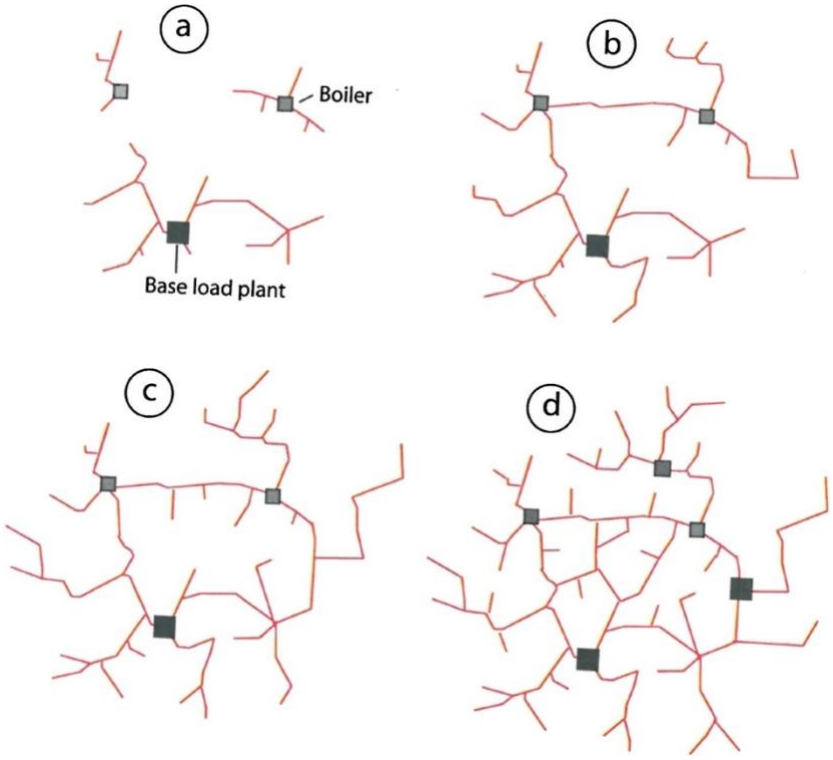

Figure 18. Conventional DHN designs evolution. (a) a network made of three islands, (b) a coherent network having a tree structure, (c) a network with a ring, and (d) a meshed network[92].

2.3.2 Intra-distance

In the conventional DH literature, the effective width approach is a common parameter defined to estimate the length of a DHN by knowing urbanistic parameters such as the land area and the building area [93][94]. Heat Roadmap Europe has extensively used this method to estimate European countries' network costs and DH potential. It was described by Persson and Werner in [62] and it is estimated as follows:

$$e = \frac{A_B}{A_L} \tag{2.7}$$

$$L = \frac{A_L}{w} \tag{2.8}$$

$$w = 61.8\, e^{-0.15} \tag{2.9}$$

where,

e= plot ratio.

A_B= building space area (m^2).

A_L= land area (m^2).

w= effective width (m).

L= total trench length of the distribution network (m).

Based on the Hotmaps layer data, the building area (A_B) and land area (A_L) are known inputs, which allows the trench length to be estimated. The concept of effective width can be used to quickly estimate network investments with a minimal number of inputs; however, it is important to note the downsides of this approach. Based on limited empirical evidence from a small set of cases, this study overestimates the effective width in low density areas, and as a result, underestimates the distribution costs. This issue is addressed in [95], where the author provides evidence of effective width behavior in sparse regions using empirical data of a DHN in Denmark. In this study, it was created a grid of one-hectare cells, and the parameters of interest (effective width, network length, building area, land area) were calculated for different aggregation of cells, by combining adjacent cells.

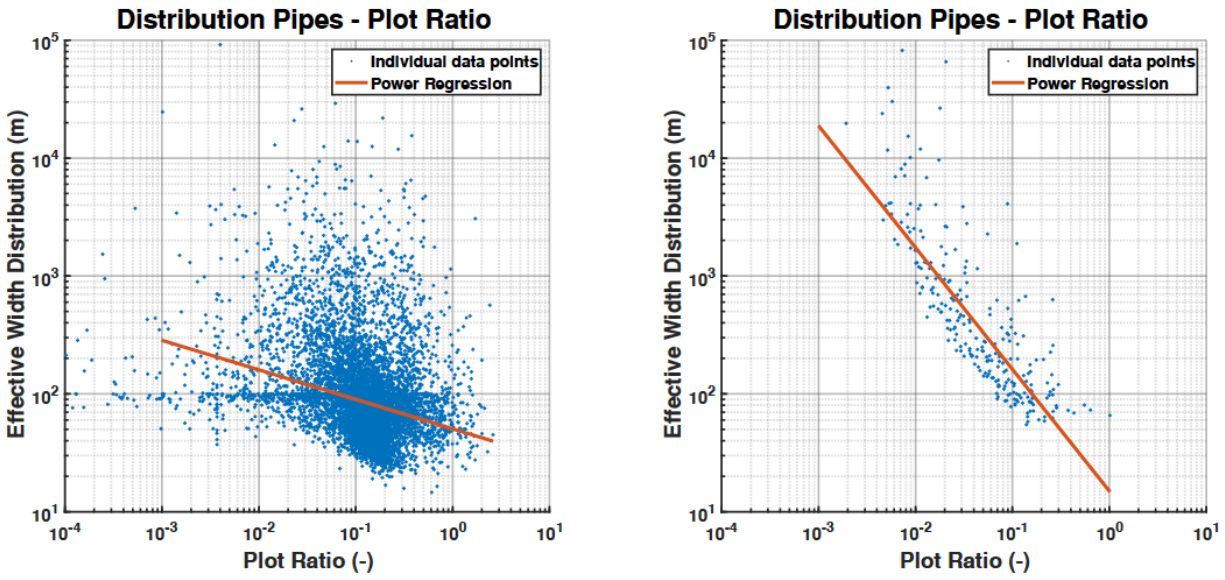

(a) (b)

Figure 19. Effective width in distribution pipes. (a) In a 1 ha cell size, data dispersion is large, showing poor regression at this scale. (b) 100 ha supercell size. It is observed a clear decreasing trend of the effective width for large plot ratios (high-density areas).

It was found that this approach statistically improves when increasing the cell size, reaching a plateau at about 10-25 ha supercell size. The fact that small scale cell sizes lead to poor regressions is another reason to keep an approach as aggregated as possible. In this model, the cells are of a size between the two plots presented in Figure 19.

The total costs of the distribution network are determined by the network length and the diameters of the network pipes (according to a pre-determined pipe configuration described in subsection 2.4.3). The maximum pipe diameter is determined by the maximum expected flow rate during peak conditions and by the constraints on the maximum velocity and pressure drop gradient accepted in the pipes. The designed pressure drop (Δp) is 100 Pa/m in each pipe [94], and the design speed based on the pipe diameter are shown in Table 20 from Appendix A.2.

The volume flow rate ($\dot{V}$) that is exchanged between the network and the reversible heat pumps is a function of the energy transferred at the evaporator(Q_{evap})in heating or condenser (Q_{cond}) in cooling mode, the heat carrier fluid density (ρ), the specific heat of the carrier fluid (c_p), and the temperature difference (ΔT) along the evaporator (or condenser):

$$\dot{V} = \frac{Q_{evap(cond)}}{\rho c_p \Delta T_{evap(cond)}} \quad 2.10$$

$$\dot{V}_{max} = max\ (\dot{V}_h + \dot{V}_c) \quad 2.11$$

where,

$Q_{evap(cond)}$=thermal power at the evaporator (in heating) and condenser (in cooling) mode [MW].

$\Delta T_{evap(cond)}$= difference between the network supply and return temperature [K].

$\dot{V}_h$=volume flow rate in heating mode [m^3/s].

$\dot{V}_c$= volume flow rate in cooling mode [m^3/s].

The maximum flow rate ($\dot{V}_{max}$) carried in the network is estimated as the highest value of the sum of the flow rates in heating and cooling modes in a year. It is used for sizing the network pipes as follows:

$$D_{max} = \left(\frac{f_F \times \rho \times L \times \dot{V}_{max}^2}{\pi^2 \Delta p} \right)^{1/5} \quad 2.12$$

Where f_F is the Fanning factor (1/4 of the Darcy friction factor f), L is the pipe length, and Δp is the designed pressure drop [96]. A good approximation for the turbulent flow regime is given by the Haaland equation, which depends on the Reynolds number (Re) and the pipe roughness (ε):

$$f = \left\{ -1.8 \, log \left(\left[\frac{6.9}{Re} \right] + \left(\frac{\varepsilon / D}{3.7} \right)^{1.11} \right) \right\}^{-2} \quad 2.13$$

It was assumed for turbulent flow $Re = 10^6$ and $\varepsilon = 0.1$ mm as recommended value for commercial steel ducts. The Darcy friction factor depends on the diameter of the pipe, but since the diameter is not known initially, the calculation is done in two steps. It is first assumed a friction factor f_F (0.02 by default), and it is then used to calculate the Darcy friction factor based on a fictitious pipe diameter. Using this new factor in the second step, the maximum diameter for the network is determined.

Figure 20 shows the theoretical framework of inter and intra distances applied to the clusters. The triangles represent the clusters centroids (VSPc) which connect with the sources centroid (VSPs) through a backbone (red and blue lines represent the supply and return network pipes). The intra-distance can be interpreted as a mesh network, whose length is measured using the Persson approach, and whose pipe size is assumed to follow a predetermined network composition.

Figure 21 presents the total length required to connect SBs with the sources' centroid. The intra-distance in this case is calculated the same way as the sources' connection: the sum of the Euclidean distances between each building and the VSP.

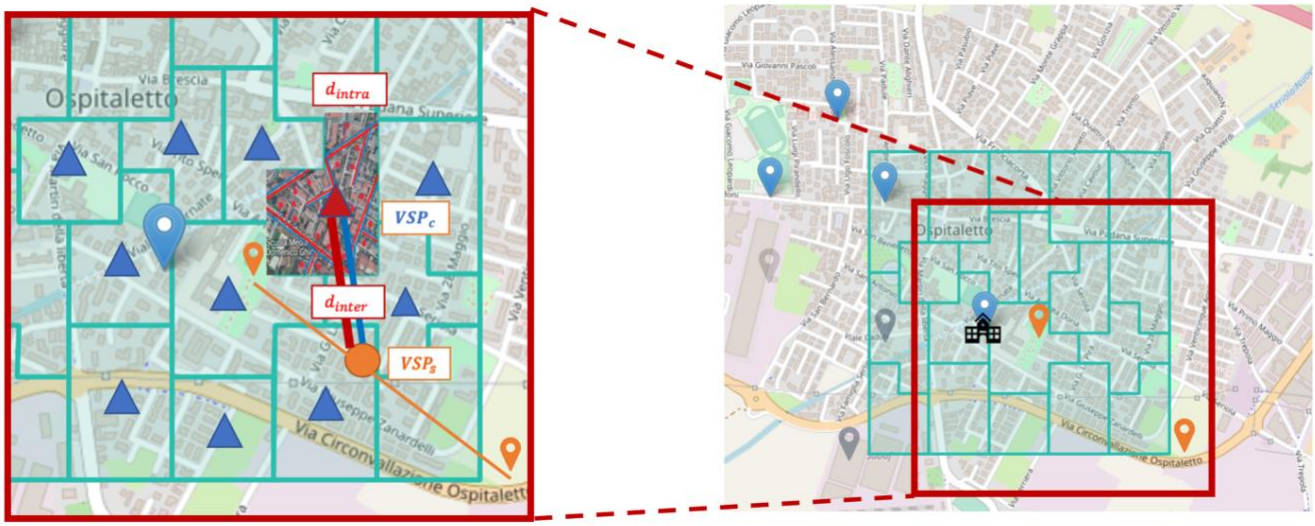

Figure 20. Theoretical representation of the total network length required to connect a cluster.

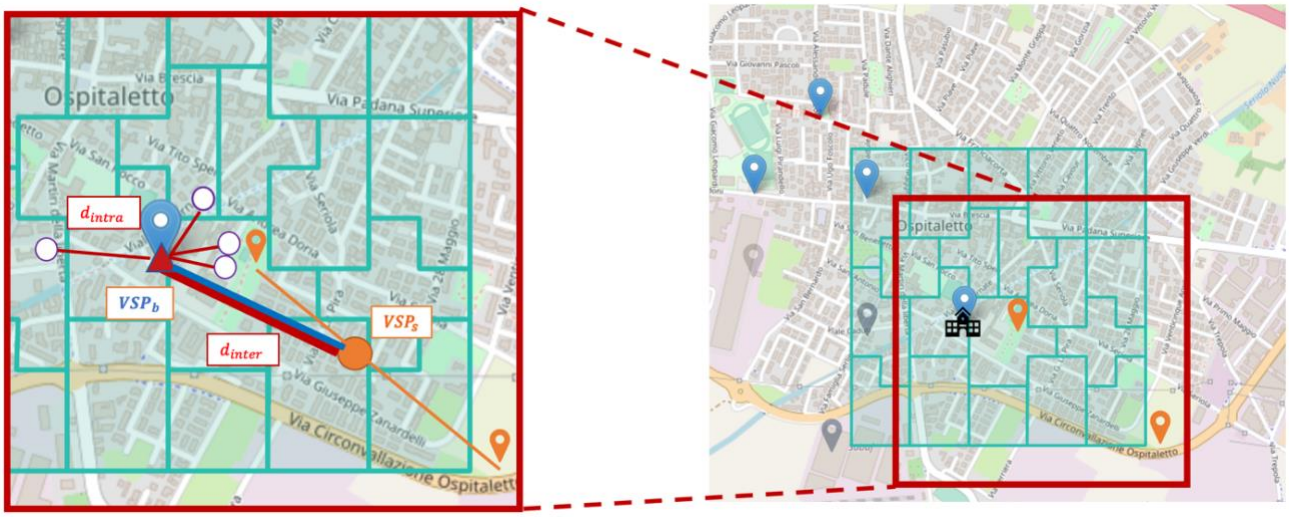

Figure 21. Theoretical representation of the network length required to connect SBs.

2.3.3 Thermal losses

The thermal losses and gains along the NT-DHC network assume a similar heat exchange of the carrier fluid with the ground as in closed horizontal GSHP systems. Due to the shallow depth of the network trench, the ground temperature is seasonally affected by the ambient temperature. The temperature of the ground around the network pipes (T_{gs}), was estimated according to a standard textbook formula [97][37] as a function of the time of the year t and the depth z below the ground surface:

$$T_{gs}(t) = T_{avg} - \Delta T_{amp} \exp\left(-z\sqrt{\frac{\pi}{t_{cyc}\,\alpha}}\right)\cos\left(\frac{2\pi}{t_{cyc}}(t - t_{min}) - z\sqrt{\frac{\pi}{t_{cyc}\,\alpha}}\right) \qquad 2.14$$

A curve that fits the data in a periodic manner is a typical problem in physics, in this case, it was applied a machine learning function in Python called "optimize-curve-fit" whose role is to apply non-linear least squares to fit a function of the type $T_{amb,fit}(t) = disp + amp \times \cos(t \times w - \emptyset)$ to some input data. The fitted curve then served as input for Eq. 2.14. The resulting ambient temperature fitting and the consequent ground curve are presented in Figure 22.

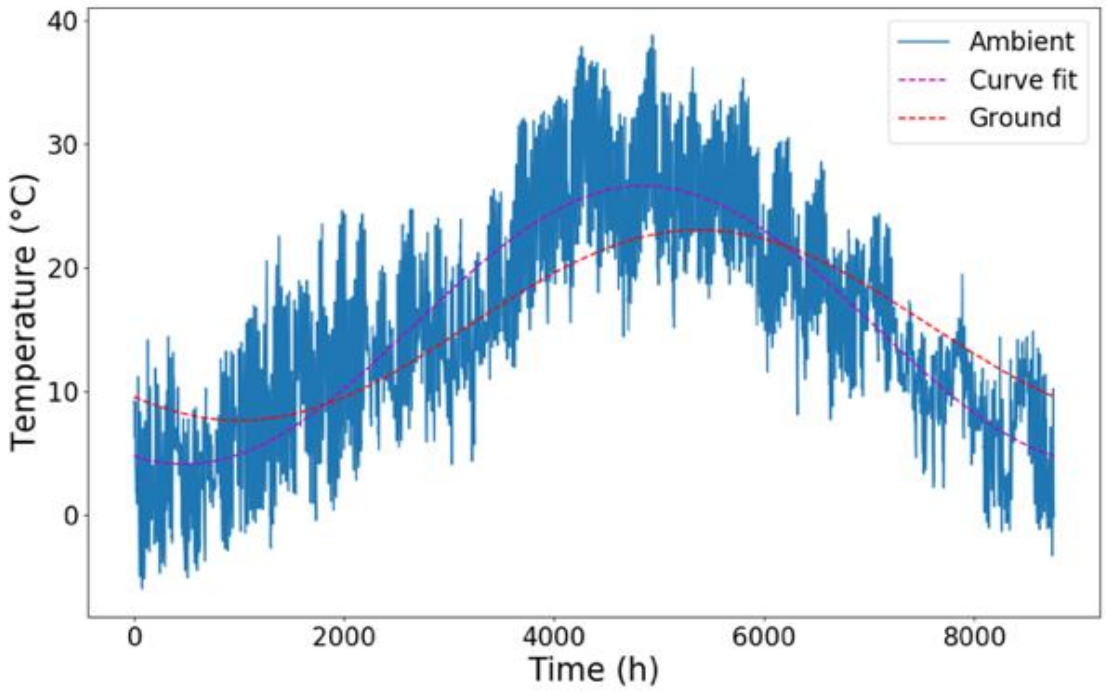

Figure 22. An illustration of the hourly ambient temperature (blue line), corresponding fitted curve (purple dashed line), and ground temperature (red dashed line). In this example, the data corresponds to the location of the case study presented in section 3.1.

The overall thermal losses on the supply ($E_{loss,s}$) and return ($E_{loss,r}$) pipes are estimated as a function of the following network characteristics: pipes lengths and diameters, pipes insulation properties given by an average overall heat exchange coefficient (U_{avg}), network supply ($T_{net,s}$) and return temperatures ($T_{net,r}$), and ground temperature:

$$E_{loss,s} = U_{avg} \times (T_{net,s} - T_{gs}) \quad 2.15$$

$$E_{loss,r} = U_{avg} \times \left(T_{net,r} - T_{gs}\right), \quad 2.16$$

$$U_{avg} = \sum_{i=1}^{n} \sum_{j=1}^{m} U_{pipe_{i,j}} \times L_{pipe_{i,j}}, \quad 2.17$$

A correction factor U_{CF} was introduced, with the aim of finding the best match with real thermal losses measurements. The default value before calibration is U_{CF} = 1.

$$E_{th,loss} = U_{avg} \times \left[\left(T_{net,s} - T_{gs}\right) + \left(T_{net,r} - T_{gs}\right)\right] \quad 2.18$$

$$E_{loss,CF} = U_{CF} \times E_{th,loss} \quad 2.19$$

2.4 Techno-economic model

2.4.1 Network heating and cooling modes

The temperature delivered to the buildings for SH purposes (T_{SH}) is estimated through a climate curve. This method assumes that the required SH level is in direct relation with the outdoor temperature (T_{amb}). This temperature is bounded within a minimum ($T_{min,i}$) and maximum ($T_{max,i}$) desired temperature that are reached based on a minimum ($T_{min,o}$) and maximum ($T_{max,o}$) outdoor temperatures. The climate curve is represented as:

$$T_{SH}(T_{amb}) = \begin{cases} T_{max,i} & if\ T_{amb} \leq T_{min,o}, \\ T_{min,i} & if\ T_{amb} \geq T_{max,o}, \\ m \times T_{amb} + b & otherwise \end{cases} \quad 2.20$$

$$m = \frac{T_{max,i} - T_{min,i}}{T_{min,o} - T_{max,o}} \quad 2.21$$

$$b = -m \times T_{min,o} + T_{max,o} \quad 2.22$$

Figure 23 displays the SH setpoints of four theoretical users in a NT-DHC network. The dashed red line represents the proportional interpolation of these values based on the amount of thermal power used by each user. The temperature required for domestic hot water (T_{DHW}) was set to 55°C by default. The network users' temperature requirements follow the same annual share of DHW and SH as that presented in section 2.2.3. In addition, the SH requirements follow the HDD distribution profile. Accordingly, applying the climate curve and the previous assumptions results in a curve whose monthly average pattern is shown in Figure 24. This curve should be viewed only as a representation of a particular case. Adaptations should be made to its application to other analyses according to climatic conditions influencing the energy share required for SH ($E_{\%sh}$), ambient temperature (T_{amb}) and building setpoints ($T_{min,i}$ and $T_{max,i}$).

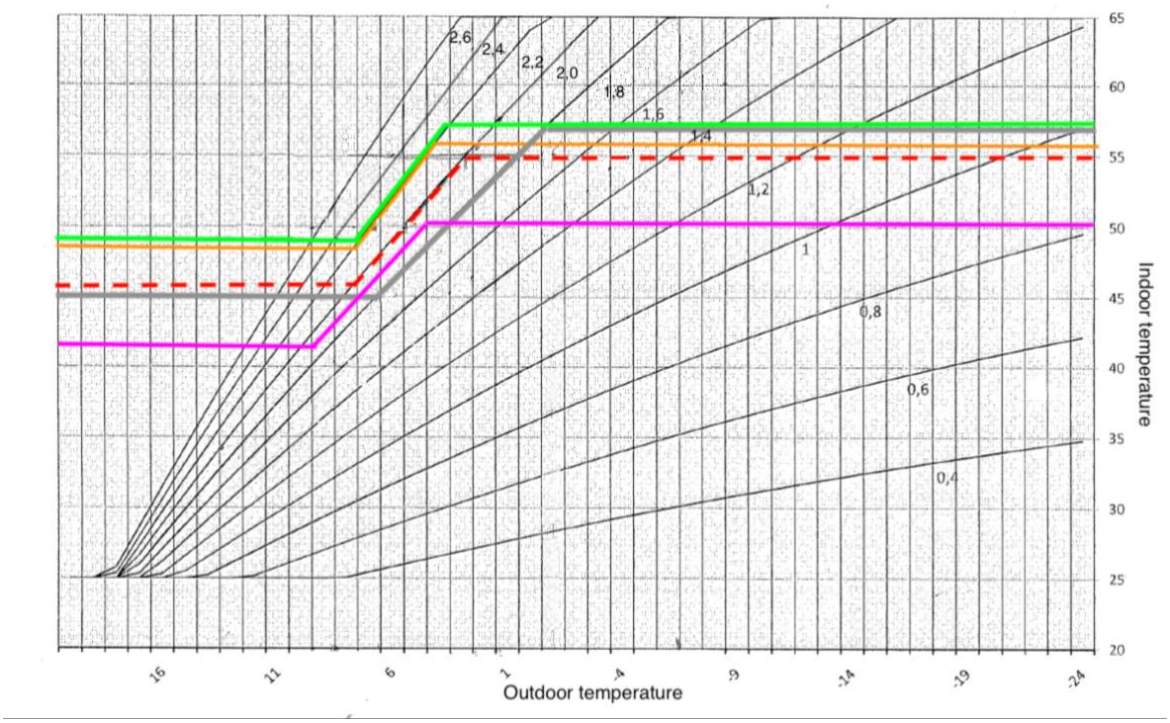

Figure 23. Climate curve implemented in the model. The red dashed line represents the temperature delivered to the buildings for space heating purposes.

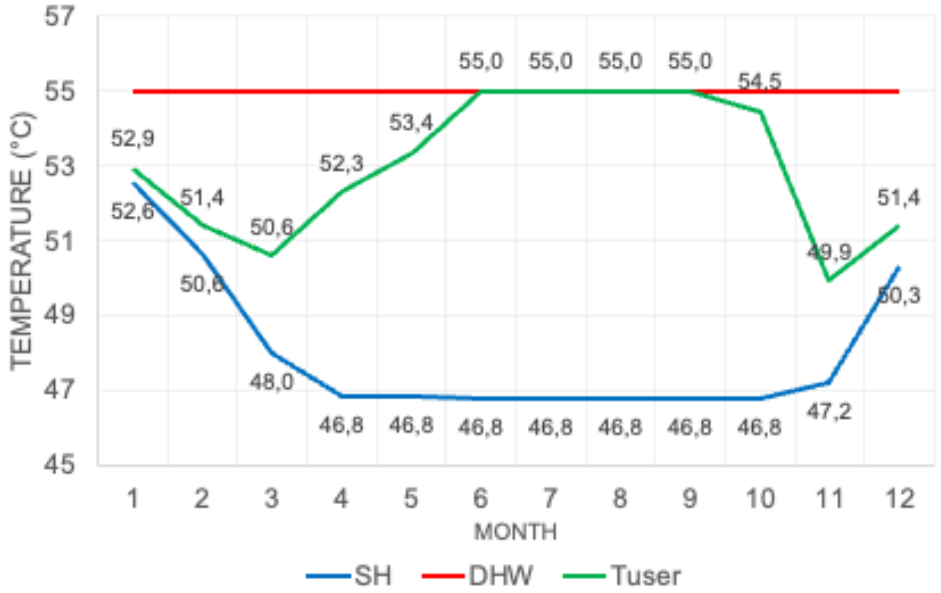

Figure 24. Monthly average HP condenser outlet temperature for the SH and DHW preparation.

2.4.2 NTDHC substation modeling

The HPs located on the users' substations work in parallel, with a variable operation depending on the load conditions. They are modelled in an aggregate manner, since the application of this tool is to be able to reproduce fast estimations of potential new DH extensions with a larger number of users, under conditions where H&C are supplied by the same network. Thus, equation *2.23* was selected from the literature [98] to represent a simplified physical understanding of the HPs pool performance. In heating mode, this COP function depends on the average temperature leaving the HPs' evaporators ($T_{e,o}$), whose values vary depending on the available sources' temperatures; and on the required temperature delivered to the users at the outlet of the HPs'condensers ($T_{c,o}$). In addition, a correction factor (η_{CF}) was included in this formula, to account for phenomenological inefficiencies of the modelled system due to other physical events beyond the scope of this analysis:

$$COP = 1 - \eta_m + \eta_m \times COP_C \quad 2.23$$

$$COP_C = \frac{T_c}{Tc - T_e} \quad 2.24$$

$$T_{c(e)} = T_{c,o(e,o)} \pm \Delta T_{HX} \quad 2.25$$

$$COP_{CF} = \eta_{CF} \times COP \quad 2.26$$

$$EER = COP - 1 \quad 2.27$$

COP_C corresponds to the Carnot COP, a function of the condenser T_c and evaporator T_e refrigerant temperatures. These variables were determined through the external fluid outlet temperatures at the evaporator and at the condenser ($T_{e,o}$ and $T_{c,o}$, respectively), adjusted by a temperature drop at the HP condenser and evaporator heat exchangers (ΔT_{HX}), assumed to be the same in both cases (Figure 25). The compressor efficiency η_m varies due to multiple factors such as the HPs model, size, and operating conditions. It was possible to retrieve both η_m and ΔT_{HX} from the suppliers' machine datasheets by fitting equations 2.23 to *2.26* yielding the values of 53% and 2.15 K, respectively. Other effects – like thermal losses in substation pipes and buffers, pumping consumptions on the users' side, differences between datasheet and real HP performances, losses due to HP on/offs, climatic curve inaccuracies, and measurement uncertainty – are comprised in the aforementioned η_{CF} factor. In the absence of

further information (e.g., a specific calibration, see below), the default value η_{CF} = 1 is used.

HPs operate in the opposite direction during cooling, with the condenser serving as a heat rejector on the network side of the HP (Figure 25b). EER (energy efficiency ratio) is the summer's coefficient of performance, obtained by applying *2.27*). During the summer season, the temperature on the user side is set to the maximum outlet temperature of 10°C. This constraint is based on the typical limits of W/W HPs used in residential applications[99]). In heating mode, the HPs outlet evaporator limits are 4°C and 18°C (although water-glycol mixtures could allow temperatures below zero), while temperatures as high as 60°C on the condenser outlet could make these HPs suitable for providing heat to conventional heating terminals such as radiators (Figure 26).

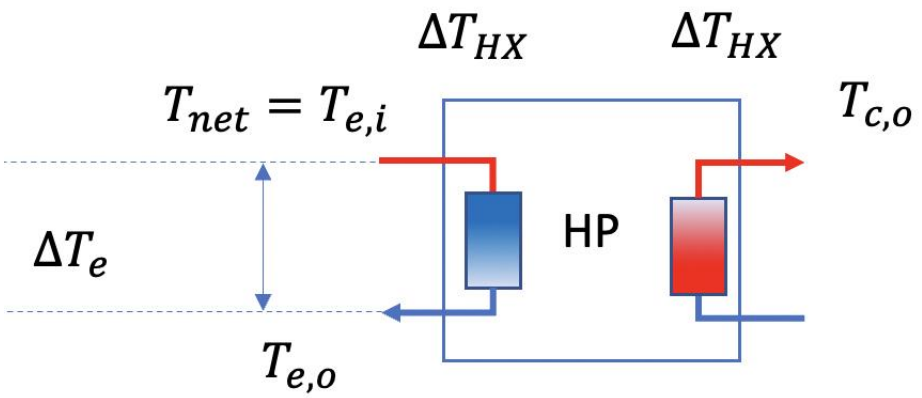

(a)

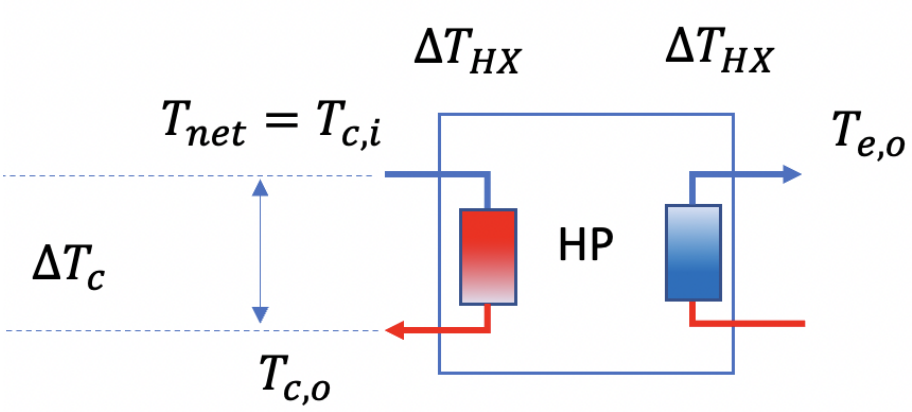

(b)

Figure 25. NT-DHC substation scheme. (a) Heating mode (b) Cooling mode

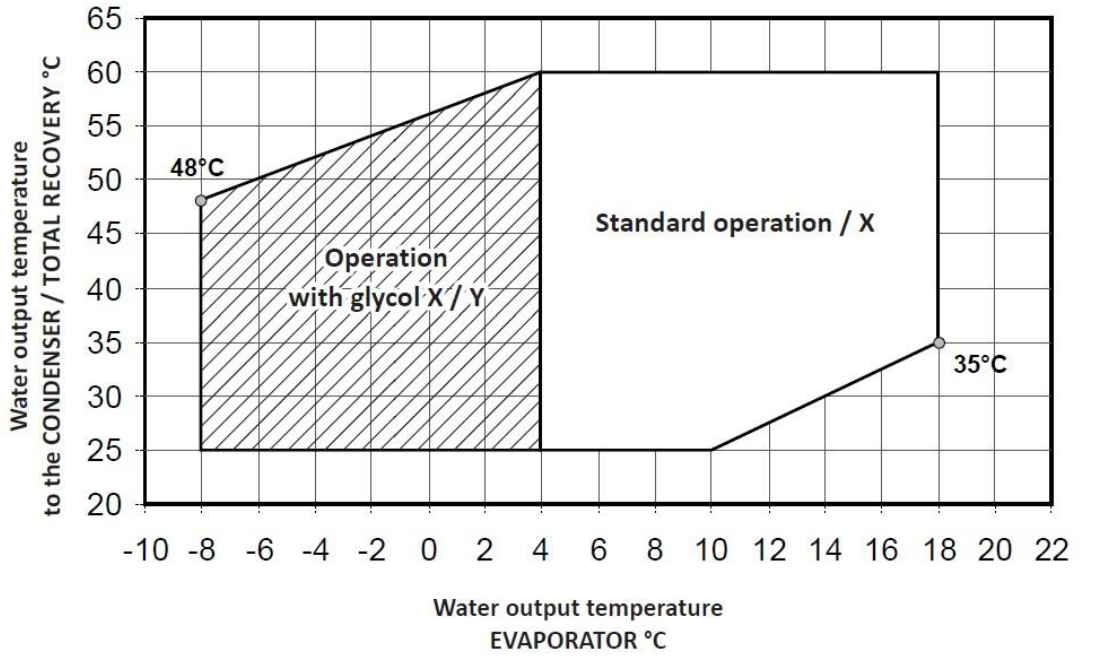

Figure 26. Operating limits of a residential W/W HP used at the EURAC laboratory (nominal heating power of 25-30 kW). The diagram shows the operating limits assuming a ΔT of 5K on the evaporator and condenser[99].

2.4.3 NT-DHC economic assessment

As opposed to the levelized cost of heat (LCOH) method commonly used in the DH literature for scenario analyses [30][100][101][102], the NT-DHC system can provide simultaneous heating and cooling through the same network, making the comparison among extension projects less straightforward. For this reason, the evaluation of total net present value (NPV) of each network extension is used as the economic indicator to measure the feasibility of a NT-DHC project.

The NT-DHC NPV is the present value of the future cashflows from the H&C sales of the NT-DHC operation at a required rate of return (r) compared to its initial investment. It is equivalent as calculating the return on investment (ROI). Converting all the future sales into today's euros and comparing with the initial investment, this indicator allows to decide whether a project is worthwhile or not.

The discount rate is company-specific, since it depends on how the funding is obtained. Generally, it is based on investors' expectations of return, or borrowing costs. The default rate of return in this assessment is assumed to be 3% unless otherwise specified. In the DHC sector, the most common business models are those owned completely by public entities, which accounts for the low rate[103]. In selecting this business model, the primary motivation is to ensure a positive impact that goes beyond

economic, but also social and environmental. This includes situations in which the economic profitability would not be enough to attract private capital despite its positive externalities.

Alternatively, the payback time (PBT) and internal rate of return (IRR) are common financial indicators when comparing projects. The advantage of NPV is that it accounts for the time value of money, it is additive (the total NPV of multiple projects is the sum of the corresponding NPVs), and it constitutes a fast and easy metric to compare an initial investment against the present value of the expected returns. In practice, this indicator is calculated for each potential extension scenario as follows:

$$NPV(r,N) = \sum_{n=1}^{N} \frac{\left(p_{heat} \times E_{th,h} + p_{cool} \times E_{th,c}\right) \times f_{inc} + C_{fix} - C_{NT-DHC}}{(1+r)^n} - I_{NT-DHC} \quad 2.28$$

where,

p_{heat}, p_{cool}= price of heating and cooling service sold through the NT-DHC network (€/MWh).

$E_{th,h}, E_{th,c}$= heating and cooling energy delivered to the network users (MWh/y).

f_{inc}= incentive factor over the energy price sold through the NT-DHC network (i.e., a factor of 1.2 would represent a 20% subsidy from a public entity. The default value is set to 1).

C_{fix}= fixed operation and maintenance fee.

C_{NT-DHC} =total annual costs of NT-DHC operation.

I_{NT-DHC} =NT-DHC investments (€).

The operating costs of a NT-DHC solution (C_{NT-DHC}) is subdivided into three components: operational expenses ($OPEX$), fixed operating and maintenance costs of reversible HPs (OM), and carbon emission costs (C_{tax}).

$$C_{NT-DHC} = OPEX + OM + C_{tax} \quad 2.29$$

$OPEX$ include all the expenses incurred by the network manager: variable costs of operating technologies such as electricity used by the HPs, auxiliary systems if any (auxiliary heater, chiller, or cooling tower), pumping consumptions and WH sources. WH recovery is assumed to be free in the default simulation, however, the model assigns a cost to this item for the user to explore different business models:

$$OPEX = E_{el,HP} \times p_{el,ind} + \sum E_{th,WH} \times p_{WH} + \sum E_{th,aux,j} \times \frac{p_{fuel,j}}{\eta_{tech}} \quad 2.30$$

OM are fixed operating costs incurred by the HPs substations. Equipment costs include all costs independent of the operation of the heating system, such as service agreements, spare parts, and insurance. Figure 27 shows the curve implemented in the model to estimate these costs. It was obtained by fitting the HPs data from the Danish Energy Agency database [104].

C_{tax} are carbon emissions costs. Based on the assumption that future use of heating systems will be taxed, the final customer is expected to pay this cost directly or indirectly based on the estimated emissions:

$$C_{tax} = c_{tax} \times f_{em,el} \times E_{el,HP} \quad 2.31$$

where,

$E_{el,HP}$ =HPs electricity consumption in H&C modes (MWh).

$p_{el,\text{ind}}$ =industrial electricity price (€/MWh).

$E_{th,\text{WH}}$ = WH supplied to the network (MWh).

p_{WH} = WH price (€/MWh).

$E_{th,\text{aux,j}}$ = thermal energy produced/rejected to/from the network by auxiliary system j (MWh).

$p_{fuel,j}$ =fuel price used by auxiliary system j (€/MWh).

η_{tech}= efficiency of the auxiliary system (MW_{th}/MW_{fuel}).

c_{tax} =carbon tax (€/t CO_2)

$f_{em,\text{el}}$ = Electricity emission factor, tCO_2/MWh

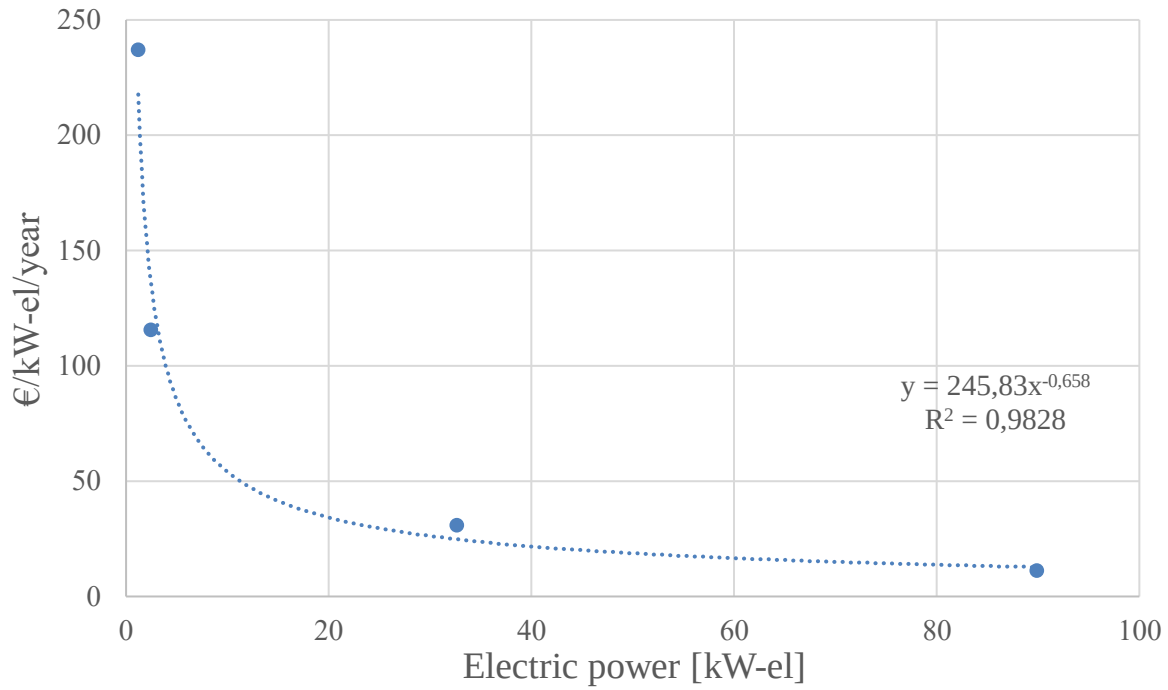

Figure 27. Fixed O&M costs of reversible HPs.

The investment in the NT-DHC solution (I_{NT-DHC}) consists of investment in the network (I_{net}), investments in reversible HPs substations (I_{HPs}), and investments in heat recovery on the production sites (I_{srcs}):

$$I_{NT-DHC} = I_{net} + I_{HPs} + I_{srcs} \quad 2.32$$

Investment in the network (I_{net}) is based on its length, diameter, and material costs. The distribution pipes conforming the intra-distance are made up of six categories of pipes of varying diameters. The fraction of each kind is scaled according to the maximum pipe diameter found in the network and is set according to standard network configurations[94]. However, these values can be customized if more information is available.

To estimate the network piping cost, the FLEXYNETS project's costs database of network pipes is used. Prices were retrieved from a Danish manufacturer of DH pipes for three types of pipes (called SERIES 1, SERIES 2, and SERIES 3, respectively). Installation prices, on the other hand, are determined by Swedish experience in groundwork. The network pipe composition, default scaling

factors, and piping prices are shown in Appendix A.2.

In addition, the investment in the network backbone (I_B) assumes the maximum pipe diameter required. About 55% of the total network cost is expected to come from the backbone, which is sized according to the peak conditions.

$$I_{net} = \left(\sum_{i=1}^{6} L_{pipe}(D_{i,}) \times p_{pipe}\right) + I_B \quad 2.33$$

$$D_i = \sqrt{SF_i \times D_{max}^2} \quad 2.34$$

$$L_{pipe}(D_i) = d_{intra} * L_{share}(D_i) \quad 2.35$$

$$p_{pipe}(m, dist) = p_{pipe,m} + p_{ins,dist} \quad 2.36$$

where,

D_i = average pipe diameter (mm) of category i ($i = 1, \dots, 6$).

SF_i =scaling factor related to pipe category i.

D_{max} = maximum pipe diameter (mm).

L_{pipe} = pipe length (m).

d_{intra} =total length composing the network intra distance (m).

$L_{share,d_{i,avg}}$ = fraction of the network of category i with diameter $D_{i,avg}$.

p_{pipe} = total piping costs (€/m).

$p_{pipe,m}$= piping costs with average diameter D_i and material m (€/m).

$p_{ins,dist}$=piping installation costs with diameter D_i in a new or existing district (€/m).

The specific investment in reversible heat pumps Inv_{HPs} was calculated using fitting data from the Danish Energy Agency database as presented in Figure 28 (red line). Rather, the blue line was retrieved from the FLEXYNETS database and obtained by applying a discount factor. It assumed that the HPs costs in Italy are slightly lower than the Danish case. The total investment is calculated as a function of the installed capacity ($Q_{max,HP}$). In [94] two alternative methods are described. In the first, the user specifies the peak electric power absorbed by a single building's HP, and then calculates the cumulated

peak power by multiplying the single HP by the number of buildings. In this model, however, the number of buildings is unknown. Therefore, the second method was chosen. The second method consists of calculating the peak electric power absorbed by the HPs in H&C modes and applying a user-defined safety factor (SF) for oversizing and diversity factor (DF) as shown in equation:

$$I_{HPs} = Inv_{HPs} \times Q_{max,HP} \quad 2.37$$

$$Q_{max,HP} = max\left(\frac{E_{th,h}(t)}{COP} + \frac{E_{th,c}(t)}{EER}\right) \times \frac{SF}{DF} \quad 2.38$$

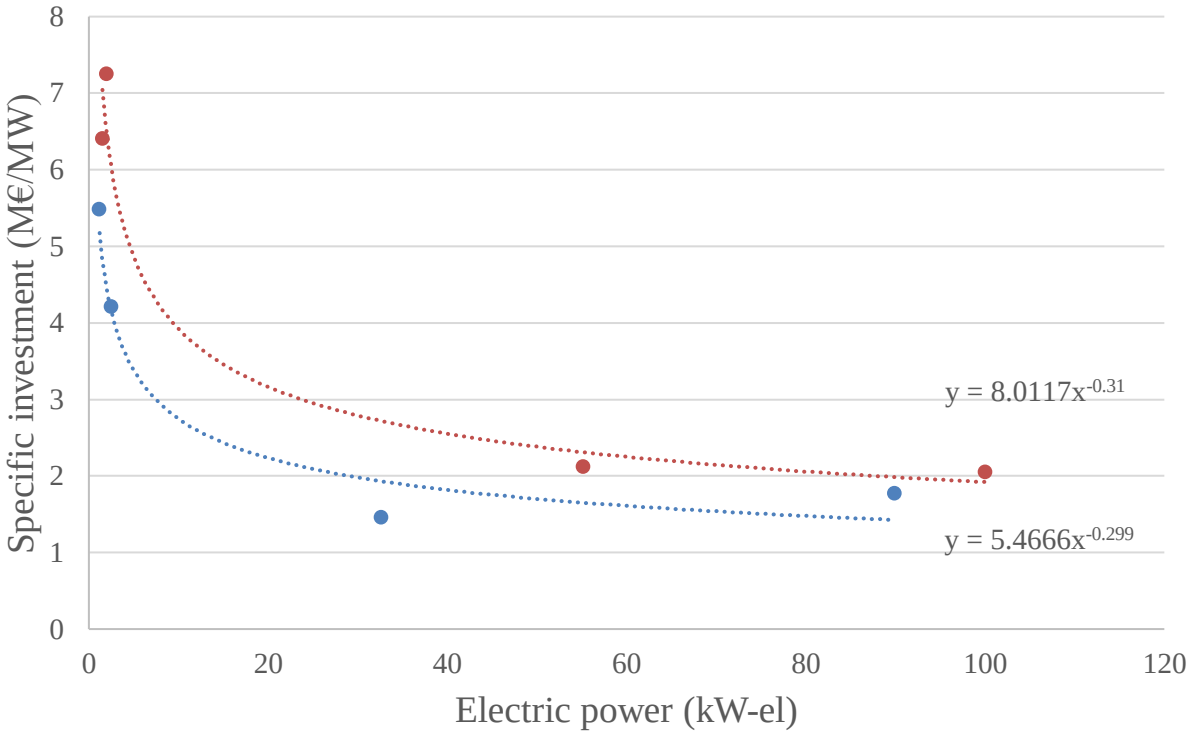

Figure 28. Reversible HPs specific investments [104]

2.4.4 Individual solutions costs

In this study, the primary motivation in choosing technologies to benchmark is to compare with the most common H&C systems in the residential market, and to compare with a similar distributed technology based on HPs, however, one that does not require a network for delivery. The following scenarios are investigated:

- Individual systems scenario: Heat demand is met by individual gas boilers and cooling demand by individual split units. Also studied in [99][58].
- A/W HPs scenario: H&C demand supplied by means of reversible air to water heat pumps (A/W HPs)

The gas boiler costs data comes from the Danish Energy Agency catalogue (DEA)[104]. This catalogue contains data from EU28 countries. As an alternative to gas boilers, it is also possible to select another technology from the following list if the user is interested in exploring another option:

- Heat pump air-to-air, air-to-water and brine-to-water
- Electric heating
- Bio-oil boiler
- Oil boiler
- Biomass boiler automatic and manual
- Wood stove
- Solar heating

The technology data is based on the type of building (single-family house or apartment building) and the renovation status (new or existing). There are four time horizons: 2015, 2020, 2030, and 2050.
In this model, the user must manually select these values, so that the factors ($k1_{inv}$, $k2_{inv}$, $k1_{fixed_{OM}}$, $k2_{fixed_{OM}}$) for each technology can be determined. Table 21 from Appendix A.3 shows the filtered data available for gas boilers, assuming the costs for an existing apartment building (MFH) and 2020 reference year.
The total costs of an individual heating system consist of four components: the annualized capital expenditures ($CAPEX_{ind}$), the fixed operating and maintenance costs (OM_{ind}), the variable operational expenses (OP_{ind}) and the carbon emissions costs ($C_{tax,ind}$):

$$C_{ind} = CAPEX_{ind} + OM_{ind} + OP_{ind} + C_{tax,ind} \quad 2.39$$

$CAPEX_{ind}$ correspond to the investment in the heating system, and OM_{ind} covers all costs not directly related to the operation of the system, including maintenance, service agreements, spare parts, and insurance, if any. Both are functions of the maximum thermal peak of the heated area under evaluation ($Q_{max,ind}$). Based on the hourly thermal heating demand (E_{th}), technology efficiency (η_{tech}), and an oversizing factor (SF), the latter is calculated as follows:

$$Q_{max,ind} = max\left(\frac{E_{th}}{\eta_{tech}}\right) \times SF \quad 2.40$$

$$CAPEX_{ind} = k1_{inv} \times Q_{max,ind}^{1+k2_{inv}} \times \alpha_{r,l} \quad 2.41$$

$$OM_{ind} = k1_{fixed_{OM}} \times Q_{max,ind}^{1+k2_{fixed_{OM}}} \quad 2.42$$

where,

$k1_{inv}$= constant factor for the investment costs.
$k2_{inv}$= exponent for the investment costs.
$k1_{fixed_{OM}}$= constant factor for the fixed operating and maintenance costs.
$k2_{fixed_{OM}}$= exponent for the fixed operating and maintenance costs.
$\alpha_{r,l}$= annualization factor, function of interest rate r and technology lifetime l.

OP_{ind} correspond to the energy costs (based on an energy price p_{fuel}) associated with running the technology:

$$OP_{ind} = p_{fuel} \times \frac{E_{th}}{\eta_{tech}} \quad 2.43$$

$C_{tax,ind}$ are carbon emissions costs. Based on the assumption that future use of fossil-based heating systems will be taxed, the final customer is expected to pay this cost directly or indirectly based on the estimated emissions:

$$C_{tax,ind} = c_{tax} \times f_{em,fuel} \times \frac{E_{th}}{\eta_{tech}} \quad 2.44$$

Even if the $CAPEX_{ind}$ is underestimated by considering the aggregated thermal peak load, this should not affect the total individual heating costs since this is mainly driven by the energy costs (OP_{ind}) as shown in Table 5. The levelized cost of heat (LCOH) was calculated as C_{ind}/E_{th} for three loads with different thermal peak, using the default data (factors for Italy, from Table 21). It was assumed a gas price of 100 €/MWh:

Table 5. Individual heating (gas boilers) cost structure example

Cluster	**Heat demand [MWh]**	**Thermal peak [MW]**	$\boldsymbol{CAPEX_{ind}}$ **[%]**	$\boldsymbol{OM_{ind}}$ **[%]**	$\boldsymbol{OP_{ind}}$ **[%]**	$\boldsymbol{C_{tax,ind}}$ **[%]**	**LCOH [€/MWh]**
1	1560	1.29	1.48	0.54	85	13	117.5
2	555	0.27	2.73	1.16	83.5	12.6	119.5
3	2741	1.33	1.41	0.42	85.2	12.9	117.3

The total costs of cooling technologies are divided into four components similar to those for heating technologies; the annualized capital expenditures ($CAPEX_{ind,c}$), the fixed operating and maintenance costs ($OM_{ind,c}$), the variable operational expenses ($OP_{ind,c}$) and the carbon emissions costs ($C_{tax,ind,c}$):

$$C_{ind,c} = CAPEX_{ind,c} + OM_{ind,c} + OP_{ind,c} + C_{tax,ind,c} \quad 2.45$$

In contrast with the method previously used for the $CAPEX_{ind}$ and OM_{ind} of heating systems, the same database provides the specific investment costs and fixed operating and maintenance cost factors (both expressed in €/kW) of the following cooling systems:

- Small split units (<5 kW)
- Big split units (>5 kW)
- Medium chillers (A/W) (<400 kW)
- Large chillers (A/W) (>400 kW)
- Medium chillers (W/W) (<400 kW)
- Large chillers (W/W) (>400 kW)

Using this information, $CAPEX_{ind,c}$ and $OM_{ind,c}$ are calculated as a function of the cumulative cooling capacity ($Q_{max,c}$). The EER is estimated based on equation *2.27*. In the cooling case, it is assumed that $T_{e,o}$ is the expected cooling temperature delivered on the building side (set at 10°C but customizable), and T_c corresponds to the ambient temperature:

$$CAPEX_{ind,c} = Inv_{cool} \times Q_{max,c} \times \alpha_{i,l} \quad 2.46$$

$$OM_{ind,c} = OM_{cool} \times Q_{max,c} \quad 2.47$$

$$Q_{max,c} = max\left(\frac{E_{th,c}}{EER}\right) \times \frac{SF}{DF} \quad 2.48$$

where,

Inv_{cool}= specific investment in cooling machines (€/kW).
OM_{cool} =fixed operating and maintenance cost factor (€/kW).
$Q_{max,c}$= cumulative cooling capacity (kW).
EER= cooling efficiency.
SF= safety factor for oversizing.
DF= diversity factor. This factor considers that the highest sum of powers coincidentally delivered by the machines of a system is still lower than the sum of the installed powers of the devices unless there is a perfect simultaneity in their operation. This diversity factor is set to 0.34 in [94]; however, the model user can modify it.
$\alpha_{r,l}$= annualization factor, function of interest rate r and technology lifetime l.

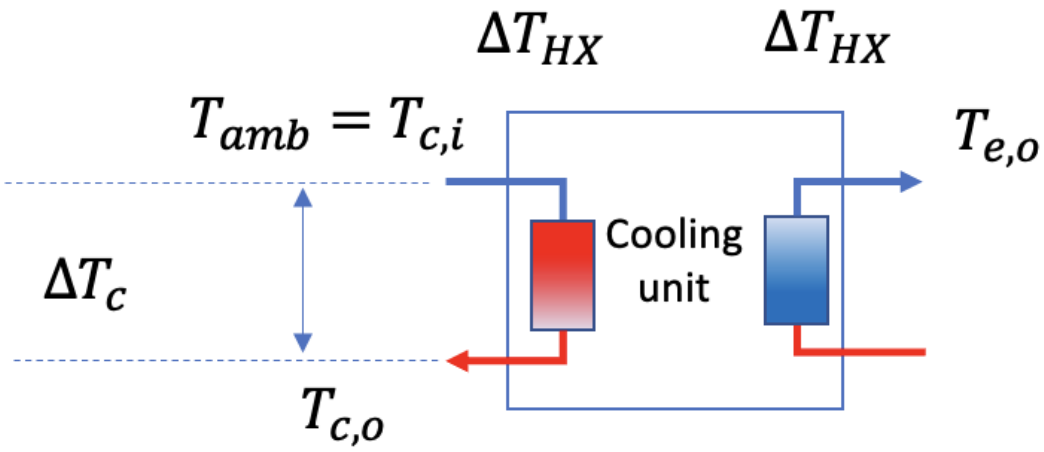

Figure 29. Scheme for the competing air-sourced solution

$OP_{ind,c}$ correspond to the electricity costs (based on the residential electricity price $p_{el,res}$) associated with running the cooling technology:

$$OP_{ind,c} = p_{el,res} \times \frac{E_{th,c}}{EER} \quad 2.49$$

The carbon emission costs ($C_{tax,ind,c}$) of this competing solution are directly related to the emissions associated with the electricity production, so the costs are calculated as follows:

$$C_{tax,ind,c} = c_{tax} \times f_{em,el} \times \frac{E_{th,c}}{EER} \quad 2.50$$

Finally, the costs associated with the competing solution of reversible A/W HPs are composed by the annualized capital expenditures ($CAPEX_{ind,AW}$), the fixed operating and maintenance costs ($OM_{ind,AW}$), the variable operational expenses ($OP_{ind,AW}$) and the carbon emissions costs ($C_{tax,ind,AW}$):

$$C_{ind,AW} = CAPEX_{ind,AW} + OM_{ind,AW} + OP_{ind,AW} + C_{tax,ind,AW} \quad 2.51$$

$CAPEX_{ind,AW}$ correspond to the annualized investment costs in reversible A/W HPs ($I_{ind,AW}$), which is estimated applying equations *2.37* and *2.38*. The COP and EER of A/W HPs are calculated using the same method as the NT-DHC substation described in subsection 2.4.2. However, in H&C modes,

the inlet temperature to the HP is the ambient temperature instead of the network temperature. It is assumed the same cost curve presented in Figure 28, unless more information is available.

$$CAPEX_{ind,AW} = I_{ind,AW} \times \alpha_{r,l} \quad 2.52$$

$OM_{ind,AW}$is assumed to be calculated analogously to the NT-DHC system. A residential price for electricity ($p_{el,res}$) is assumed similarly to individual cooling units:

$$OP_{ind,AW} = p_{el,res} \times \left(\frac{E_{th,h}}{COP_{AW}} + \frac{E_{th,c}}{EER_{AW}}\right) \quad 2.53$$

The carbon emission costs associated with the operation of A/W HPs ($C_{tax,AW}$) are based on the electricity used, hence this emission factor is used:

$$C_{tax,AW} = c_{tax} \times f_{em,el} \times \left(\frac{E_{th,h}}{COP_{AW}} + \frac{E_{th,c}}{EER_{AW}}\right) \quad 2.54$$

2.5 Optimization

2.5.1 Knapsack approach

The knapsack approach is a direct way to explain how investment decisions can be made in potential network extensions with a limited number of WH sources and loads each with a maximum thermal power (MW) to be covered and an economic value (the NPV estimated in € as described in subsection 2.4.3). This is the most common version of the knapsack problem, called the 0-1 knapsack. Its application dates back to 1896 and has been considered for over a century[105].

The adaptation of the knapsack problem to this case consists of n items, each with a weight w and value v. The objective is to identify a subset of the n items that maximize the overall value of the knapsack:

$$Maximize \sum_{i=1}^{n} v_i \, x_i \quad , \, n \, items$$

The total weight of the n items (or total thermal power) cannot exceed the capacity W (or maximum WH potential expressed in MW):

$$subject \, to \sum_{i=1}^{n} w_i \, x_i \leq W$$

The candidates to be incorporated into the knapsack are either included or excluded:

$$x_i \in \{0,1\}$$

Evaluation will be limited to those items that add value to the overall knapsack (only those extensions whose NPV has a positive outcome):

$$v_i \geq 0 (i = 1, \dots, n)$$

Finally, based on the clustering process described in subsection 2.2.2, the items must be smaller than the knapsack to avoid trivial solutions:

$$w_i < W (i = 1, \dots, n)$$

The knapsack problem is considered to be NP and a hard optimization problem [106]. A trivial attempt to solve it would be to make an exhaustive search of all 2^n possible subsets of n items. A brute force

approach to solving this problem would require more than 30 years if 60 items are considered, assuming that a computer runs 1 billion vectors per second. This is because when increasing the number of items by one, the number of possible combinations doubles.

In 1952, however, Bellman was the first that introduced the dynamic programming approach to solve the 0-1 knapsack problem [107]. Using dynamic programming, each of the smaller subproblems is solved once, and the results are recorded in a table, rather than solving overlapping subproblems repeatedly. This table is then used to solve the original problem. The classical dynamic programming approach works bottom-up [108].

Dynamic programming obtains a better running time compared to a brute force approach (also called naïve algorithm) since its time complexity is O(nW) vs. $O(2^n)$[109]. The pseudo-code of the algorithm is presented in Figure 30.

```
Knapsack
{
   for (w = 0 to W)
        V[0, w]=0;
   for(j = 1 to n )
        for (w = 0 to W)
          if (w[j] <= w)
             V[j,w]=max{V[j -1, w],v[j] + V[j -1, w-w[j]]}
          else
             V[j, w]= V[j -1, w]
  return V[n.W];

}
```

Figure 30. Pseudo-code of the dynamic programming algorithm to solve the 0-1 knapsack problem[106]

The computational effort to solve the network extension problem depends on the number of periods selected and the number of items to optimize. Figure 31 shows an example with three consecutive knapsack problems solved in steps. The evaluation of the NPV of each item is linear (the current non-optimized version of the techno-economic model takes 0.2 s). After the value of each item has been calculated, the average time to solve a knapsack problem is 0.05 s. Appendix A.4 contains the Python

script [110] which was adapted for this application.

Finally, it is worth noting that this approach fits well with NPV as a KPI choice to measure value. In the knapsack approach, the optimal selection is determined by exploring the cumulative benefits of a group of projects. Other economic indicators that are not absolute value measures, such as the IRR, cannot be summed to represent the value of a portfolio of projects. Alternatively, this could be viewed as a limitation of the model since this approach tends to prioritize large clusters with larger absolute economic margins, whereas other economic indicators such as IRR may provide additional information on the relative benefit of individual investments (it may exist that a small investment creates a higher relative return as opposed to a large investment).

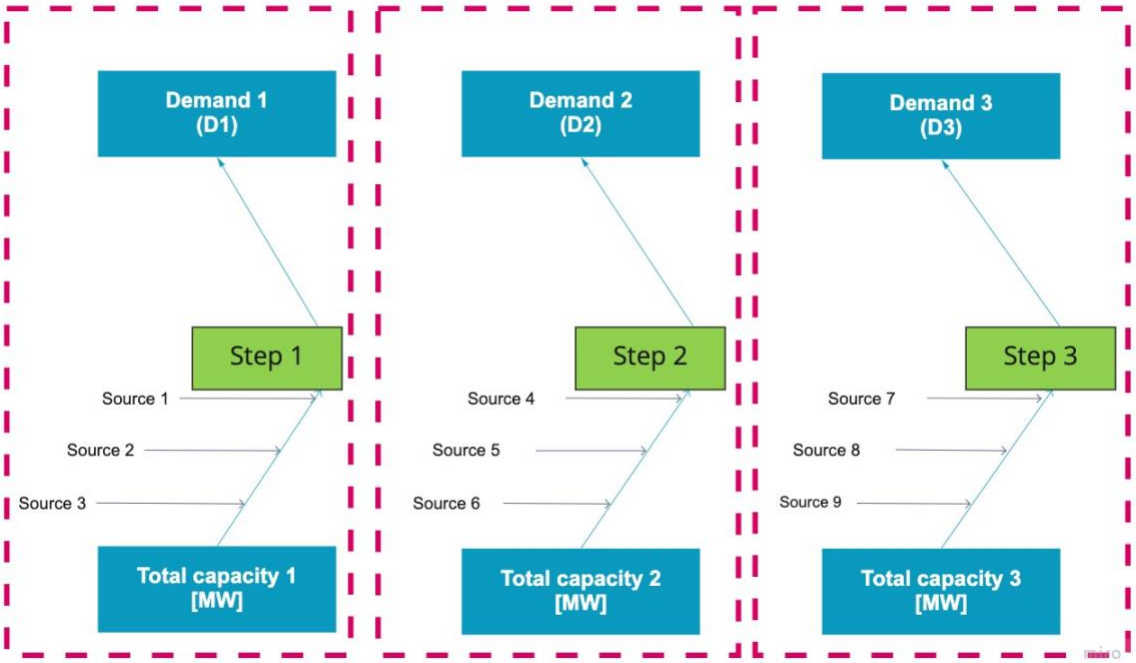

Figure 31. Three extension scenarios formulated as consecutive knapsack problems. The algorithm, given a total capacity, identifies the best subset of loads that can join the system in a first step. By considering the remaining loads, a second subset is identified that can optimally join the network. The process can be repeated as many times as necessary.

2.6 Conclusion

In this chapter, it is presented in detail a new methodology for the TEA of NT-DHC systems and the identification of future spatial expansion scenarios. The model simulations are executed with an hourly resolution, allows the integration of multiple WH sources, thermal availability, and temperature. The network control allows the implementation of specific operation strategies based on sources' merit order.

In the beginning of the chapter, spatial and heat density inputs are presented through an open-source mapping tool. A discussion is held about the key aspects to consider when planning a network expansion, and how this leads to load aggregation through clustering. A comparison of clustering algorithms is presented, and a test was conducted to find the most suitable for this type of application. The network model proposes two types of network components: the intra-cluster distance, corresponding to the service pipes required to connect buildings within a cluster/group of SBs; and the inter-distance, the primary network backbone that connects the sources with the loads. In this framework, the first category is calculated using literature-supported methods, whereas the second (star-like approach) is a novel addition to the whole methodology. Hydraulic and network sizing calculations are supported by previous research in the DHC sector.

This method allows for a comprehensive TEA suitable for scenario analysis through its cost database. It is presented the main equations for estimating energy and investment costs of both NT-DHC and H&C benchmark solutions.

By the end of the chapter, a knapsack approach is proposed for solving the optimal expansion problem of a NT-DHC system. A mathematical formulation of the 0-1 knapsack problem in the DHC context is provided. The computational advantages are discussed and its limitations.

Consequently, this approach extends the State of the Art by modeling the performance of a network system based on decentralized HP substations, as well as incorporating economic factors that are not considered in DH physical models and optimizing the selection of the best system extension.

3

Verification and calibration

This chapter has been presented in the following publications:

M. Cozzini, S. Calixto, S. Buffa, and R. Fedrizzi, “Reti di teleriscaldamento e teleraffrescamento basate su pompe di calore decentralizzate,” *AICARR J.*, vol. 60[58].

M. Cozzini, R. Fedrizzi, S. Calixto, and G. Manzolini, “Modelling of an Existing Neutral Temperature District Heating Network: Detailed and Approximated Approaches,” presented at the Sustainable Development of Energy, Waterand Environment Systems, Cologne, Germany, 2020[66].

S. Calixto, M. Cozzini, and G. Manzolini, “Modelling of an Existing Neutral Temperature District Heating Network: Detailed and Approximate Approaches,” *Energies*, vol. 14, no. 2, Art. no. 2, Jan. 2021[67].

S. Calixto, C. Köseoğlu, M. Cozzini, and G. Manzolini, “Monitoring and aggregate modelling of an existing neutral temperature district heating network,” presented at the The 17th International Symposium on District Heating and Cooling, Nottingham Trent University, Nottingham, United Kingdom, Sep. 2021.[68].

S. Calixto, C. Köseoğlu, M. Cozzini, and G. Manzolini, “Monitoring and aggregate modelling of an existing neutral temperature district heating network,” *Energy Rep.*, vol. 7, pp. 140–149, Oct. 2021[69]

This chapter will focus on the base TEA model for NT-DHC network scenario analysis (represented as a yellow box in Figure 6). It is based on the approach of an Excel tool developed within the FLEXYNETS project [94]: the tool's objective was to carry out feasibility studies on implementing the NT-DHC concept under different scenarios. The model has a lumped parameter approach: all the network users are considered a single aggregated load. A single representative day per month time-slicing is used for all profiles. The thermal sources consist of only WH plants. This feature was a limitation when introducing multiple thermal sources/sinks with different temperature levels in the study of the intra-week synergies that affect the performance of an NT-DHC network.

It was first used for the scenario analyses related to implementing a NT-DHC that provides H&C services to a FU located in a typical Mediterranean area (Rome climate was chosen as a reference) with different availability levels of neutral-temperature WH. A parametric analysis was carried out to compare the conditions in which the performance of a DH system of this kind is more competitive than a traditional network and individual solutions. The results show an economic margin for the applicability of NT-DHC solutions, with an important role played by cooling [58].

The base model approach (also called “lumped model”) was verified with a physical model and monitored data from a real NT-DHC network located in Ospitaletto, Italy, as stated in the first specific objective of this project. The results were presented in [66] and then published in [67]. Some upgrades to the initial model consisted of implementing an average climatic curve to estimate temperature levels required for SH on the buildings' side (as described in subsection 2.4.1) and a more accurate system Coefficient of Performance (COP) function (see subsection 2.4.2).

The validation with experimental data was presented in [68], and then published in [69]. By the end of this chapter, an improved version of the initial aggregate model had been translated into Python, and the upgrades described in Table 2 had been implemented.

3.1 Case study

The NT-DHC network in Ospitaletto, Italy, began operating in the fall of 2018. It extracts heat from two sources (industrial WH and aquifer wells at about 25 °C and 15 °C, respectively). The users are mainly schools, all endowed with HPs substations, which raise the temperature to 55 °C, with variations depending on the balance between space heating (SH) and sanitary hot water (SHW) production. The network extends around 2 km, built with primarily non-insulated pipes, a simple tree structure, and a conventional 2-pipe system. The layout is shown in Figure 32a, along with the location of the users and sources (industrial waste heat and aquifer wells corresponds to source 1 and 2, respectively). In this approximate model, the aggregated thermal load of all the network users is shown in Figure 32b (with a pattern of 24 h for each month).

The four users correspond to rather different sizes, with thermal powers (on the condenser side of the HPs) in the range of 300-800 kWth. With the operating temperatures, the COP is expected to be around 4-5. The thermal power on the network side (i.e., at the HP evaporators) is correspondingly lower than the power on the user side.

The aggregated hourly load profile (sum of the four users) shown in Figure 32b served as input for the physical model. This profile was estimated as follows:

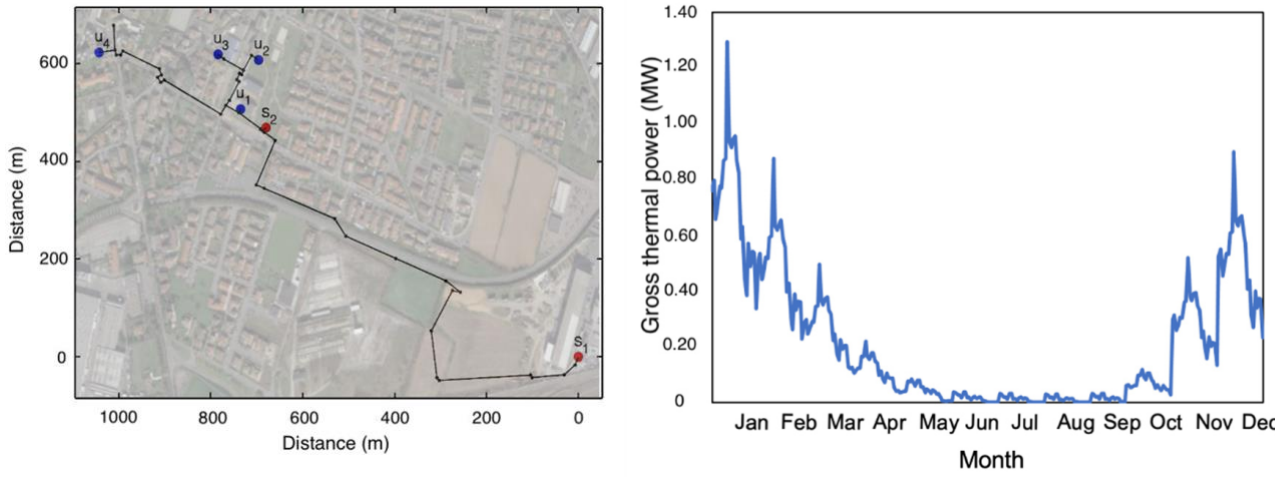

(a) (b)

Figure 32. (a) Network outline. The red markers display the sources, and the blue markers the users. Distances are measured from source s1. s = sources and u = users. (b) Aggregated load profile of all the network users for 1 year (2019) with a time resolution of one single day per month.

- Monthly consumptions were known from (approximately) weekly readings available at each user for year 2019.
- Single day consumptions were then estimated by distributing monthly consumptions proportionally to heating degree days, which in turn were calculated from the ambient temperature data retrieved by a nearby weather station.
- Hourly consumptions were finally obtained by assuming fixed patterns for space heating (SH) and sanitary hot water (SHW). The SH pattern was built by averaging the available high-frequency data measured in a few winter days. Sanitary hot water (SWH) consumptions, assumed basically constant daily throughout the year, were estimated from summer weeks, with a random pattern in the interval 06:00-23:00.

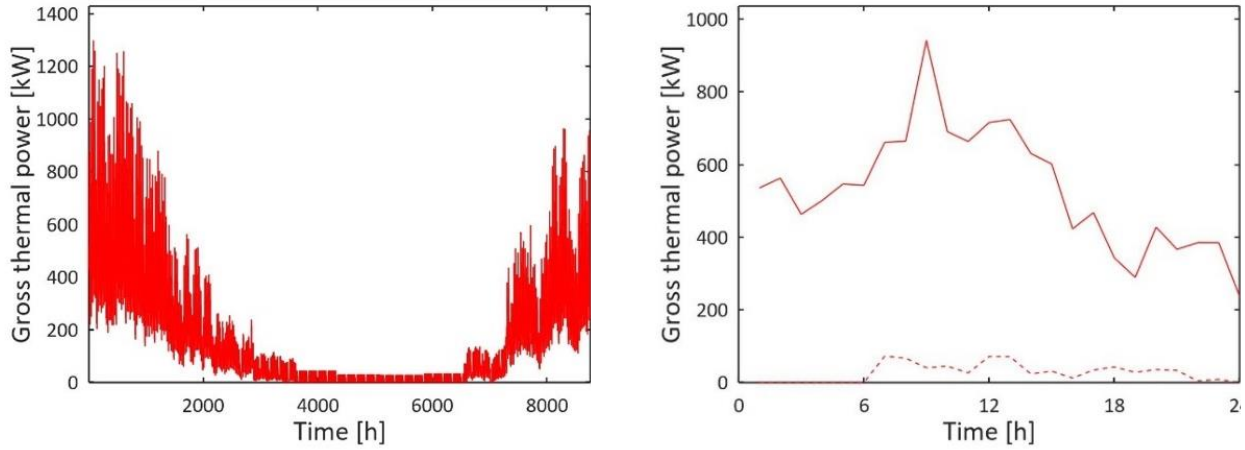

(a) (b)

Figure 33. Aggregated user load profiles (condenser side of HPs). (a) Aggregated hourly load profile for 1 year (2019); (b) Aggregated hourly profile for a typical winter day (16 January 2019). Solid line: overall load; dashed line: SHW only.

The second source, operating when waste heat is not available, is provided by aquifer wells, pumping ground water in an open loop from a depth of about 40 m. The supply temperature is mostly constant throughout the year and equal to 15 °C (corresponding to the average ambient temperature, as seasonal fluctuations do not affect the ground at this depth).

The temperature of the ground around pipes (T_{gs}), which is important to calculate the network heat losses, was calculated as described in subsection 1.2.2. Whenever $z \neq 0$, an exponential decay factor and a delay term appear in equation 2.14, both depending on the ground thermal diffusivity α, which

is here assumed to be 7×10^{-7} m^2/s[37]. The network pipes are at a depth of about 1 m and the corresponding calculated ground temperature is represented by the black solid line in. One can recognize the smaller amplitude and the delay (depending on ground capacity) with respect to the approximated surface temperature (as seen in Figure 22). Due to the exponential term, oscillations quickly decrease with depth, converging towards $T_{gs} \simeq T_{avg}$.

The thermal losses were estimated as described in subsection 1.2.2. The supply-return network temperature was assumed to be at a constant 5 °C difference. As the network geometry and pipes characteristics were known, all the material properties were obtained from data sheets.

The model also includes economic inputs (e.g., investment costs, energy prices, interest rates), which are however not discussed here.

The model main outputs provide:

- HP electricity consumptions
- Thermal energy delivered by the network (on the evaporator side of the HPs)
- Thermal losses
- Pumping consumptions
- CO_2 emissions

For this analysis, several default options of the original model were modified according to the input list provided above. Moreover, the COP function and the formula for pumping consumptions were updated.

3.2 Verification with a physical model

The physical model used here was developed by EURAC within the LIFE4HeatRecovery project. It is coded in Octave (preserving compatibility with MATLAB), and it describes the hydraulic and thermal dynamics of the network. The network geometry is implemented as a graph, with vertices positioned according to Figure 32a. Hydraulic boundary conditions are provided by flow rates at user vertices (which are calculated from the user load profiles assuming a constant supply-return temperature difference of 5 °C, controlled by regulating valves at HP substations) and by the pressure at a reference vertex. Thermal boundary conditions are provided by source temperatures. The hydraulic part is solved independently from the thermal part by using Kirchhoff laws at network nodes. The relation between pressure losses Δp and flow rate F is assumed to be of the type

$$\Delta p \propto F^n \tag{3.1}$$

while pump control basically assumes a fixed pressure difference. The solution of the thermal part depends instead on the hydraulic solution, as it uses a one-dimensional heat transfer equation which depends on velocity (and neglects thermal diffusion), namely [111]

$$(\partial_t + v\partial_x)\, T = -\frac{T - T_{gs}}{\tau} \tag{3.2}$$

where T is the fluid temperature, T_{gs} is the ground temperature around the pipes, v is the fluid velocity, and τ is a time constant. The latter is related to the overall pipe heat loss coefficient U (which can be found in pipe data sheets or can be calculated with standard formulas on the basis of pipe geometric data and material thermal conductivities) by $\tau = \rho\, c_p\, \pi\, (D/2)^2/U$, where D is the pipe diameter and ρ and c_p are respectively the water density and specific heat. Solution of Eq. *3.2* can be written as

$$T(t,x) = T_{gs} + \left[T\left(t_0, x - \int_{t_0}^{t} v(t')\, dt'\right) - T_{gs}\right] e^{-(t-t_0)/\tau} \tag{3.3}$$

where t_0 is some initial time. Exploiting this semi-analytical solution, the outlet temperature of a pipe section can be calculated as a function of the inlet temperature at previous times. In practice, this was implemented by coding in MATLAB the analogous of the Modelica spatialDistribution() function[112].

The main inputs of the detailed model correspond to the list provided for the approximate model, though they of course need to be more detailed. In particular:

- A load profile for each single user needs to be provided.
- All profiles are included as full hourly profiles.

Indeed, while the detailed model can in principle be run with any time step, for this analysis simulations were carried out with an hourly time step for a full year (i.e., 24 h × 365 = 8760 h). Flow rates, pressures, and temperatures are available at each vertex at any time step.

The comparisons could only be carried out on the aggregated values and at monthly level, given that these are the spatial and temporary scales of the approximate model. The overall thermal consumptions on the user side are clearly the same for both models, as these are inputs. However, differences can be expected in the overall electric consumptions of the HPs (due to different detail levels in the calculation

of the network and user temperatures) and consequently on the network heat flows. Moreover, significant differences could exist for thermal losses and pumping consumptions, given the very simplified assumptions used in the approximate model.

Integrating energies monthly, it is possible to get the consumptions used for the comparison. Electric and evaporator energies for the HPs are shown in Figure 34. These are crucial quantities for this type of networks, where the operating consumptions of HPs provide a major contribution to costs and carbon emissions (through electricity). One can see that the two models are in reasonable agreement. The COP function used in the two cases is the same, however the network-side and user-side temperatures are different:

- Network-side temperature: the approximate model uses a constant temperature given by the weighted average of the source temperatures, while the detailed model uses the temperature derived from the propagation of the time-dependent source temperatures along the pipes (considering all thermal losses).
- User-side temperature: the approximate model uses an average climatic curve, while the detailed model uses the actual climatic curves of the single users.

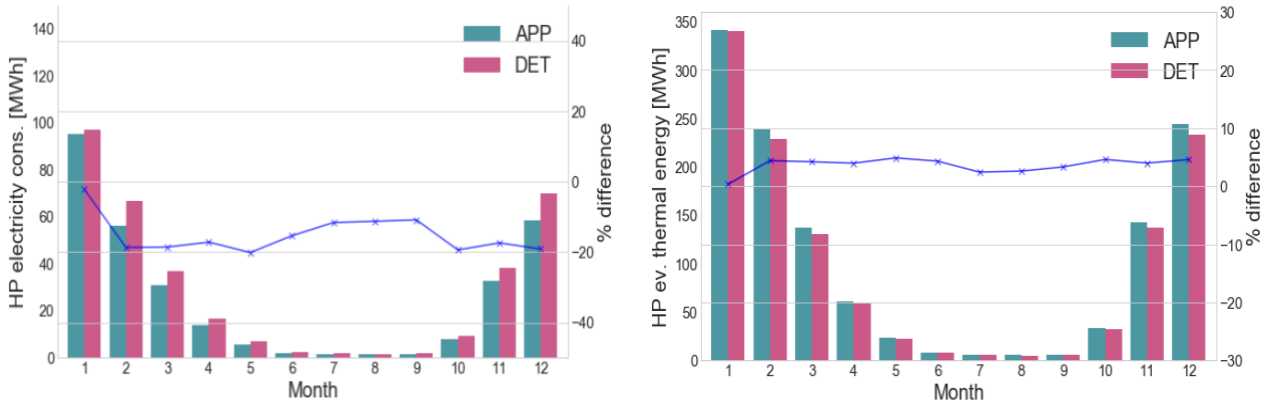

(a) (b)

Figure 34. Aggregated monthly energy balances for user substations. The blue curve (right axis) in both figures represents the percentual difference of the approximate model with respect to the detailed model. (a) Electric consumptions of HPs.; (b) Heat absorbed from the network (i.e., at HP condenser).

The energy delivered on the HP condenser side, assuming an adiabatic system, is the sum between the HP electric consumptions and the heat absorbed on the evaporator (i.e., network) side. Taking the ratio between the condenser side heat and the HP electricity, one can get an average COP. This is reported

in Figure 35a. One can see that the approximate model estimates a higher COP than the detailed model. This is mainly due to the higher temperature assumed at the evaporator side.

Concerning thermal losses, the predictions of the two models are reported in Figure 35b. The approximate estimate is typically higher than the detailed one. A major difference appears in summer. Here the approximate model estimates the presence of significant thermal gains, as the ground temperature can be higher than the network temperature, especially when waste heat is not available. The approximate model calculates gains and losses based on this temperature difference, regardless of the network operation. In the detailed model, losses and gains are calculated considering the network operation: during the long summer periods without significant demand, in the detailed model the network temperature reaches equilibrium with the ground temperature and no further heat exchange occurs. On the other hand, during winter the thermal losses predicted by the two models show similar values, showing that the general network structure assumed by the approximate model reasonably applies to this case. Similar conclusions can be reached based on pumping consumptions, where the predictions of the approximate model are about 50 % higher than the detailed model.

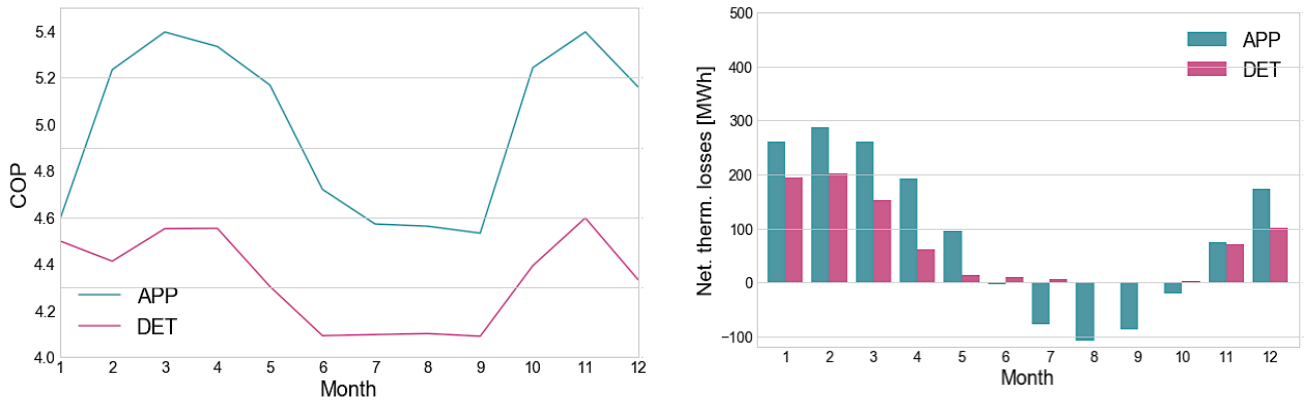

(a) (b)

Figure 35. a) Monthly values for HP COP; (b) Network thermal losses

Regarding the overall yearly performance of the network, one has the results reported in Table 6. Here, it is observed the seasonal COP (SCOP), corresponding to the average HP COP, the yearly thermal energy supplied at the condenser side of the HPs ($E_{th,HP,c}$), corresponding to the user consumptions provided as an input, the yearly thermal energy at the evaporator side ($E_{th,HP,e}$), corresponding to the energy delivered by the network at user substations, the yearly electric energy consumed by HPs ($E_{el,HP}$), the network thermal losses ($E_{th,loss}$), the electricity consumptions for network pumping

($E_{el,pump}$), and, finally, the carbon emissions calculated from overall electric consumptions ($E_{el,HP} + E_{el,pump}$) multiplied by an emission factor of 0.327 tCO_2/MWh_{el}, estimated for the production mix of the Italian electric grid in Ref.[113].

Table 6. Yearly performances and energy balances for the two considered models

Quantity	Unit	Approximate model	Detailed model
SCOP	arb.u.	5.0	4.5
$E_{th,HP,c}$	MWh/y	1558	1559
$E_{th,HP,e}$	MWh/y	1249	1206
$E_{el,HP}$	MWh/y	309	350
$E_{th,loss}$	MWh/y	1045	816
$E_{el,pump}$	MWh/y	38	20
CO_2	t/y	113	121

In this work, models provided results in reasonable agreement: a 15% difference in the overall electricity consumed by the HPs (Figure 36). According to the approximate and detailed models, the estimated thermal losses to the ground were 46% and 40%, respectively, due to uninsulated pipes. According to both models, the pumping consumptions were 2% of the total thermal energy delivered at the HPs' evaporators.

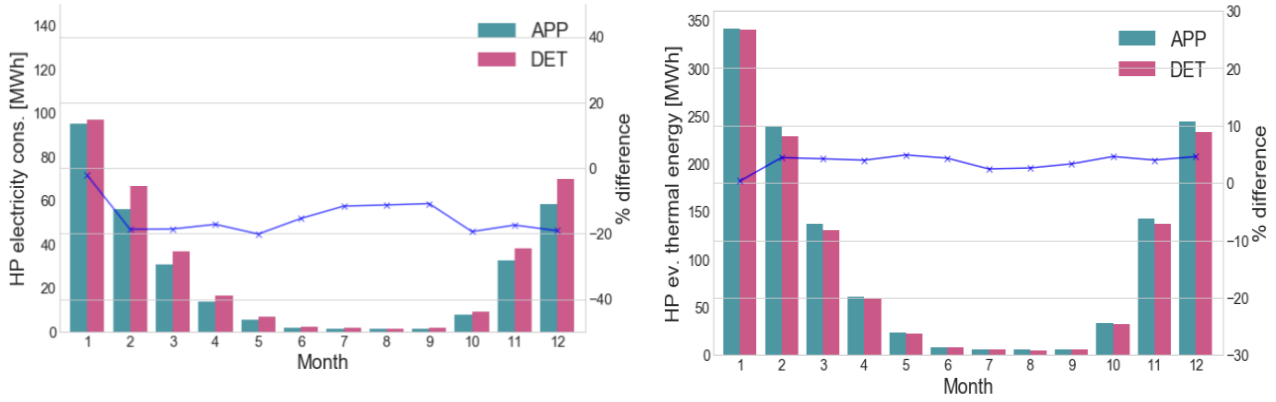

(a) (b)

Figure 36. Aggregated monthly energy balances for user substations result from comparing the approximate (APP) and detailed (DET) models. (a) Electric consumptions of HPs; the blue curve

represents the percentual difference between the two models. (b) Monthly consumption retrieved from quasi bi-weekly data made in 2019. Monthly users' demand and HP electricity consumptions are measured at the condenser side of the HP. Curves show the cumulative energy.

As mentioned above, HP electric consumption, heat absorbed by HPs from the network, and average COP are all closely linked, and discrepancies between the two models are explained by the different temperature values. The detailed model also does not consider some effects: substations are very simplified and transient effects in the operation of multiple HPs are not considered.

Thermal losses results (without calibration) are very strong even at such low temperatures, due to the use of non-insulated pipes. The detailed model indicates that 40 % of the heat injected into the network (via waste heat and aquifer wells) is lost in the ground (46 % according to the approximate model, considering a compensation between gains and losses occurring at different times of the year). In the network considered, waste heat is abundant and free: choosing non-insulated pipes can reduce investment costs without affecting operating costs. In other cases, however, it might be more convenient to use pre-insulated pipes (possibly with the thinnest thicknesses available).

Both models estimated relatively low pumping consumption despite a temperature difference of only 5°C between supply and return. According to the detailed model, the electric energy needed for pumping is about 1.7% of the thermal energy delivered at the HP evaporators (or about 1.0 % of the thermal energy injected at the sources), whereas according to the approximate model is almost twice as high. This is related to the sizing of pipes diameters. The discrepancy between the two models is rather high in this case. Additionally, improvements would be needed for the detailed model, which is currently neglecting some losses (e.g., head losses at pipe geometric changes), resulting in a likely underestimation of the actual values.

Carbon dioxide emissions are directly related to electric consumption in this case. In fact, this is the only non-renewable energy source in this type of network. To properly estimate the sustainability of this type of district systems most attention should be devoted to the proper modeling of HPs and to the proper calculation of network and users' temperatures, to obtain an accurate estimation of COP.

Finally, it is useful to report about the numerical performance of the two approaches. While the execution of the approximate model is basically immediate, the detailed model requires about 30 min to solve the considered network (about 50 vertices) for a full year with hourly time steps on a standard laptop with a quad-core CPU. This reveals the differences between the two kinds of models: while intermediate approximation levels could be chosen, a detailed model would be impractical for parametric analysis or optimization, where the model needs to be solved for hundreds or thousands of times.

3.3 Calibration with experimental data

The model was then translated into Python to improve its flexibility. The lumped approach was preserved, but time-slicing was abandoned, upscaling the time analysis at an hourly level for an entire year. This also allowed the introduction of a simplified storage modeling, whose satisfactory implementation was previously prevented by the discontinuities created by time slicing, even though not required for this case study. Figure 37 shows some representative results (not reported in [67]) for a slight variation of the current Ospitaletto case, assuming cooling is included.

Following the cross-verification in [67] of the approximate and detailed models, real data validation was undertaken. The utility that runs the Ospitaletto network made available weekly/biweekly data for 2019 (Figure 38) and hourly data for 2020. Hourly data for 2020 also included specific measurements (temperatures and flow rates at different points of the network). Unfortunately, due to the Covid-19 emergency, the overall operation of 2020 is far from being representative (schools were closed from early March until the reopening in September). Hence, to analyze the overall network performance a mixed approach was used: the yearly performance analysis was based on 2019 data, while the detailed analysis of single aspects (e.g., daily profiles and thermal losses) was carried out using selected 2020 data.

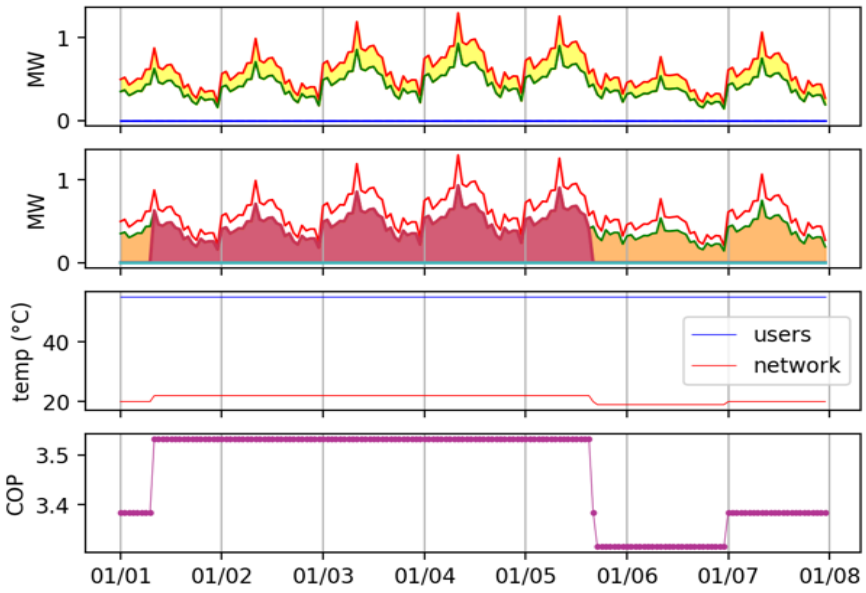

(a)

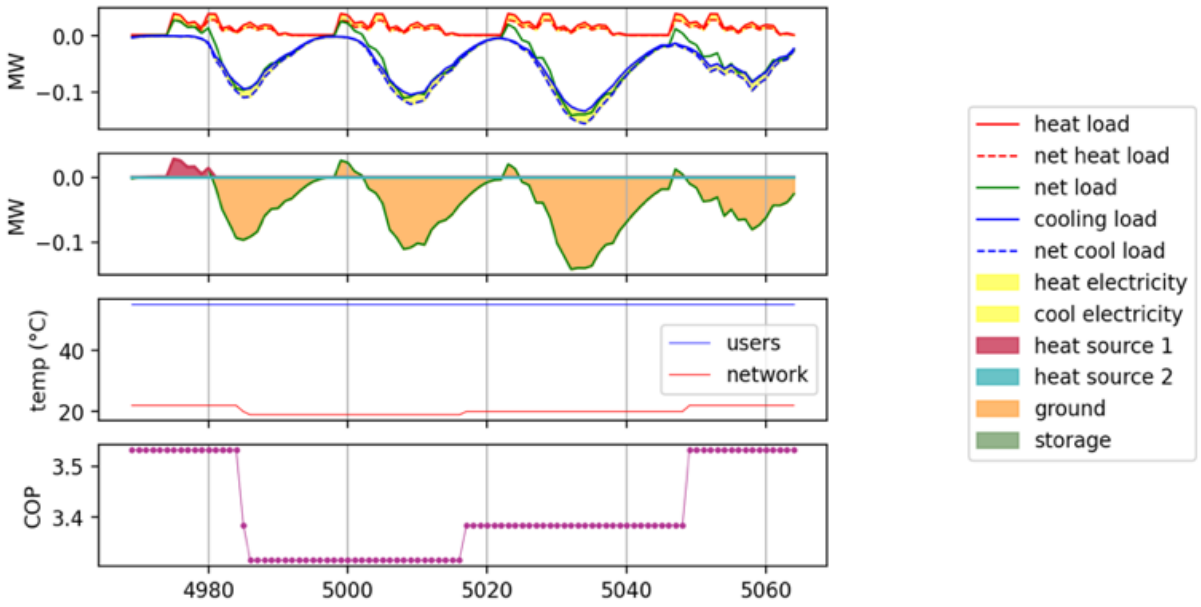

(b)

Figure 37. Model outputs corresponding to the energy balance estimated in a scenario for the Ospitaletto network. (a) One representative winter week. (b) One summer week, including space cooling and heating for SHW.

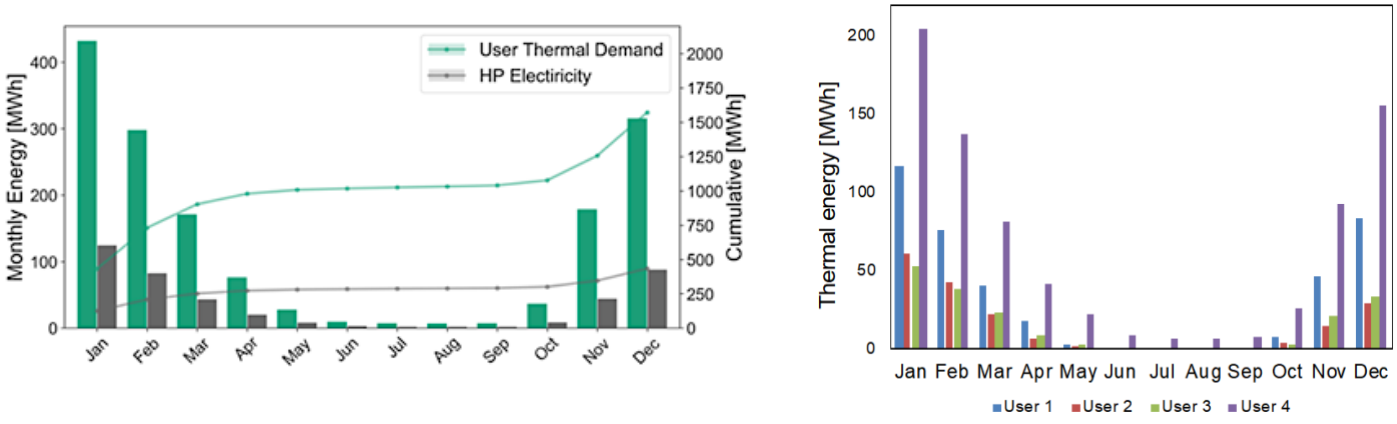

(a) (b)

Figure 38. a) Estimated monthly consumption from quasi-biweekly measurements in 2019. Users' monthly thermal demand and HP electricity consumptions are measured at the HP's condenser side. (b) Monthly thermal demand by user.

Data from 2020 was used to carry out a more detailed analysis, in which different temperature conditions in the network are shown in Figure 39. These conditions highly depend on the sources' availability. The most common situation in this case study occurs when source 1 ($s1$) is active (refer to Figure 32 for positions). The peak is at about 25°C. The supply temperature on position $s2$ (where the pumping station and the aquifer wells are located) has a peak at about 23°C, and the return temperature in the same position has a peak at 18°C. On the weekends, the network is tempered to a 15°C supply and 11°C return levels when the industry is off. Finally, Figure 39c shows the overall temperature distributions at the pumping station (for all source cases). The supply-return temperature difference is of the order of 5 K, in reasonable agreement with the expected HP control.

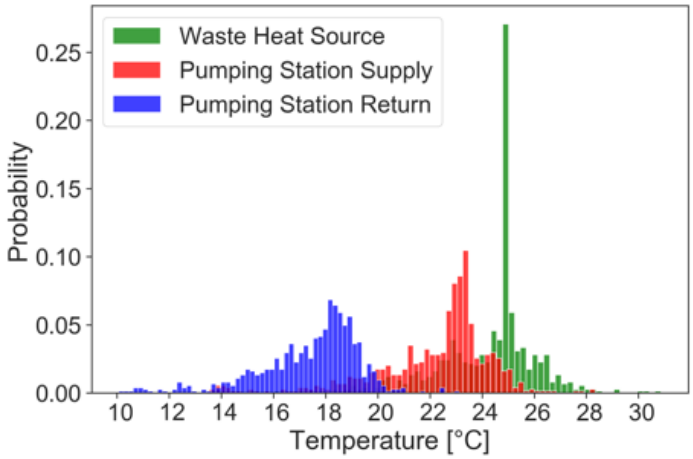

(a)

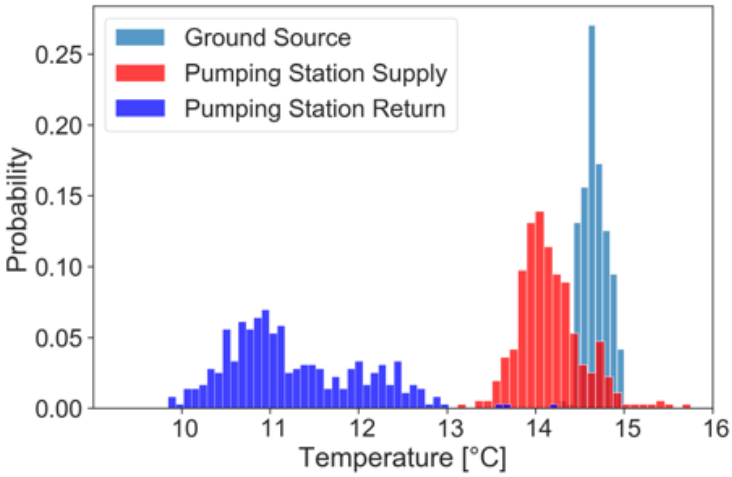

(b)

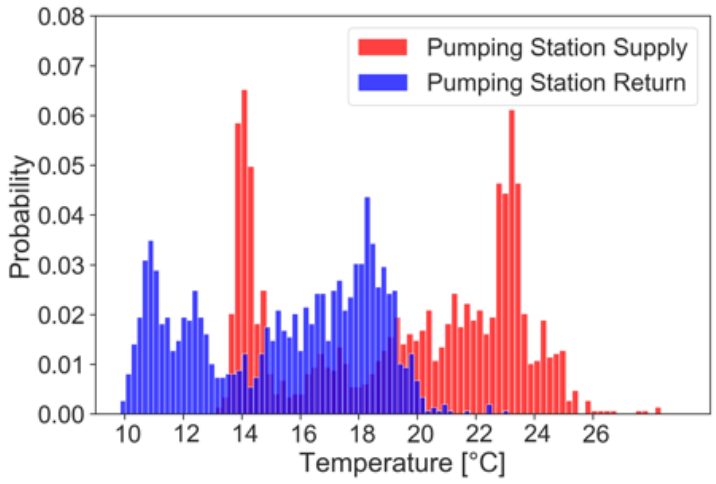

(c)

Figure 39. Temperature distribution in different points of the network for different operating conditions. (a) Distribution when source s_1 is active; (b) Distribution when source s_2 is active; (c) Overall distribution at the pumping station. January-March 2020 data.

To understand the consumers' consumption behavior, it is worthwhile to differentiate summer and winter operation, since this corresponds to the difference between SHW and SH operating conditions, respectively. HPs are modeled according to a climatic curve, so their COP is influenced by the ambient temperature and the type of demand. Figure 40a shows the typical distribution of SHW throughout the day. The profiles correspond to a few days of May 2020 (18^{th}-23^{rd}). During the night, all users have a much lower consumption (zero for Users 1-3 and schools only). From 06:00 to 23:00, a random pattern can be observed instead. The observed order of magnitude of SHW is expected to hold for most of the year, so it is possible to estimate the SH demand by subtracting the estimated SHW from the overall measured consumption. Figure 40b analyses SH demand and their relationship with heating degree days (HDD): A linear relationship is observed (hourly data are used for the period January-March 2020, so any errors associated with the SHW estimate are of less significance). This result suggests that a reasonable interpolation of the weekly/biweekly data of 2019 at a daily level can be done based on HDD. A typical daily SH profile can also be retrieved using the 2020 hourly data for interpolation at an hourly level.

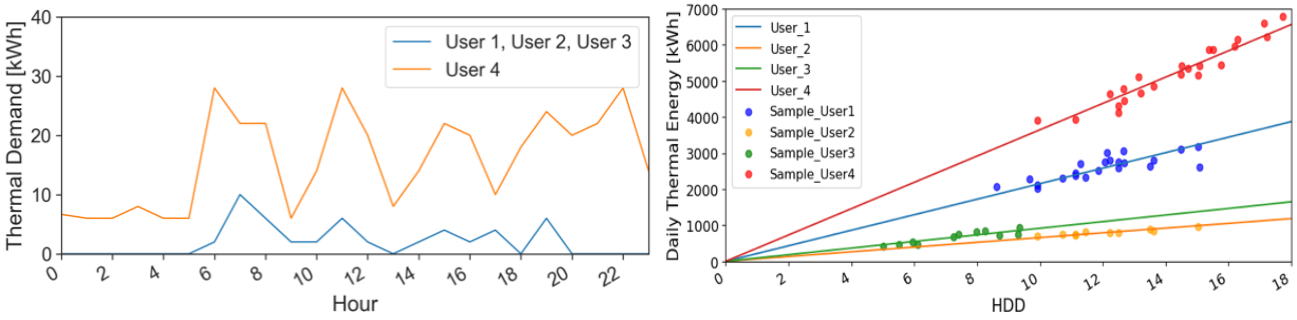

(a) (b)

Figure 40.(a) Sanitary hot water profile of all the users. (b) Linear regression between thermal energy and heating degree days.

The analysis of the 2020 data was used to interpolate 2019 data at an hourly level. Heat demands, measured in the user substations condenser side (E_{th,tot,h,u_i}), are the sum of the heat used for SHW preparation (E_{th,SHW,h,u_i}) and SH (E_{th,SH,h,u_i}). In summary, assuming that the daily total heat demand for SH is proportional to HDD ($C_{user_i} \sim E_{th,SH,d,u_i}/HDD$), a proportionality constant (C_{u_i}) is estimated from linear regression applied to HDD and daily SH demand bas on data collected from Jan 2020 to Nov 2020. As a result, it was possible to estimate the daily SH heat demand for 2019, which is then distributed according to the users' hourly relative profiles as shown in Figure 41. Using the data collected between February 2020 and March 2020, relative profiles are generated, assuming the schools are operating normally and have not been affected by Covid-19 related measures.

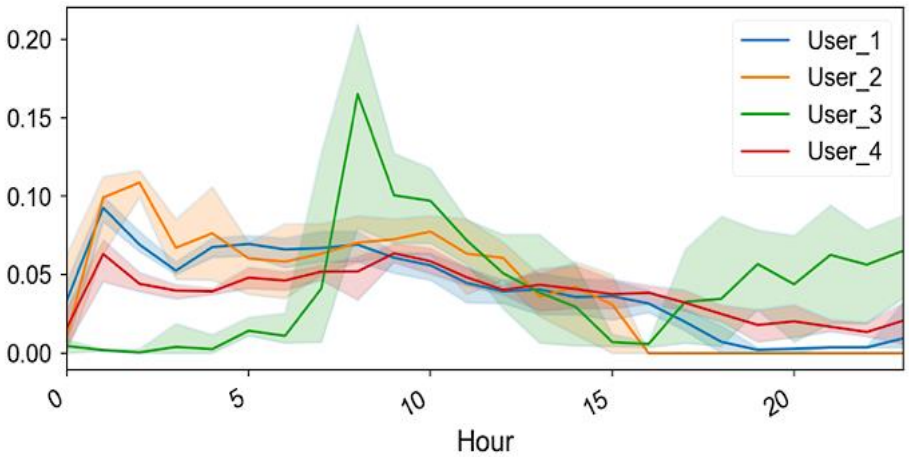

Figure 41. February-March 2020 user profiles data

The determination of the ground temperature was done as explained in subsection 1.2.2**.** In this description of the ground behavior, the ground responds in daily or seasonal temperature cycles. Thermal losses on the entire network were modeled as a function of pipe lengths and diameters, pipe insulation properties given by an average overall heat exchange coefficient, network supply and return temperatures, and ground temperature. The supply-return network temperature difference (ΔT_{evap}) was assumed to be at a constant 5 K due to the heat pumps' control settings, however, a sensitivity analysis in the range from 3-5°C was performed in alignment with the monitoring values (Figure 39). As the geometry of the network and the characteristics of the pipes were known, the properties of the materials could be sourced from the datasheets. As with the COP estimate, a correction factor U_{CF} was introduced to find the best match with actual thermal losses.

Actual network thermal losses ($E_{th,loss,ntw}$) were estimated by the difference between the total source thermal energy ($E_{th,WH} + E_{th,g}$) and the total thermal energy delivered to the evaporator side of user substations' HPs ($E_{th,HP,e}$). This was estimated from the difference between the thermal energy delivered on the HP condenser side ($E_{th,HP,c}$) and the HP electricity consumption ($E_{el,HP}$), assuming an adiabatic system. The efficiency (η_{ntw}) was then estimated as the ratio between the delivered energy to the users $E_{th,HP,e}$ and the total energy produced ($E_{th,WH} + E_{th,G}$). The timeframe considered was between Jan 22nd -31st of 2020, which was the only period of available data with all the necessary measurements.

3.3.1 Key performance indicators

Experimental data was typically collected on a biweekly basis, so key performance indicators (KPIs) were selected for comparison by integrating energy data on a monthly and annual basis. The energy carried by the network to the HPs evaporator side ($E_{th,HP,e}$), assuming an adiabatic system, was estimated as the difference between the heat delivered to the users ($E_{th,HP,c}$) and the HPs electric consumptions ($E_{el,HP}$). In addition, the seasonal COP (SCOP) is calculated as the ratio between the annual thermal energy on the condenser side and the yearly electric energy consumed at the user substation (SCOP = $E_{th,HP,c}$/ $E_{el,HP}$), this represents the performance of HPs only. SPF, on the other hand, measures the overall efficiency of the system. This includes the electricity used by the HPs and the pumps in the network ($E_{el,pump}$). Finally, $E_{el,pump}$ was estimated as a function of the network flow rates and the pump capacity in each of the network circuits (primary and secondary loops, and the aquifer wells circuit). Additionally to the yearly analysis, evaluating these indicators monthly allowed us to evaluate the seasonality effects.

The correction factor η_{CF} was evaluated to find the best fit with the experimental data. Several simulations were performed, and the modeled parameters were compared according to two metrics: an accuracy metric with respect to the SCOP, represented by equation *3.4*), and the mean squared error (MSE) of the monthly COP estimates of the model according to equation *3.5*); where $f_i(COP)$ is a vector of residuals, $m(COP_i)$ is the COP predicted by the model in month i, and COP_i is the observed value.

$$Accuracy = (SCOP_{real} - SCOP_{corr})/SCOP_{real} \quad 3.4$$

$$MSE = \frac{1}{N}\sum_{i=1}^{N} f_i(COP)^2 \quad 3.5$$

$$f_i(COP) = m(COP_i) - COP_i \quad 3.6$$

3.3.2 Sensitivity analysis and calibration

This analysis did not include temperature data from the user's substations on the network side. However, monitoring data at the pumping station could be used to estimate them. The most relevant case is when source s_1 is active (since this occurs for more than 80 % of the time), where the estimate yields T_{s_1} = 22°C and ΔT_{evap} = 4°C for the temperature at the HP inlet and the supply-return temperature difference, respectively. When these conditions apply, the hourly COP values are distributed in the range 4-5.6 (Figure 42). The best performance is obtained in climatic conditions where the outdoor air is in the range 7-20°C and when the maximum temperature supplied to the users is below 50°C. T_{s_1} and ΔT_{evap}, have a degree of uncertainty, so a sensitivity analysis was performed using these values, varying T_{s_1} between 18 and 22°C and ΔT_{evap} between 3 and 5°C. The hourly COP values barely change because of these changes, namely less than 5%.

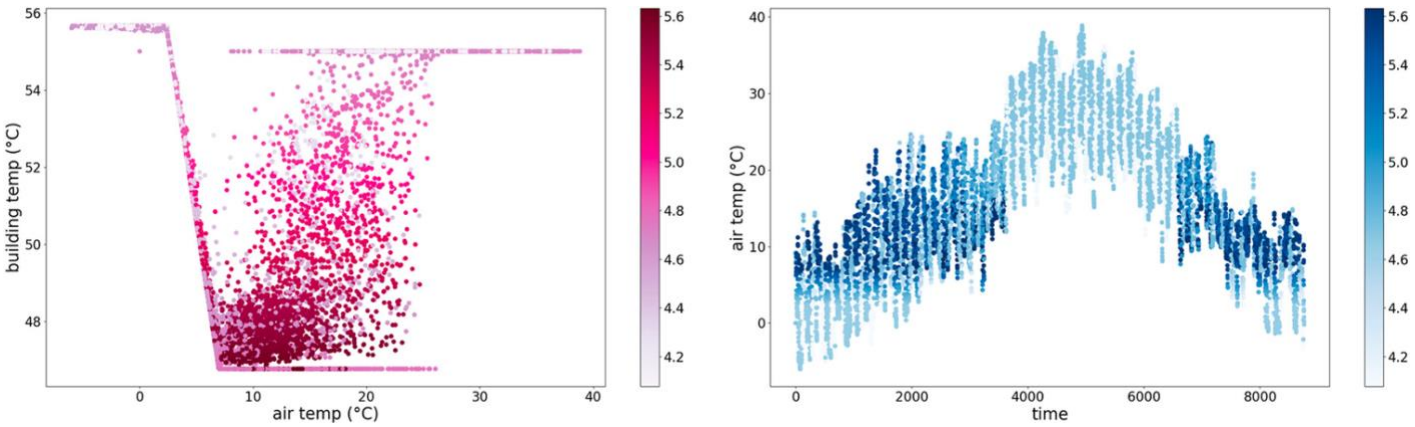

(a) (b)

Figure 42. COP performance map. The colors represent hourly values in the range of the color bars. (a) Effect of the climatic curve implemented in the model. (b)Climate influence in the COP. The points in dark blue indicate better performance in the spring and autumn seasons.

The period from January 22nd to January 31st was used to validate the thermal loss calculation. The total measured losses in this period were 26 MWh, significantly lower (37 %) than the uncalibrated model prediction based on nominal values. Therefore, a corresponding correction factor was introduced. This large discrepancy is related to a shortcoming in the "default" calculations: the thermal losses are estimated assuming an undisturbed ground temperature at the pipe wall. This approach is appropriate when it comes to insulated pipes (where the insulation represents most of the thermal resistance) and is also applicable to district heating models, but it fails when it comes to non-insulated plastic pipes. The observed U_{CF} corresponds with the point at which the undisturbed ground temperature is reached at about 0.25 m from the pipe wall (this corresponds to assuming that an effective ground insulation layer of 0.25 m is present around uninsulated pipes).

The experimental data was aggregated in a monthly basis, to compare with the predicted COP and SPF. Table 7 presents the model's accuracy and the MSE when using different correction factors (η_{CF}) according to equation *2.26*. The best fit is obtained for η_{CF}= 75%. This means that the overall substation inefficiencies are on the order of 25%. While a 15% of performance loss can be expected, this is a relatively high correction, which might be due to the existing substations' performance and the various approximations of the model.

Table 7. Sensitivity analysis of COP correction factor

η_{CF}	SCOP	Accuracy (%)	MSE
74	3.57	1.43	0.00268
75	3.62	0.0499	3.26×10^{-6}
76	3.67	1.33	0.00232

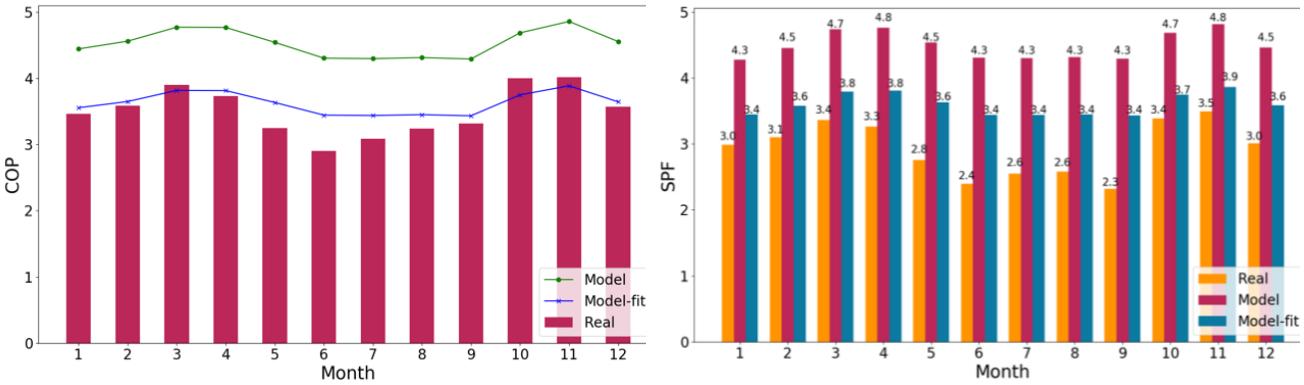

Figure 43. COP and SPF outputs before and after applying the correction factor that best fits the experimental data.

Table 8. Annual performance and energy balances comparison

Quantity	Unit	Model		Monitoring Data	%Diff
$E_{th,HP,c}$	MWh/y			1557.63	
T_{S_1}	°C	20	22	24.28±1.9	
T_{aq}	°C	15.33		14.67±0.14	3.79 - 55
SCOP	arb. u.	3.61	3.64	3.62	0.27 - 0.55
SPF	arb. u.	3.16	3.17	3.11	1.61 - 2.57
$E_{th,HP,e}$	MWh/y	1125.94	1127.61	1128.9	0.11 - 0.26
$E_{el,HP}$	MWh/y	431.69	427.54	433.5	0.42 - 1.37
$E_{el,pump}$	MWh/y	49.66	50.47	65.2	22.59 - 23.83

3.4 Conclusion

The TEA model validation and calibration are discussed in this chapter. It is built on the lumped approach of the Excel tool developed during the FLEXYNETS project. In an initial stage, a parametric analysis was carried out in a theoretical FU in a Mediterranean climate to assess the performance of a NT-DHC system using different shares of WH. The results show economic advantages of the network solution with an important role of cooling.

At the beginning of this chapter, it was introduced the case study of the NT-DHC network in Ospitaletto, Italy. The lumped model and the physical model (also called "detailed") are described, and the main technical results are compared. Due to the lump model's spatial and temporal scales, comparisons could only be performed on aggregated values and at the monthly level.

It was concluded that the models provided results in reasonable agreement: a 15% difference in the overall electricity consumed by the HPs. According to the approximate and detailed models, the estimated thermal losses to the ground were 46% and 40%, respectively, due to uninsulated pipes. According to both models, the pumping consumptions were 2% of the total thermal energy delivered at the HPs' evaporators. Electric consumption of decentralized HPs, heat absorbed by the HPs from the network, and average COP are all closely linked, and discrepancies between the two models are explained by the different temperature values.

Finally, the computational performance of both models was also reported. The lumped model can be executed immediately, while the detailed model takes about 30 min to solve the whole network (about 50 vertices) for an entire year with an hourly time step. The difference between the two types of models is evident: whereas intermediate approximation levels can be chosen, a detailed model is impractical for parametric analysis or optimization.

The second part of the chapter discusses the calibration of an upgraded lumped model with experimental data: the characteristics described in Table 2 had been implemented in Python. An integrated approach was used to analyze the overall network performance: 2019 data were used for the annual analysis, while selected 2020 data were used for the detailed analysis (e.g., daily profiles and thermal losses).

The network relies on source temperatures between 15 and 25 °C and exhibits an SPF of 3.11. Large parts of the network pipes are not insulated, resulting in thermal losses of about 30%. Electric pumping consumptions are of the order of 4 % of the users' thermal consumptions. The lumped model provides proper order of magnitudes for these values even using simplified default estimates. However, for a good agreement (a few percent of the difference in the most important indicators), two simple phenomenological coefficients must be calibrated.

Based on this analysis, we concluded that a lumped approach seems appropriate for such a simple network (most deviations can be explained by physical details unrelated to individual differences). A lumped model offers a quick tool for scenario analysis (the model includes costs estimates as well), a needed application for this innovative NT-DHC network strongly coupling electrical and thermal consumptions.

4

Model application

Chapters 4 and 5 have been partially presented in:

S. Calixto, M. Cozzini, and G. Manzolini, “Techno-economic tool for the evaluation of neutral-temperature district heating and cooling networks and individual solutions”. Euroheat & Power conference, Hilton Brussels Grand Place, Brussels, Belgium, June 2022.

The model can be applied to any city if the proper heat density data is available. However, the approach was applied to the case study mentioned above for simplicity. The parameters required and assumptions in a default simulation for the Ospitaletto case study are detailed in the following subsections. The results are susceptible to these inputs; therefore, careful data collection must be executed a priori, and well-justified assumptions are required to perform a sensitivity analysis in the most critical variables.

4.1 Sources selection

The first step is to identify the potentially exploitable sources. In the following Figure, a survey is presented. Sources of different types (WH of twenty industrial sites, six supermarkets, and six parks), temperature level, estimated thermal capacity, and location were identified within the municipality's boundaries. The three groups of sources that were selected based on temperature availability and proximity among them are presented in Table 9.

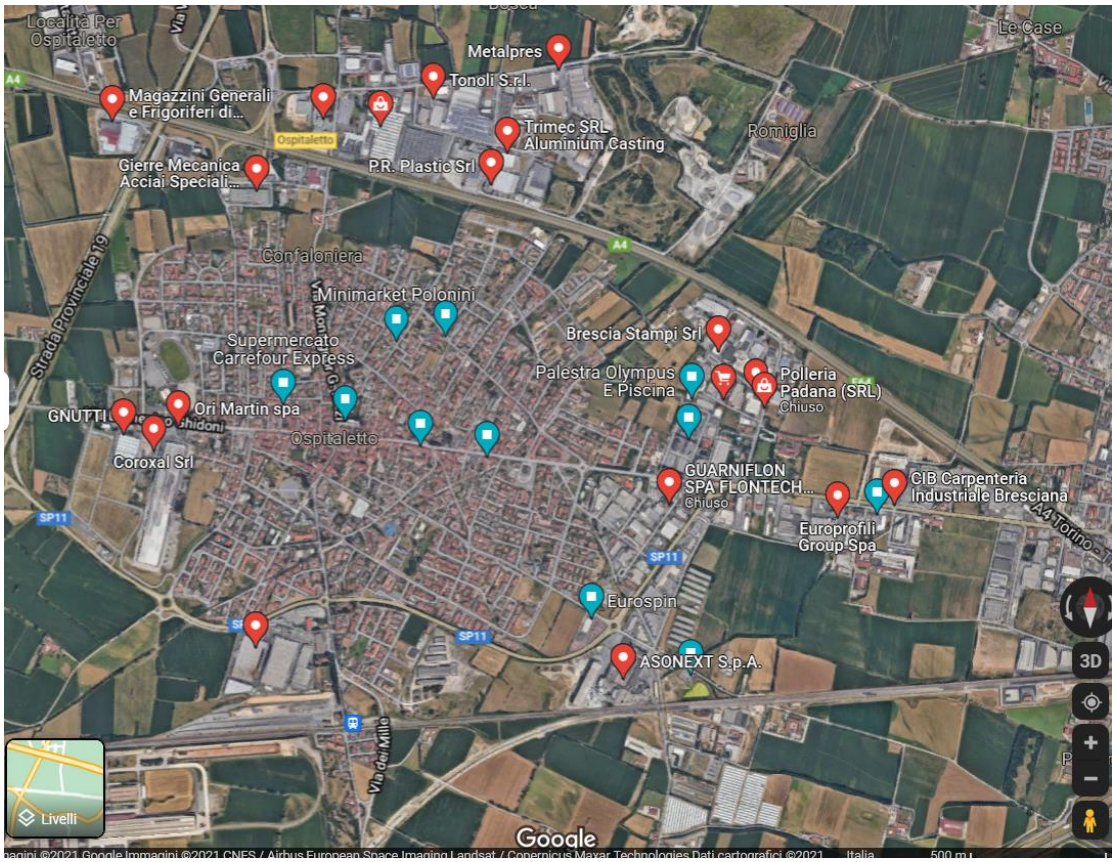

Figure 44. Neutral temperature sources survey in the Ospitaletto municipality. The red markers represent the location of industrial sites.

It is assumed that the sites with industrial waste heat have a higher exploitation priority since their operating schedule is typically stable and continuous. Moreover, their temperature level is superior to the ground sources and therefore beneficial towards the performance of the NT-DHC system.

Table 9. Sources characteristics and grouping selection

Source	Category	Capacity [MW]	Temperature [°C]	Group
Baden Powell Park	Park	1.14	15	G1
Steel plant	Industry	1.58	22	G1
SABAF	Industry	6	25	G2
Piazza Mercato	Park	12.3	15	G2
Carrefour	Supermarket	0.1	18	G3
Ori Martin	Industry	15	25	G3
Manzoni Park	Park	3.15	15	G3

4.2 Loads

Heat density data of residential buildings at the hectare level is the smallest data unit retrieved from the online Hotmaps database [60]. An arbitrary FU of 1 km^2 from the Ospitaletto municipality was selected, as presented in Figure 45. The total heat demand is 35.726 MWh/y, with a peak demand of 17.28 MW.

The Spectral Clustering method from scikit-learn [61] is applied iteratively. Starting from one big cluster and increasing the granularity of the FU, the algorithm provides an output when a configuration is found where the largest cluster does not exceed the sources' capacity limit (see section 2.2.2 for more details). This threshold should be set taking into consideration the industrial sources' capacity in each group because their stable schedules and constant heat supplies are critical to network operation. It is observed in Table 9 that this limit comes from the smallest industrial waste heat plant available of 1.58 MW, giving a configuration as shown in Figure 45. WH sources such as supermarkets, small shops, bakeries, among others, should be considered complementary sources to meet the total load, but not for sizing. Parks or other ground source sites are assumed to be auxiliary systems to meet the demand durig weekends and other times when WH plants are unavailable (see Figure 8).

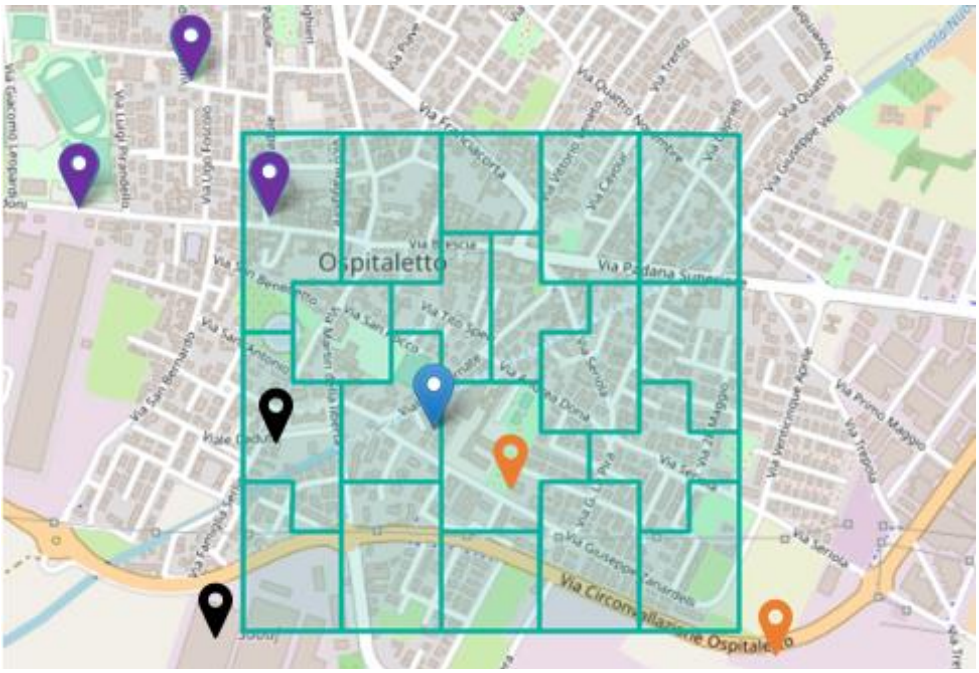

(a)

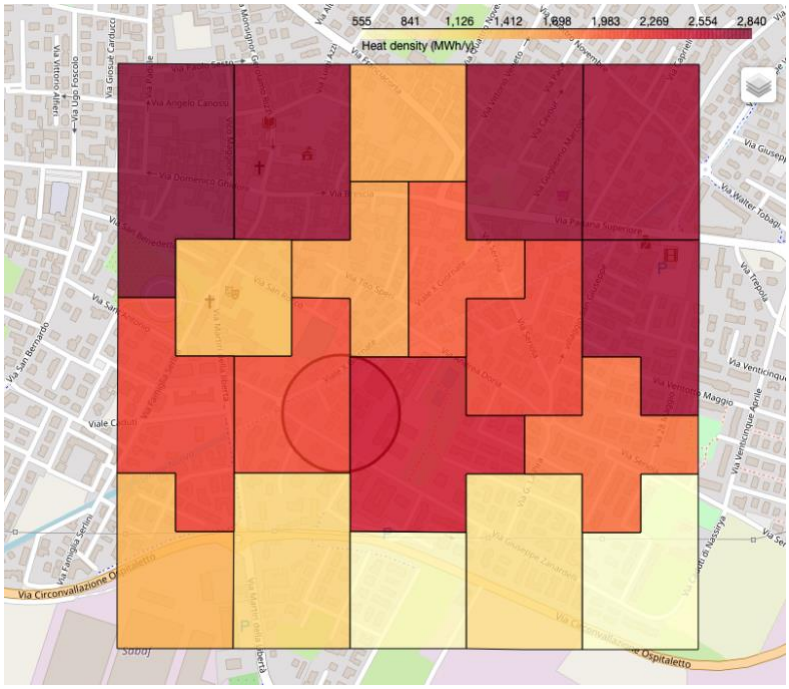

(b)

Figure 45. (a) Clusters and source groups' locations are symbolized in different colors. G1 in orange, G2 in black, and G3 in purple. The blue marker represents the centroid of SBs. (b) Heat density map of the clusters ranging from 555 to 2840 MWh/y.

4.3 Technical, economic, and environmental inputs

4.3.1 Energy prices

The energy prices vary considerably depending on the type of customer (residential or non-residential) and taxation. According to Eurostat data, the residential electricity price in Italy during the second semester of 2020 was 0.215 €/kWh (0.15 €/kWh corresponding to taxes and other costs)[114]. On the other hand, the non-residential electricity price was 0.15 and 0.175 €/kWh without and with taxes, respectively.

Italy's average residential gas price has fluctuated between 0.060 to 0.080 €/kWh from 2018 to 2021, excluding taxes. The total gas price, including taxes and levies, varied from 0.07 to 0.095 €/kWh in the same period. The comparison of energy prices with and without taxes among European countries is shown in Figure 46.

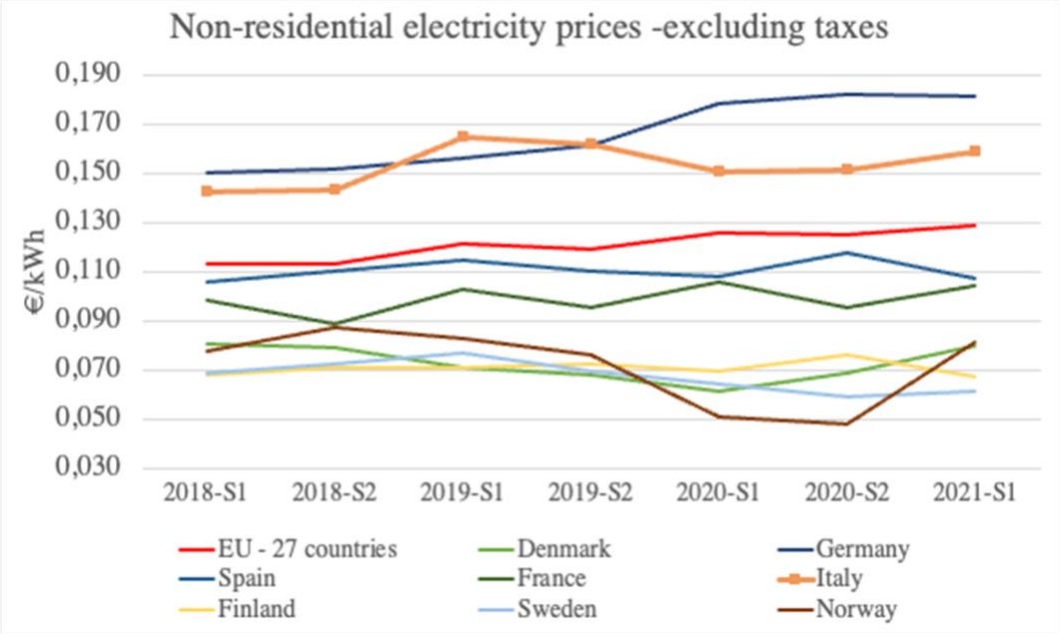

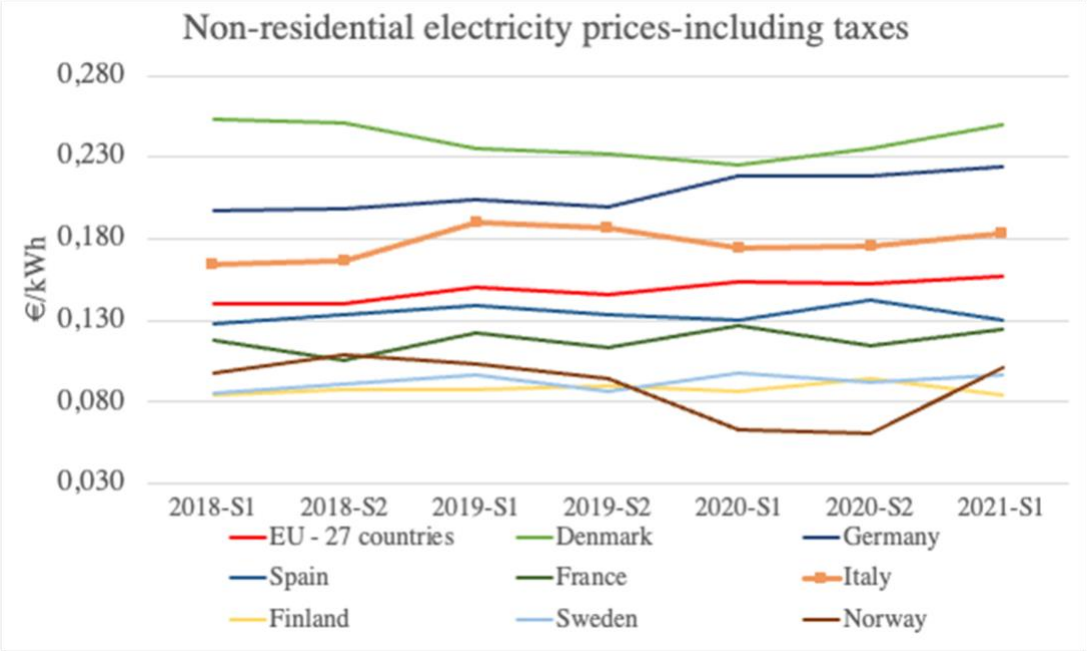
Non-residential electricity prices-including taxes
€/kWh
0,280
0,230
0,180
0,130
0,080
0,030
2018-S1
2018-S2
2019-S1
2019-S2
2020-S1
2020-S2
2021-S1
EU - 27 countries
Denmark
Germany
Spain
France
Italy
Finland
Sweden
Norway

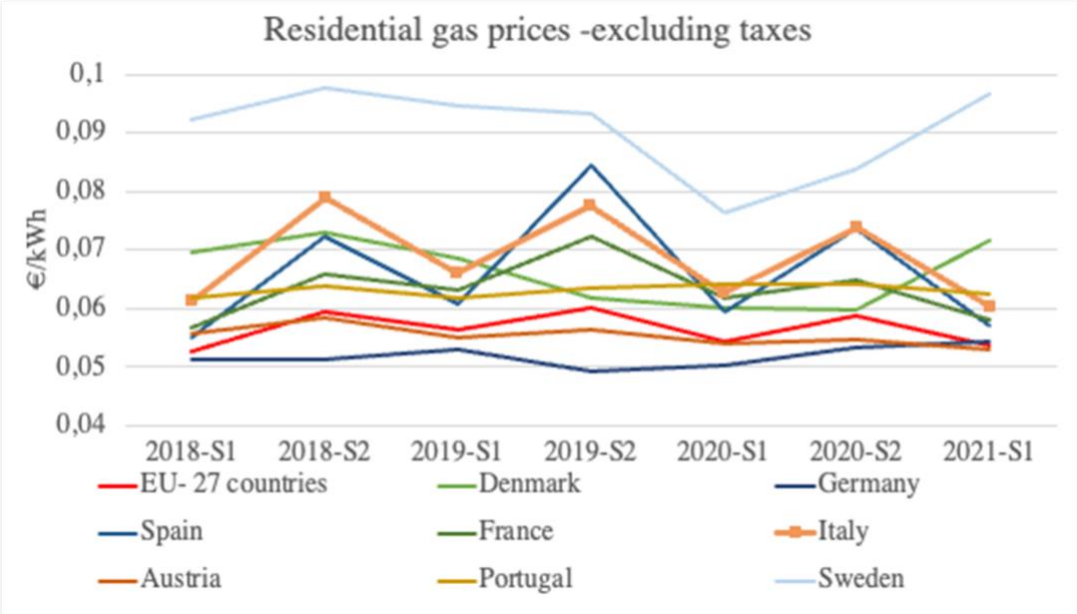
Residential gas prices -excluding taxes
€/kWh
0,1
0,09
0,08
0,07
0,06
0,05
0,04
2018-S1
2018-S2
2019-S1
2019-S2
2020-S1
2020-S2
2021-S1
EU- 27 countries
Denmark
Germany
Spain
France
Italy
Austria
Portugal
Sweden

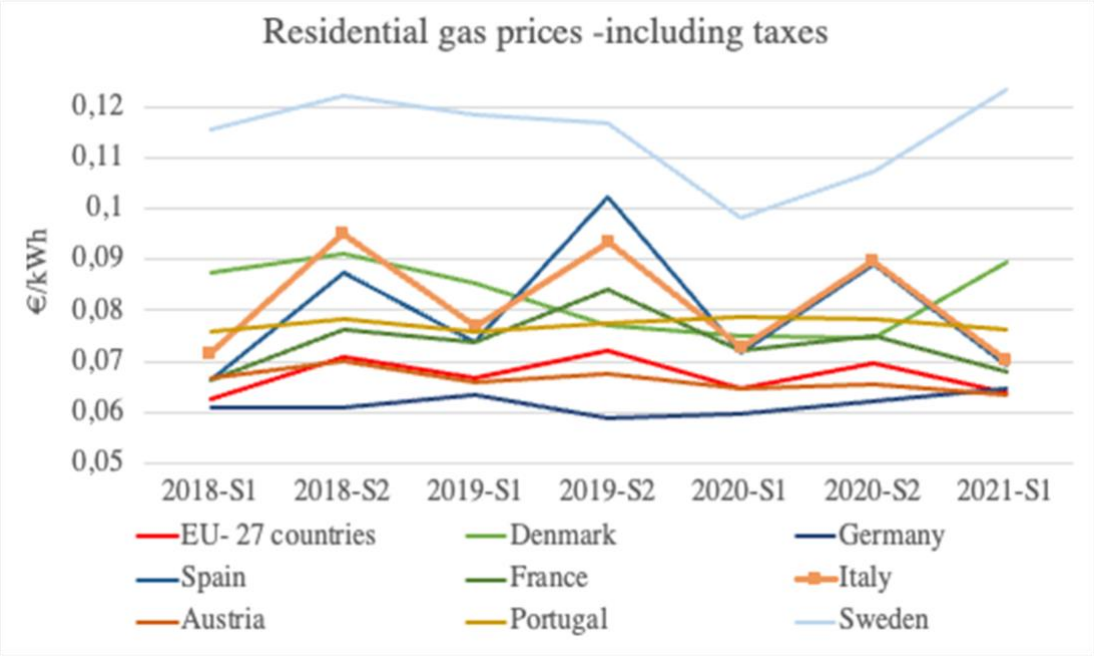

Figure 46. Energy prices with and without taxes in EU countries. Source: Eurostat [114].

Table 10 summarizes the assumptions used for a default simulation. The first assumption is that NT-DHC systems would benefit from no taxes on electricity. In contrast, the competing solutions of individual boilers are compared at the residential gas price, including taxes and levies, and split cooling units and A/W HPs operate under residential electric pricing. Finally, H&C sales assume a maximum heat price equal to the competing solution price (gas boilers).

These assumptions are made since the network operator may benefit from a pricing scheme that residential users may not have access to. In the default scenario, it is expected that OPEX from the NT-DHC scenario, and possibly a good SCOP/SEER will provide an advantage over the OPEX of individual gas boilers and A/W HPs. Assumed H&C pricing aims at assessing feasibility by comparing at least the most common and current technologies. If it is possible to find feasible solutions at this energy pricing level, this does not limit other business cases that the energy analyst could consider.

Table 10. Energy prices selected for a reference scenario (€/kWh)

Variable	Value	Description
Gas	0.100	Residential price in Italy, including taxes.
Electricity, non-R	0.150	Non-residential price in Italy, excluding taxes, based on 2020 data.
Electricity, R	0.200	Residential price in Italy, including taxes.
Heating	0.100	Assumed equal to gas price.
Cooling	0.100	Network services are assumed to be equal for H&C.

4.3.2 Emission factors

In the default simulation, the selected electricity and natural gas values for the Italian case are presented in Table 11. The 2020 edition of emission factors in the electrical Italian grid and the main European countries from the Institute of Research and Environmental Protection (ISPRA for its Italian acronym) provides a more up-to-date value for the electricity emission factor[115]. In this report, 0.281 tCO_2/MWh corresponds to electricity consumption emissions (the equivalent of the reported values from [54] using a standard method) for the reference year of 2018:

Table 11. Emission factors used in the default simulation ($tCO_{2\text{-}eq}$/MWh)

Energy carrier	Value	Description
Electricity	0.281	2018 reference year (ISPRA,2020)
Natural gas	0.202	Standard method (IPCC-2006)

4.3.3 Techno-economic inputs

A series of technical inputs for a default simulation are presented in the following table, based on the current operating conditions of the network located in Ospitaletto [69]. Detailed information about their application can be found in subsection 1.2.2 for the estimation of ground temperature and heat losses, subsection 2.2.3 for the application of DHW and SH temperature setpoints, subsection 2.4.2 for NT-DHC substations modeling, and 2.4.3 techno-economic assessment.

Table 12. Techno-economic inputs used in the default simulation

Parameter	Value	Description
T_{DHW}	55	DHW temperature (°C)
$T_{max,i}$	55.66	Maximum indoor SH temperature delivered to the buildings (°C)
$T_{min,i}$	46.77	Minimum indoor SH temperature delivered to the buildings (°C)
z	1.3	Network pipes depth (m)
η_m	53	HPs compressor efficiency (%)
ΔT_{evap}	4	Supply-return network temperature difference
COP_{CF}	1	Correction factor applied to the COP formula
U_{CF}	1	Correction factor applied to the thermal losses' formula
i	3	Discount rate of the project (%)
$f_{disc,inv}$	1	Subsidy to the total NT-DHC investments (discount factor from 0-1)
f_{inc}	1	Incentive factor for the heat delivered through the NTDHC network (i.e., a factor of 1.2 would represent a 20% subsidy from a public entity).
c_{tax}	75	Carbon tax (€/tCO_2).

4.4 Sensitivity analyses

This study requires a sensitivity analysis to answer the research questions presented in subsection 1.4:

- RQ1. Is it feasible to expand a NT-DHC network efficiently using available waste heat sources?

The feasibility of the NT-DHC solution should be examined depending on when groups of WH sources become available. Thus, the expansion results will be examined if the phasing of sources is changed (see Figure 31) from the default phasing shown in Table 9 (from G1, G2, G3 to G3, G2, G1).

- RQ2. Which conditions (technical, economic, environmental) make the NT-DHC solution more competitive than individual solutions?

Three factors will be analyzed to assess the competitiveness of the NT-DHC concept against conventional H&C solutions (individual gas boilers and split units or reversible A/W HPs): energy price conditions, electric grid environmental performance, and cooling penetration scenarios. Table 13 presents future scenarios that could occur in the electricity and gas markets. The renewability of the Italian grid and how does this impact the solution compared with individual solutions is analyzed through the cases presented in Table 14. Finally, a comparison with individual H&C solutions will be performed according to the cooling scenarios presented in Table 15.

- RQ3. Is it possible to identify optimal expansion strategies, minimizing the overall costs and emissions (through carbon taxes)?

In addition to assessing the effects of energy market pricing on optimal expansion strategies and costs, sections 5.2 and 5.3 will analyze the effects of source temperature (and therefore network) conditions and the renewable energy potential of electricity.

Table 13. Energy prices scenarios. Favorable cases for the NT-DHC

Variable	Value	Description
Electricity, non-R	0.10 €/kWh (-33% of reference)	Subsidy to the NT-DHC energy cost component
Electricity, non-R	0.20 €/kWh (+33% of reference)	Electricity price increase for the non-residential sector
Electricity, R Electricity, non-R	0.30 €/kWh and 0.225 €/kWh (+50% of reference)	Electricity price increase (residential and non-residential)
Electricity, R	0.20 €/kWh	Residential customers' price remains stable or becomes cheaper
Gas	0.15 €/kWh (+50% of reference)	Residential gas price increase
Gas	0.10 €/kWh	Residential gas price remains stable

Table 14. Sensitivity analysis of electric grid renewability

Variable	Value	Description
Electricity emission factor	0.141(-50% of current factor)	Optimistic case. A high share of renewables in the Italian electric grid
	0.483(2005 Italian electricity factor)	Pessimistic case. A grid with a low share of renewables.

As mentioned in the introduction, global heating energy demand is projected to increase until 2030, then stabilize. However, it is predicted that cooling demand will overtake heating demand worldwide. Using 2020 as a baseline, cooling accounts for 10.6% of the heating demand in the default simulation. However, future cooling scenarios with increased demand are worth investigating. In 2030, assuming

that cooling demand increases by 10% a year, this exponential growth translates into a cooling factor of 27.6%. This represents a net increase of 17% with respect to the 2020 value, or an annual increase of roughly 1.7%. If the exponential growth stabilizes and then increases linearly with the same order of magnitude (17% every 10 years), at this rate, cooling penetration could reach over 50% by 2050. The following table summarizes the future cooling scenarios that will be considered:

Table 15. Cooling scenarios

Case	Description	Cooling factor (%)
2020	Current cooling demand	0.106
2030	An exponential growth in the cooling demand of 10% per year	0.275
2050	A linear growth starting from 2030 with an approximate rate of 1.7%.	0.60

5

Results

This chapter will be publicly available at:

Deliverable D.1. “Impact scenarios at the three demonstration networks”. LIFE4HeatRecovery project. http://www.life4heatrecovery.eu/en/

5.1 Default simulation

This approach provides a phasing schedule of sources and loads according to the expected thermal capacity to be utilized and the number of periods selected. In the default simulation, it is assumed that three groups of sources become available in the order shown in Table 9 and represented geographically in Figure 45a.

In Figure 47, it is shown that the model first estimates the NPV of each potential extension project. The clusters with a higher NPV appear in red on the heatmap, while the less economically attractive ones appear in yellow. The markers correspond to the locations of sources in group G1. The model then finds the optimal subset of clusters that, combined, adds the highest value to the portfolio, without exceeding the thermal capacity threshold (Figure 47b).

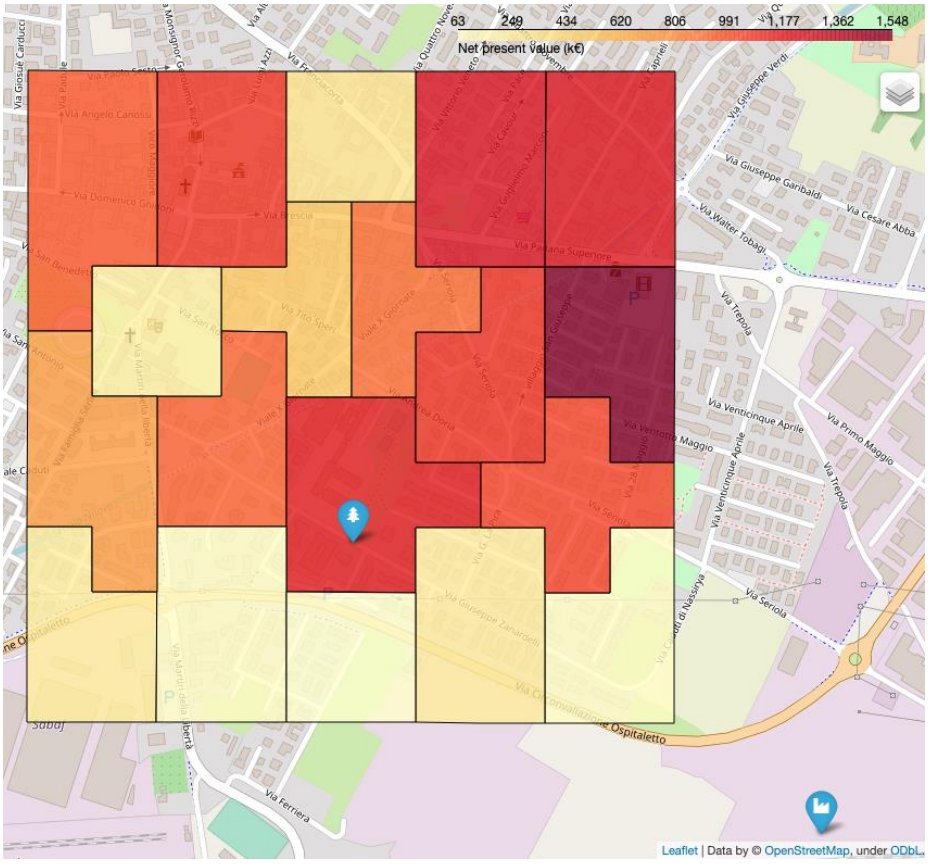

(a)

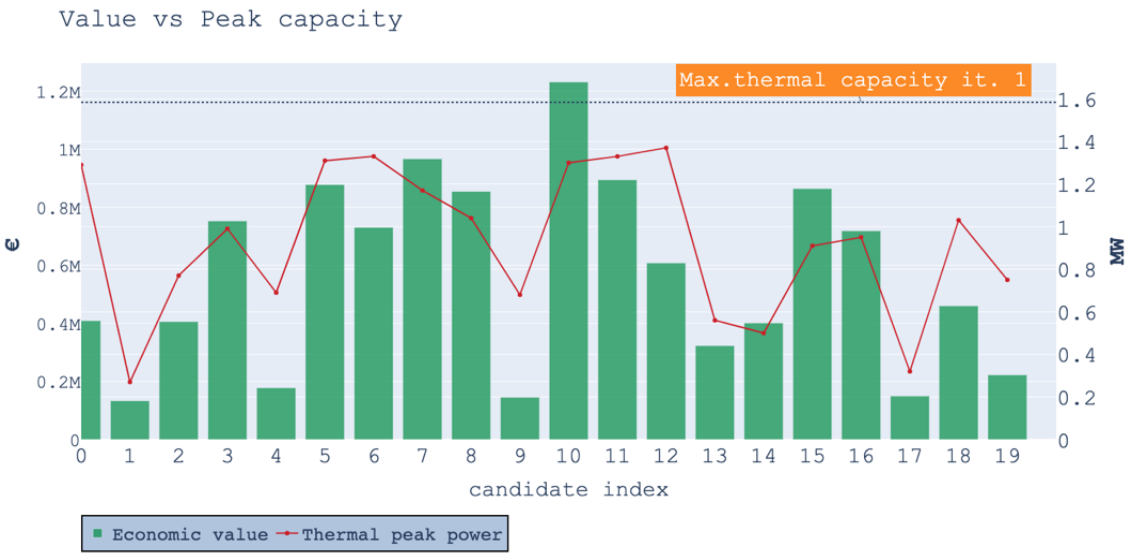

(b)

Figure 47. The first optimal extension considers the available thermal power of 1.6 MW. (a) The calculated NPV for each cluster. (b) The cost-benefit analysis.

This first iteration of the model prioritizes cluster 10 (the one with the highest NPV). Cluster 1, despite its marginal economic convenience, is chosen because it meets the 1.6 MW capacity restriction, while other more attractive zones have thermal peak demand that exceeds the source limit (see Figure 50a). In the second iteration, the model recalculates the NPV of the remaining candidates (excluding the selected zones from the previous scenario), considering there are 6 MW of WH capacity available. Figure 48 shows the markers representing the locations of sources in group G2 (from Table 9), as well as the heatmap of the calculated NPV of each cluster. The model selects the zones shown in Figure 50b based on the best compromise between economic value and peak capacity.

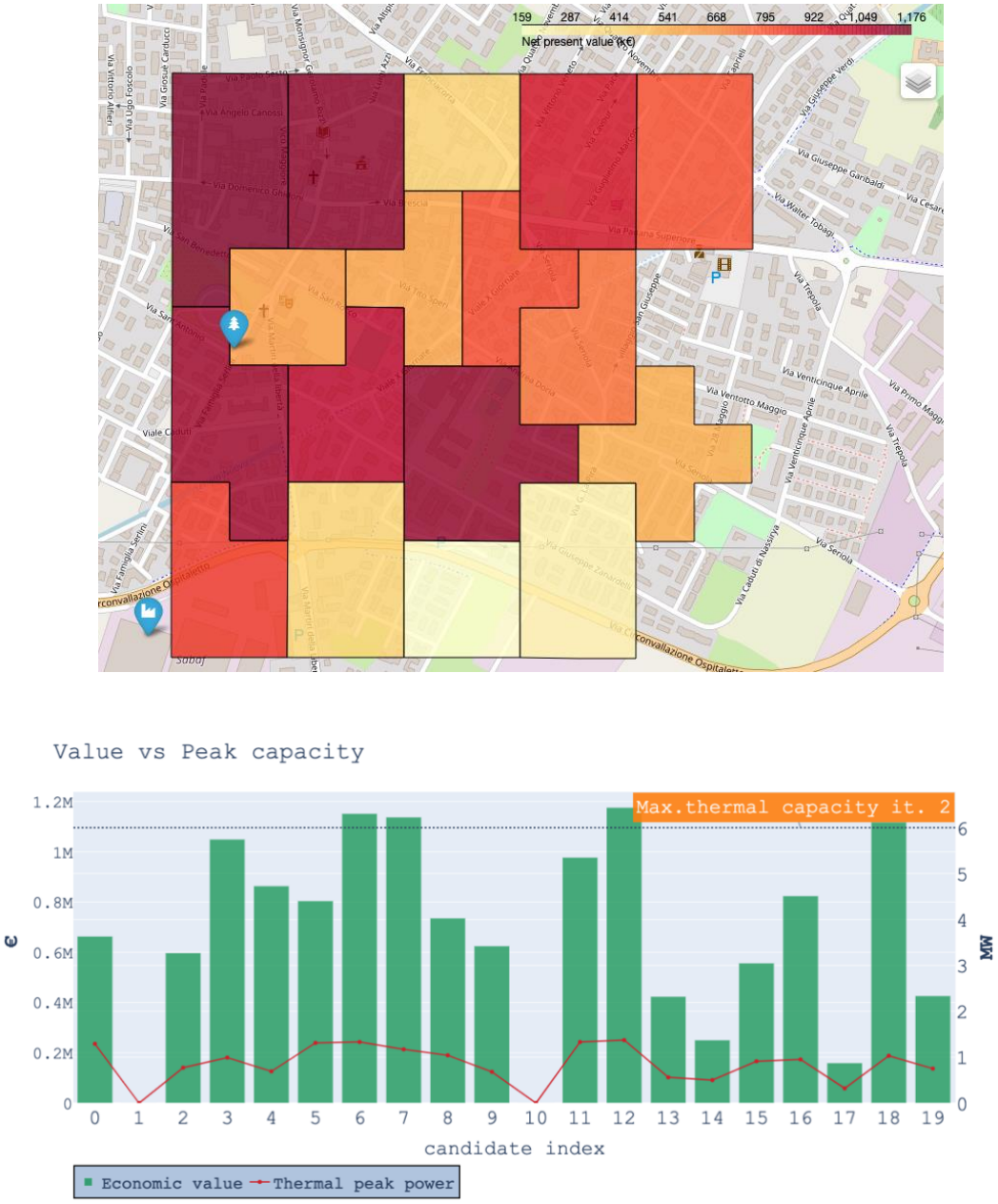

Figure 48. (a) Heatmap representing the NPV of each cluster in the second network extension. (b) Cost-benefit analysis. The first axis represents the NPV of each extension scenario, while the second represents the peak power required by each candidate. The dotted line indicates the maximum capacity that can be exploited from the WH plants (6 MW in this scenario).

In the third iteration, the model determines the NPV of the remaining loads, including the SBs shown in Figure 49. As a result of the high thermal capacity in this step, all the feasible candidates can be served by the NT-DHC system. Finally, the process ends if the algorithm cannot reach a better scenario than the BaU case or if the NT-DHC fully covers the FU. Figure 50 presents the transition pathways

for the NT-DHC system expansion based on default values. Zones located on the southern part of the FU are not connected to the network for two reasons: not only clusters 13, 14 and 17 generate revenues not sufficient to offset the high network connection costs (Figure 49), clusters 13 and 14 can use reversible A/W HPs at a lower cost than the NT-DHC solution (Figure 51).

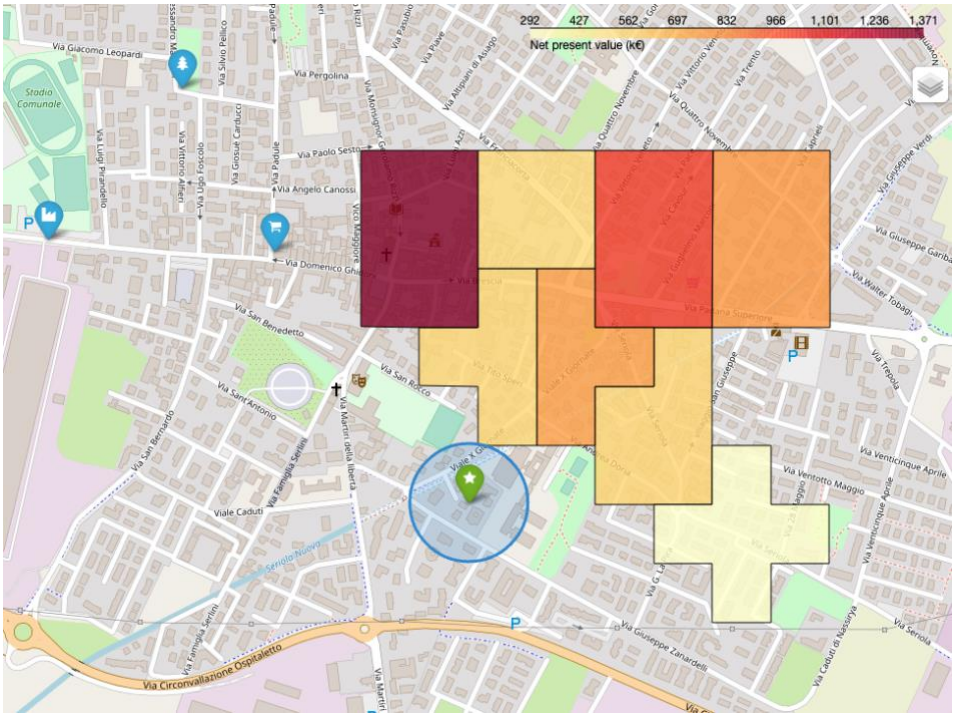

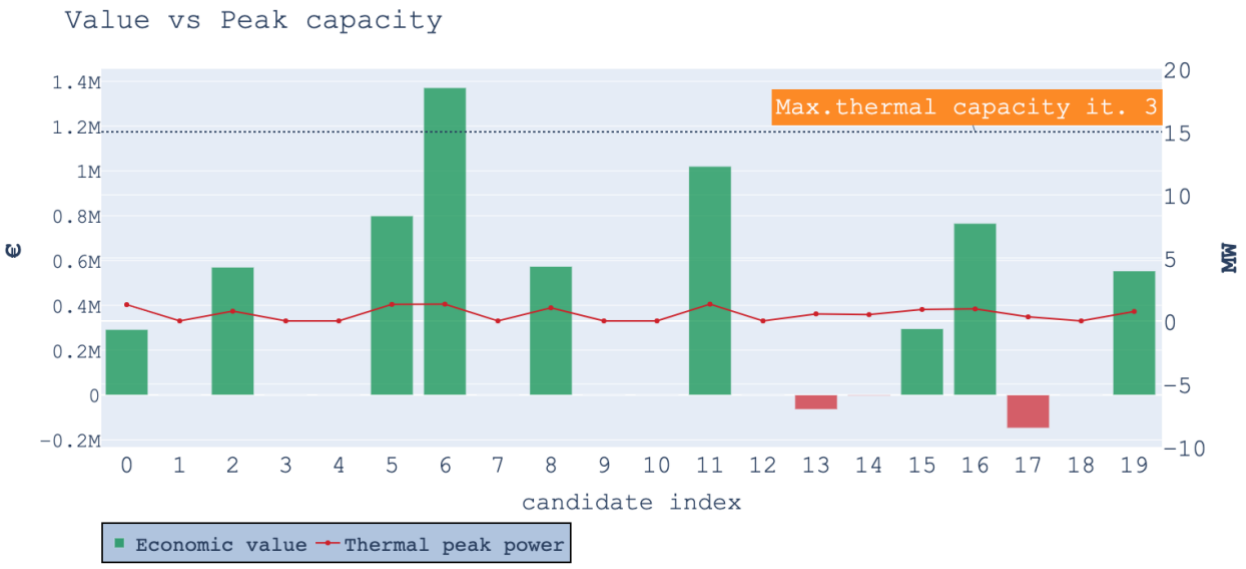

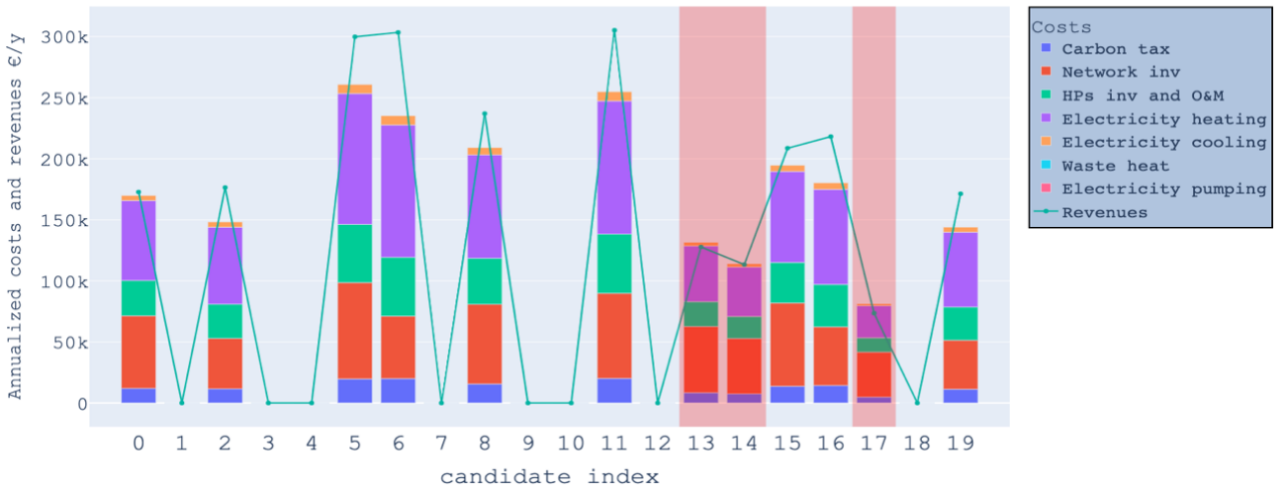

Figure 49. The optimal extension when 15 MW of thermal heat becomes available in the third phase. Clusters 13, 14, and 17 produce unfeasible scenarios, mainly because the revenues from the H&C sales are insufficient to cover the costs of the network to connect with the sources in group G3.

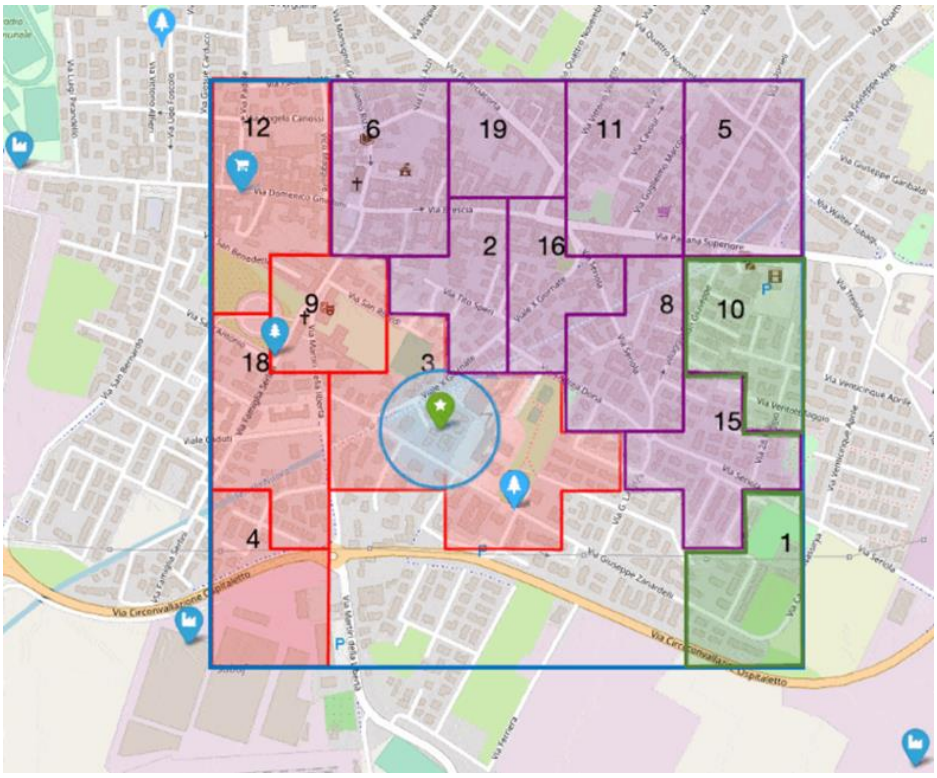

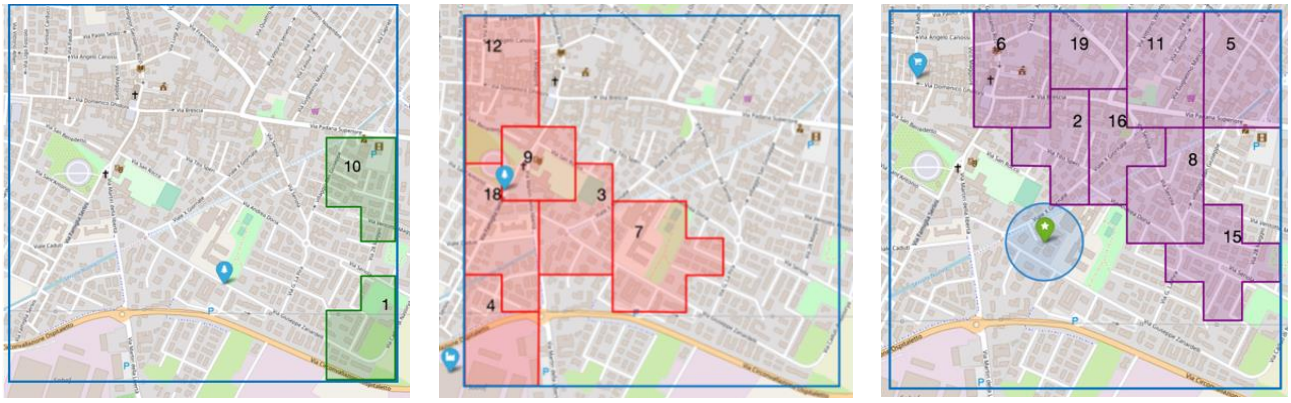

(a) (b) (c)

Figure 50. NT-DHC network extension tool applied to the case study. (a) The first optimal extension considers the available thermal power of 1.6 MW. (b) This second iteration assumes 6MW of waste heat is available. (c) The optimal extension when 15 MW of thermal heat becomes available at a later stage.

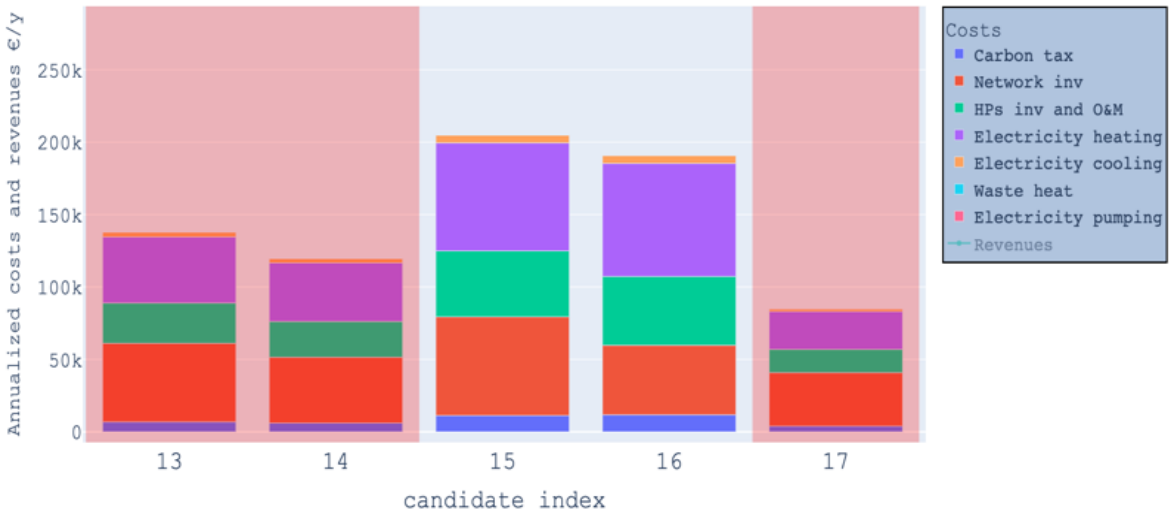

(a)

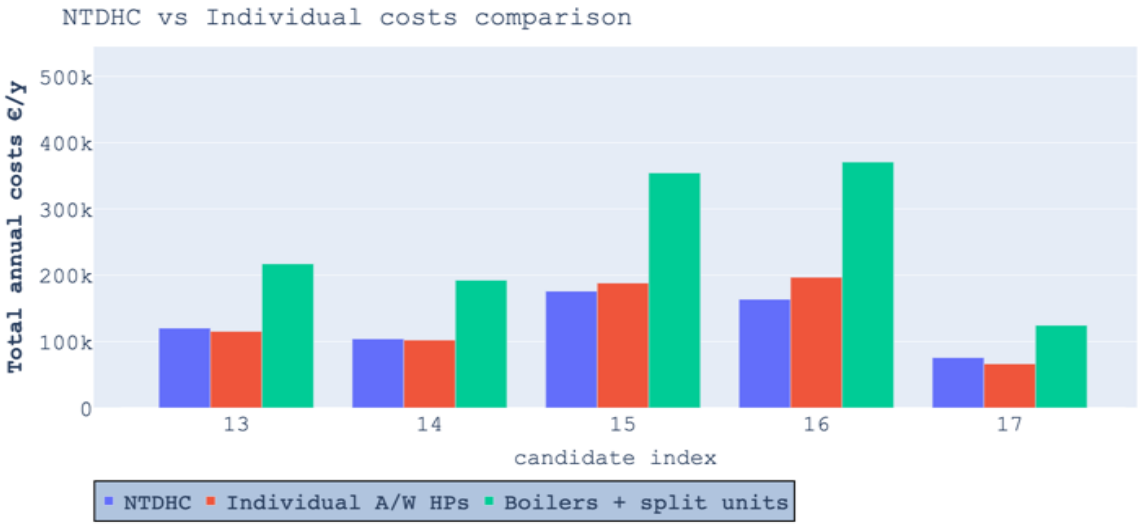

(b)

Figure 51. (a) Cost breakdown for NT-DHC. Red denotes an unfeasible scenario (higher costs than revenues). (b) Costs comparison among H&C alternatives. In Cluster 13, 14, and 17, A/W HPs are positioned as a superior solution over NT-DHC due to their lower cost.

In

Figure 52, a different phasing schedule is tested when varying the order in which the sources become available. The 15 MW WH plant in this example is assumed to be the first to be utilized, followed by the 6 MW WH plant in the second group, and finally the 1.6 MW plant in the third group. It is observed that at the end of the planning, the entire FU is covered under these conditions. In the beginning, there is higher availability of WH supply, so more clusters can join the network. The first iteration prioritizes the clusters near the sources, at the top of the FU.

It is worth noting that the southern clusters 1, 13, 14, and 17 are unfeasible in the first iteration since the H&C sales are not sufficient to offset the high network connection costs of these sources located in the north. Furthermore, in this scenario, A/W HPs are a better option for these clusters (see Figure 53). In the second iteration, NPV is recalculated considering sources from G2, and clusters 4, 13, 14, and 17 are found to maximize the overall value. As cluster 1 is the only one left and near the sources from G3, the algorithm provides a feasible extension scenario.

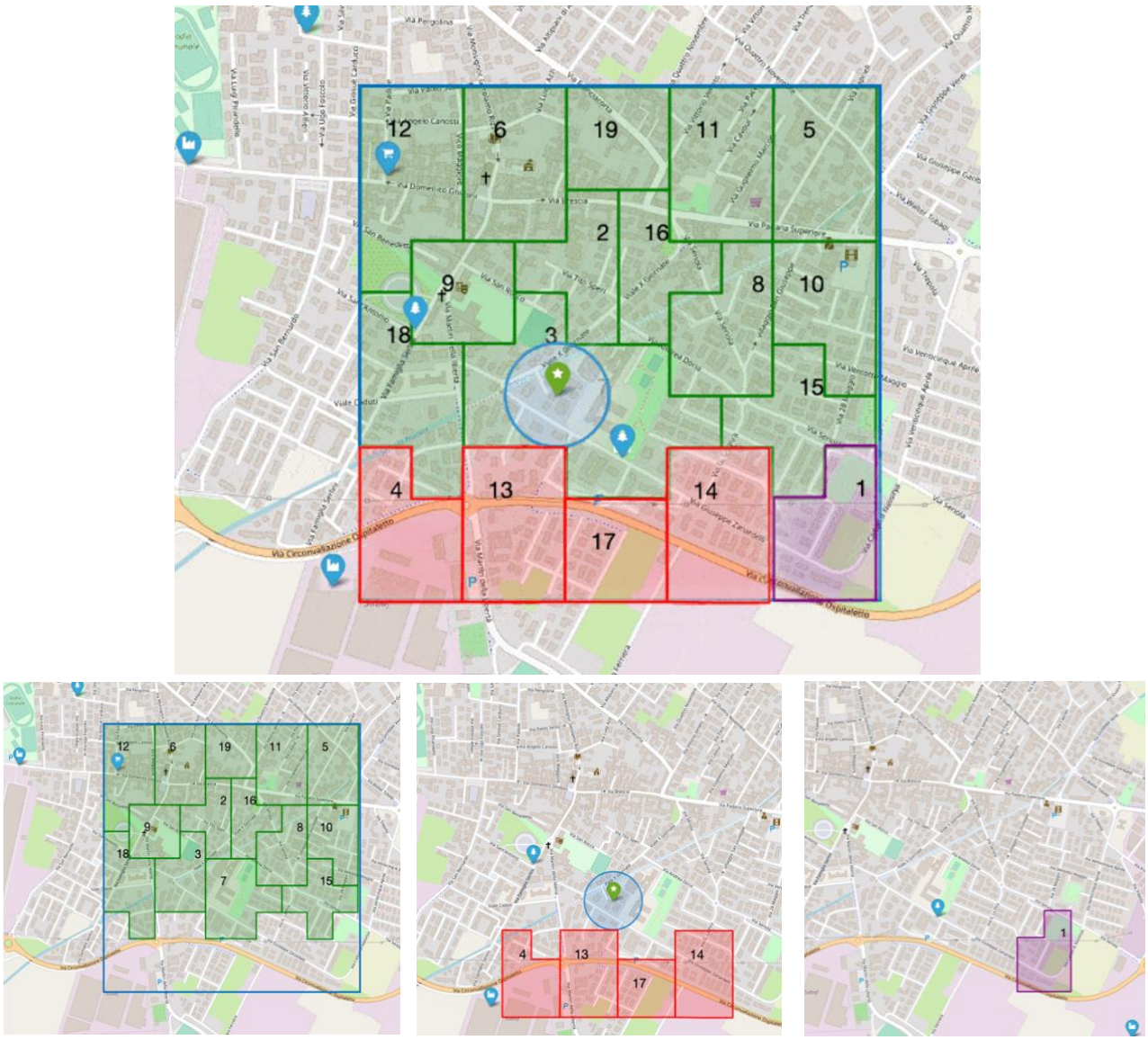

(a) (b) (c)

Figure 52. NT-DHC network extension tool applied to the case study. (a) The first optimal extension considers the available thermal power of 15 MW. (b) This second iteration assumes 6MW of waste heat is available. (c) The optimal extension when 1.6 MW of thermal heat becomes available at a later stage.

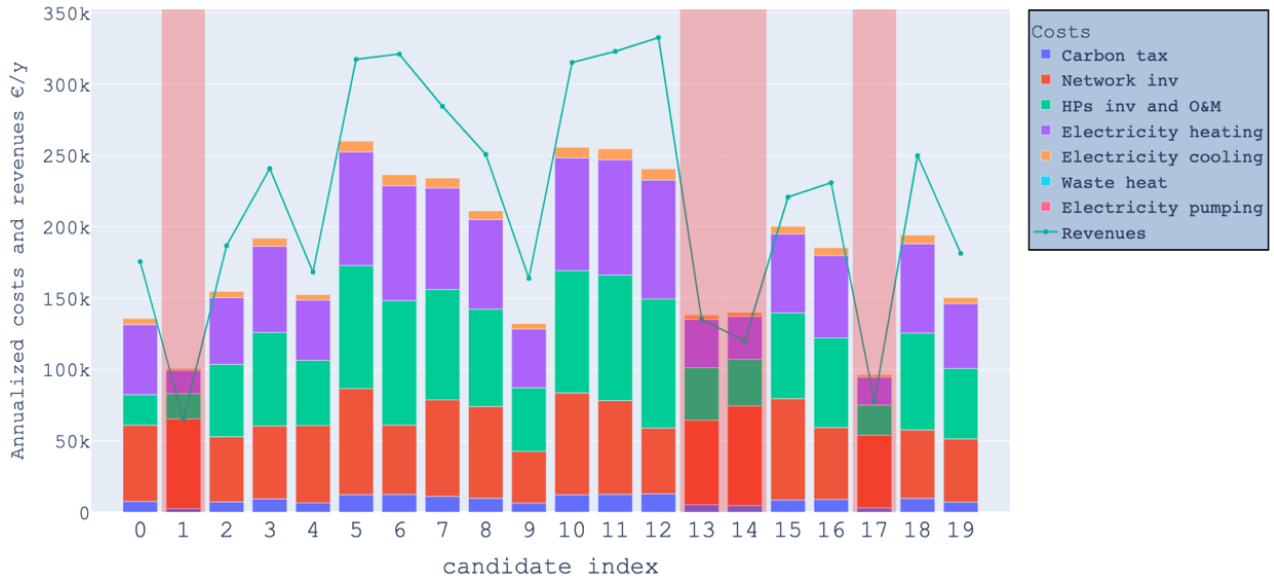
Annualized costs and revenues €/y
350k
300k
250k
200k
150k
100k
50k
0
0 1 2 3 4 5 6 7 8 9 10 11 12 13 14 15 16 17 18 19
candidate index
Costs
Carbon tax
Network inv
HPs inv and O&M
Electricity heating
Electricity cooling
Waste heat
Electricity pumping
Revenues

(a)

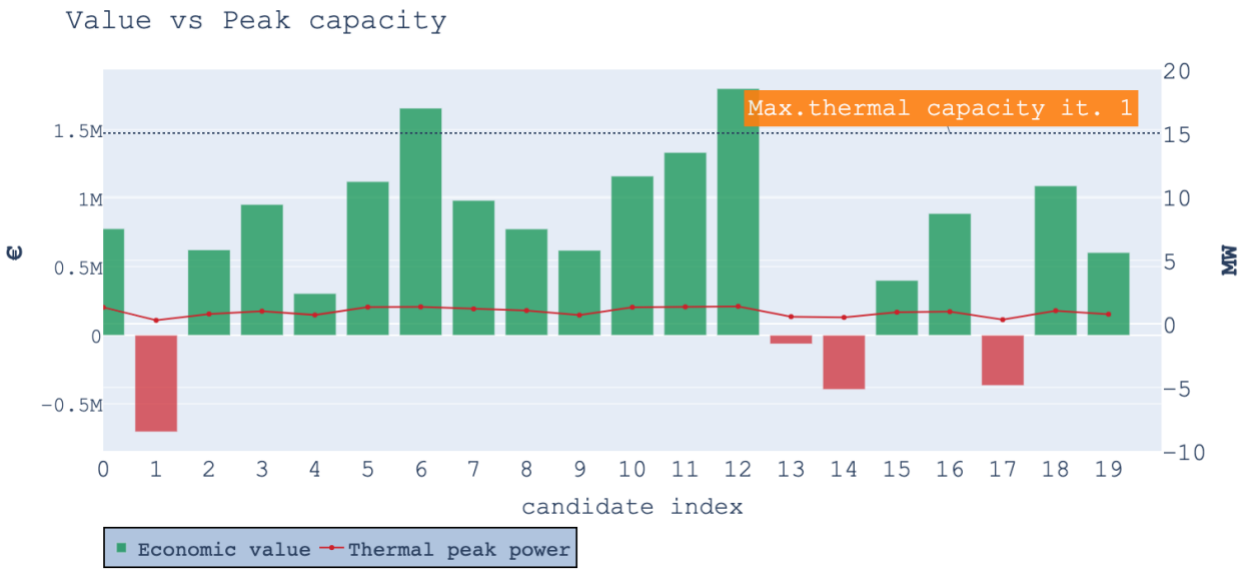
Value vs Peak capacity
Max.thermal capacity it. 1
1.5M
1M
0.5M
0
-0.5M
€
20
15
10
5
0
-5
-10
MW
0 1 2 3 4 5 6 7 8 9 10 11 12 13 14 15 16 17 18 19
candidate index
Economic value
Thermal peak power

(b)

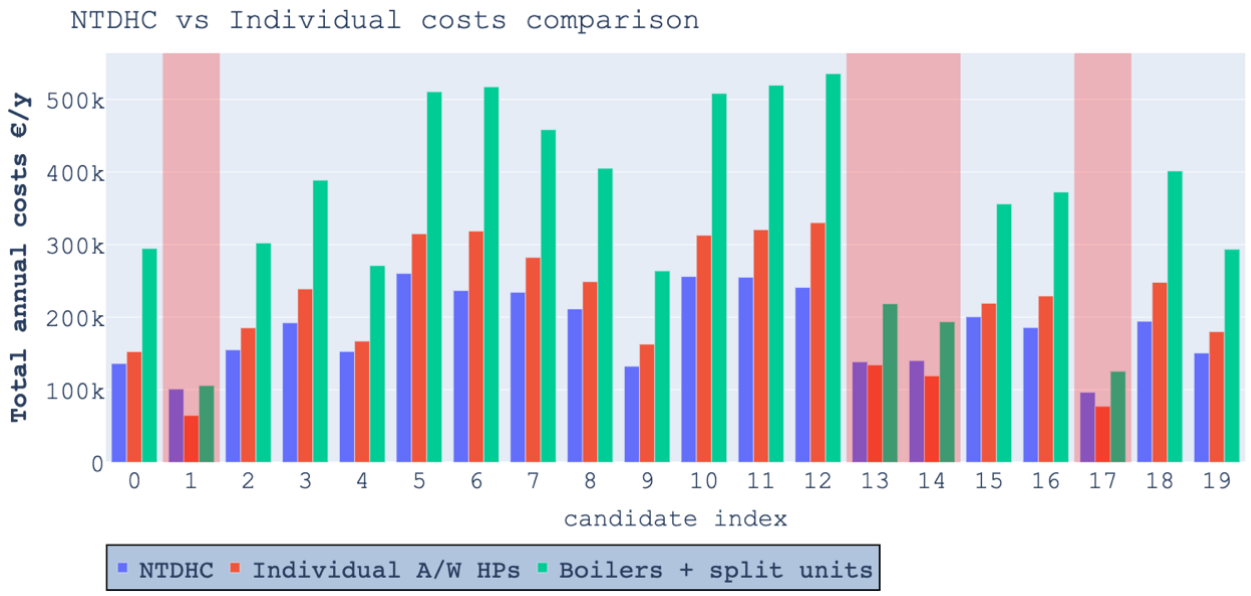

(c)

Figure 53. This scenario assumes 15 MW of thermal capacity in the first extension step. (a) Breakdown of costs and revenues in the NT-DHC system scenario. (b) NPV of each extension under these conditions. (c) A comparison of the NT-DHC system and alternative H&C solutions. Red panels indicate the scenarios in which AW HPs are a better choice.

In contrast to traditional DH business models, this type of network involves a variety of stakeholders (industry, service sector infrastructure, supermarkets, shopping centers, etc.). As shown in the previous example, the tool is flexible when it comes to scheduling WH plants and grouping them geographically. Due to the significant capital ties involved in DH investments, this feature becomes relevant in designing and testing various possibilities, reducing risks.

5.2 Energy price scenarios

The sensitivity analysis of increasing the default electricity price for non-residential customers by 33% (0.2 €/kWh from 0.15 €/kWh) shows an increase in the number of non-feasible extension scenarios (up to 45% in the first iteration). As a result, the NT-DHC functional unit coverage is reduced from 92.38% to 81.65% under these conditions (see Figure 54).

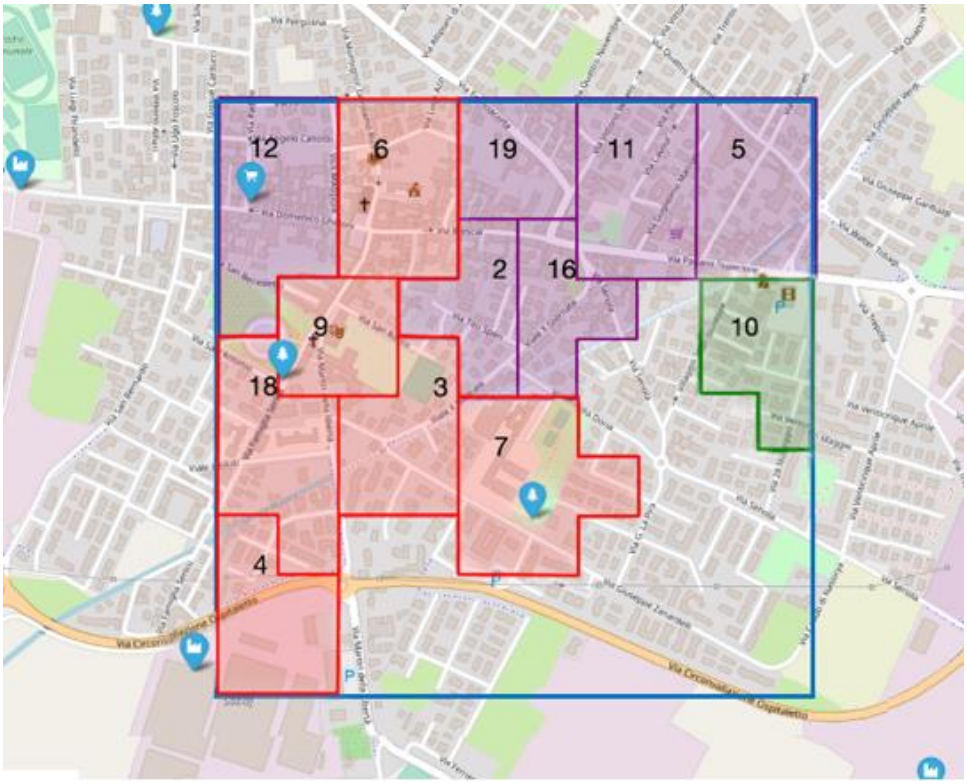

(a)

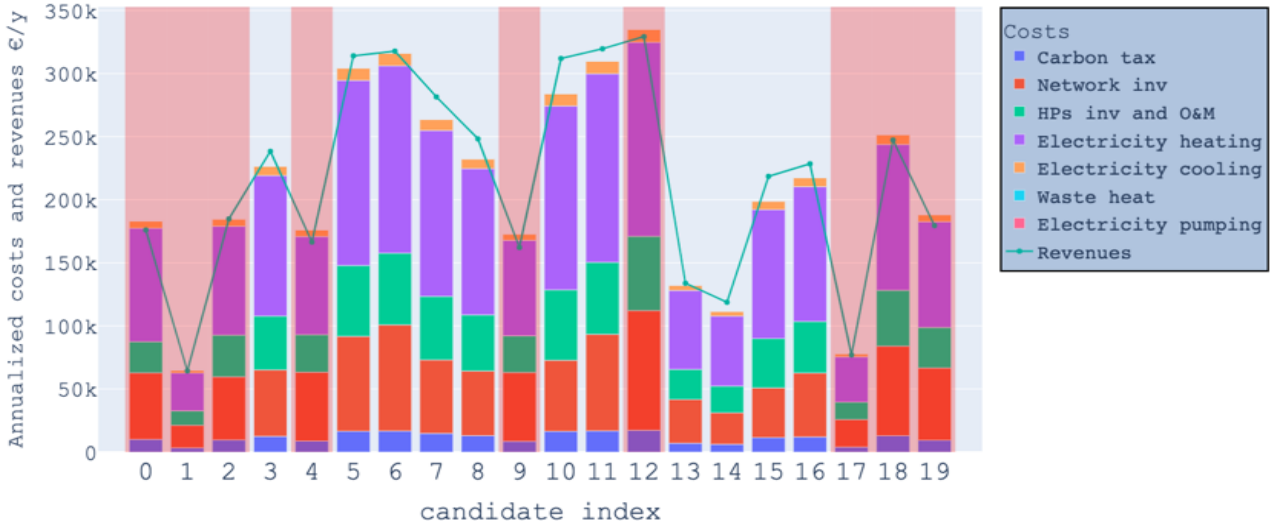

(b)

Figure 54. Optimal extension results after a 33% increase in the electricity price for the non-residential sector. (a) Final extension covering 81.65% of the FU. (b) Red panels represent unfeasible scenarios in the first extension step.

The maximum electricity price that a feasible scenario would yield is 0.35 €/kWh, based on an average SCOP of 4.68 for the highest performing HPs. If the SCOP of the HPs is reduced by 25% (as found in the study presented in [69], and also presented in subsection 3.3.2), this value drops to 0.265 €/kWh (Figure 55). This situation arises when SABAF, the primary waste heat provider from the second group, provides 1436 MWh/y of heat to a nearby area (covering only 3.85% of the total FU heat demand).

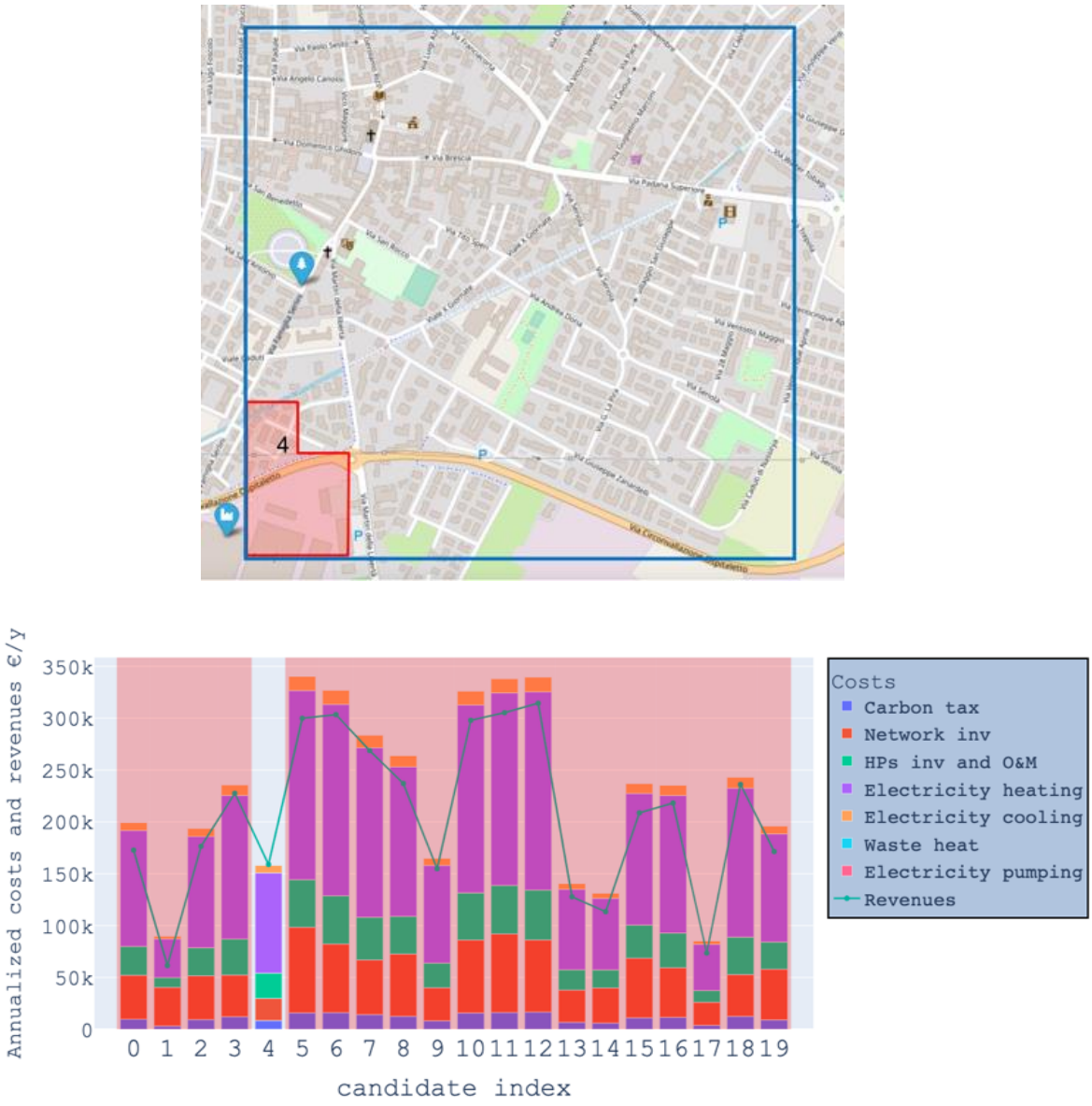

Figure 55. The maximum non-residential electricity price scenario yields a total extension of 3.85% of the total heat demand.

The best scenario for the NT-DHC solution occurs when subsidizing the energy costs by 33%, i.e., the electricity for non-residential customers is 0.1 €/kWh. The system can cover up to 95.47% of the total FU demand (see Figure 56). Because the network costs dominate in clusters 14 and 17, and the energy costs reduction is insufficient to justify the investment, the extension solutions generated by them are unfeasible. The price for non-residential customers, if the goal is to cover the entire FU, should be about 0.4 €/kWh (if all other costs remain constant and the phasing of WH plants remains unchanged).

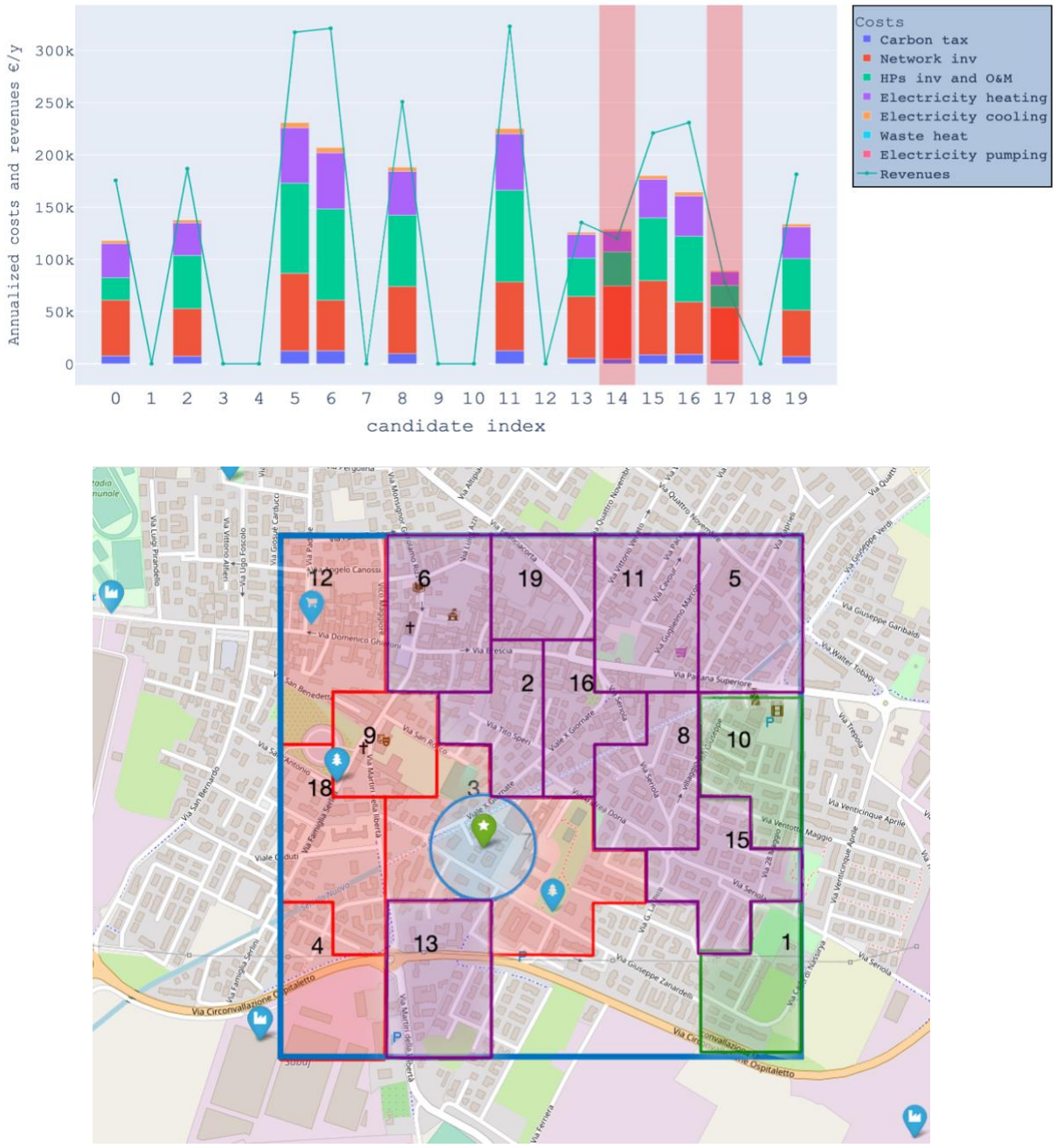

Figure 56. Subsidy on the non-residential electricity price scenario. 95.47% of the FU is covered under this condition.

Regarding the difference between decentralized HP technologies employing a network and individual A/W HP technologies, it is observed that the electricity costs are always higher for A/W HPs as compared to W/W HPs employed in the NT-DHC solution. Due to the favorable conditions of the source temperature during the heating season, the SCOP is higher for the latter case. Moreover, it was assumed that the NT-DHC solution could benefit from a non-residential electricity price that is 25% lower compared to the residential electricity used by the A/W HPs. A/W HPs always have higher installation and maintenance costs than networks. Even if both scenarios assume the same cost data, a worse SCOP implies a larger installed capacity. In contrast, the network costs of the NT-DHC solution are a disadvantage, especially in areas where heat is low in density. Minor items such as carbon taxes and electricity for cooling do not significantly impact the overall difference.

If the electricity price goes up by 50% (0.225 €/kWh for non-residential users and 0.30 €/kWh for residential users, respectively), the NT-DHC is always cheaper than A/W HPs and individual H&C systems, as shown in Figure 57(a). The NT-DHC solution offers a more significant advantage for larger clusters. However, even though the A/W HPs solution is less convenient for clusters 13 and 14 than the results in Figure 51, the NT-DHC solution's feasibility is compromised by the higher operating costs (Figure 57(b)).

On the contrary, if the residential electricity price is lowered below 0.20 €/kWh, NT-DHC becomes less competitive against A/W HPs, as observed in Table 16. In this table, the winning NT-DHC scenarios are quantified in each of the three extension steps (S1, S2 and S3). 1 means that 100% of the scenarios find NT-DHC the best solution compared to the individual H&C solutions, and 0 means the opposite. Combined with Table 17, these results show that the electricity market affects the competitiveness of H&C solutions. It is a fact that electricity-based solutions should be backed by a stable, secure, and affordable energy supply. Electricity, like many other resources, is traded in global markets as a commodity. Consequently, it can be subject to a high volatility for several reasons, from market signals, political conflicts, to pure speculation. In order to reduce the risks and vulnerability of global markets, which can ultimately affect the final consumers, it is crucial to create mechanisms to decouple from these effects. By diversifying the sources of electricity production and investing in local RES, this can be accomplished. To understand the mechanisms that may lead to favouring one solution over another, there needs to be a further analysis of the factors causing decoupling between residential and non-residential electricity pricing. The analysis of these factors, which can vary according to the market, taxation, country regulations, company agreements, etc., is outside the scope of this study.

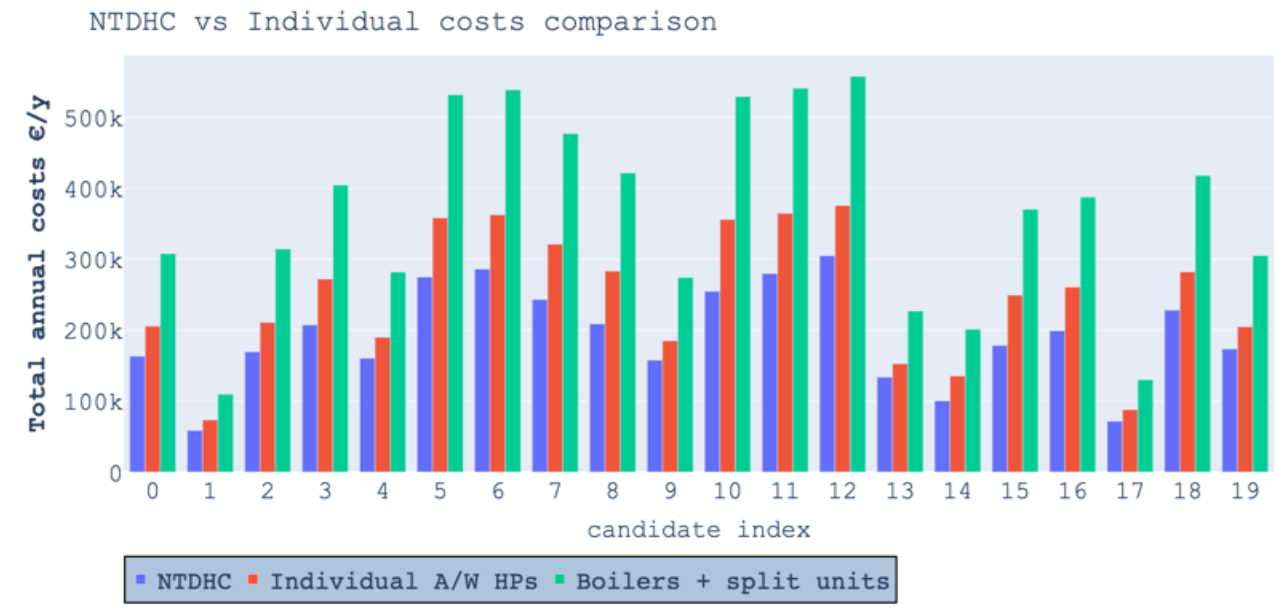

(a)

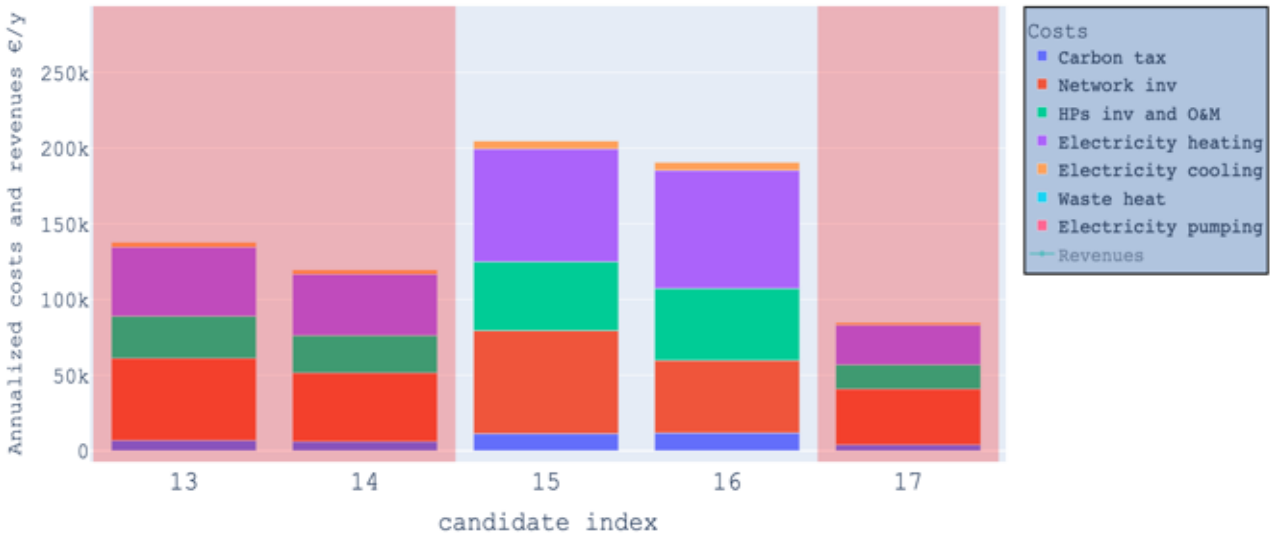

(b)

Figure 57. (a) A 50% increase in electricity prices shows how the NT-DHC solution outperforms the benchmark technologies. (b) The increase in the energy price and its impact on the NT-DHC solution.

Table 16. Pricing conditions where the NT-DHC solution is more competitive than individual H&C scenarios. The colors represent the probability of a winning scenario based on the pricing conditions.

	Individual H&C								
NT-DHC	Electricity price [€/kWh]	0.150			0.20			0.30		
		S1	S2	S3	S1	S2	S3	S1	S2	S3
	0.10	0.90	0.83	0.75	1	1	0.83	1	1	1
	0.15	0.5	0.79	0.54	1	0.94	0.75	1	1	1
	0.225	0	0	0	0.45	0.79	0.54	1	0.95	0.77

Table 17. Percentage of the FU demand covered after three extensions under different electricity pricing scenarios

% FU demand vs. electricity pricing scenarios	Individual H&C			
NT-DHC	[€/kWh]	0.15	0.20	0.30
	0.10	92.38	95.47	95.47
	0.15	81.65	92.38	92.38
	0.225	0	81.65	85.83

Since the NT-DHC solution has network costs (and not explicitly quantified administrative costs) that individual solutions lack, its competitiveness largely depends on favorable conditions leading to lower operating costs. In this regard, the HPs in the network solution must perform at their highest level. The factors that may reduce the HPs' performance must be monitored; this includes systemic inefficiencies brought about by the HP's on/off cycles, thermal losses in substation pipes and buffers, and differences between datasheet and actual HP's performance [68].

Finally, Figure 58 and Figure 59 illustrate how the temperature of the leading waste heat source, and therefore the network, impacts the HPs SCOP and SEER. A compromise between a high efficiency in heating and cooling modes is achieved at a temperature of 27-30°C. Nevertheless, higher temperatures are desirable for a network that primarily supplies heating.

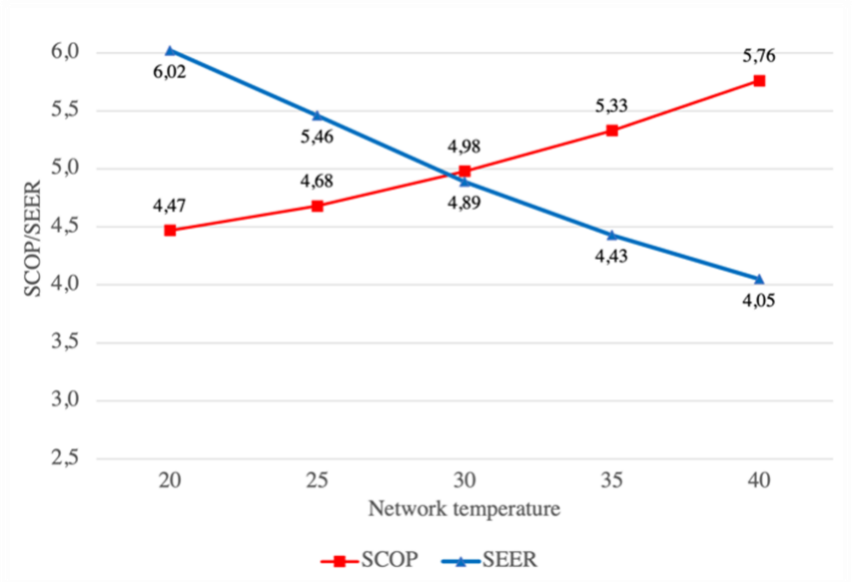

(a)

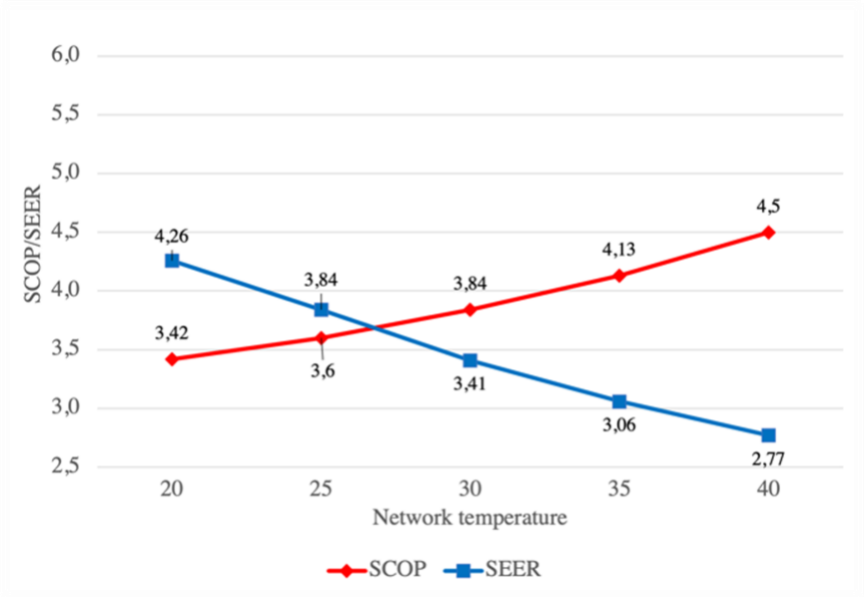

(b)

Figure 58. (a) Network temperature conditions and their impact on the theoretical network HPs performance (SCOP and SEER).(b) Theoretical performance was reduced by 25% due to operational inefficiencies independent from the source temperature.

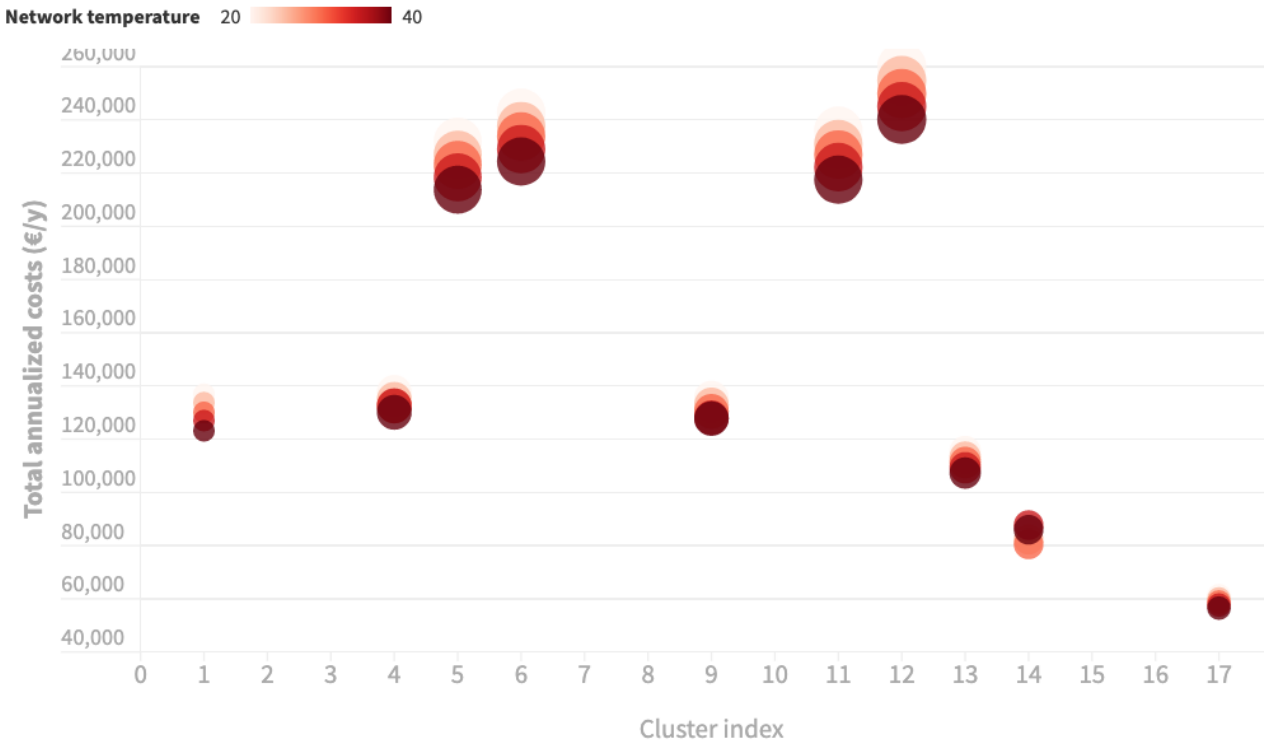

Figure 59. Impact in the total annualized costs based on different network operating temperatures. The size of the bubble represents the cluster peak power. Increasing the network temperature leads to maximum savings in larger clusters.

Concerning gas prices, the reference simulation always shows an economic advantage compared to the individual H&C solution (the costs are on average 2.2 times higher than the NT-DHC costs). If the gas price goes up 50%, the costs difference becomes almost three times.

5.3 Emission factors

A reduction in the renewable energy potential of electricity barely affects the techno-economic feasibility of the network extension. As a result, a scenario with a high share of renewables on the electricity grid (a reduction of 50% of the 2018 emissions) could save only 2.22 - 3.07% of the total costs. On the other hand, a grid based on emission levels from 2005 in Italy shows a maximum cost increase of 4.43%. Due to the electricity used by the HPs, the overall costs could have been even lower since these scenarios assume the network manager needs to pay a carbon tax of 75 €/tCO_2 (relatively high taxation compared to the current European situation).

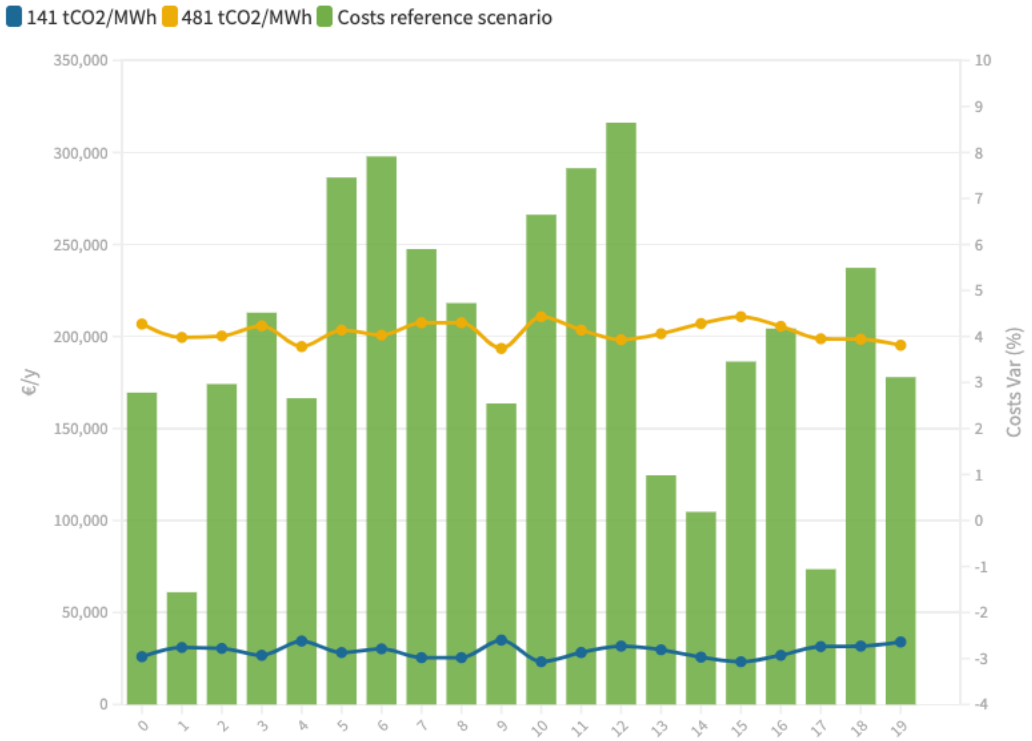

Figure 60. Total costs variation concerning the default emission factor. Results of the first extension scenario.

Table 18. Minimum and maximum costs variation in all extension scenarios.

Extension scenario	**Electricity emission factor**			
	0.141 tCO_2/MWh		**0.483 tCO_2/MWh**	
	Min var (%)	Max var (%)	Min var (%)	Max var (%)
1	-3,07	-2,6	3,74	4,43
2	-3,20	-2,67	3,84	4,62
3	-3,06	-2,22	3,2	4,42

Figure 61 illustrates the relationship between heating demand and CO_2 emissions in all the extensions. According to the top figure, carbon emissions associated with electricity increase with the clusters' size. The distances between sources and sinks vary in each extension, affecting the total costs. The figure at the bottom displays the difference in the total CO_2 emissions based on the selected electricity emission factor. Most significant variations occur in larger clusters; for example, the largest cluster exhibits a 49.8% emissions reduction (115 tCO_2 savings) using an electricity emission factor half that of today, and a 71.8% increase (166 tCO_2 more) when using a factor representative of the 2005 electric grid.

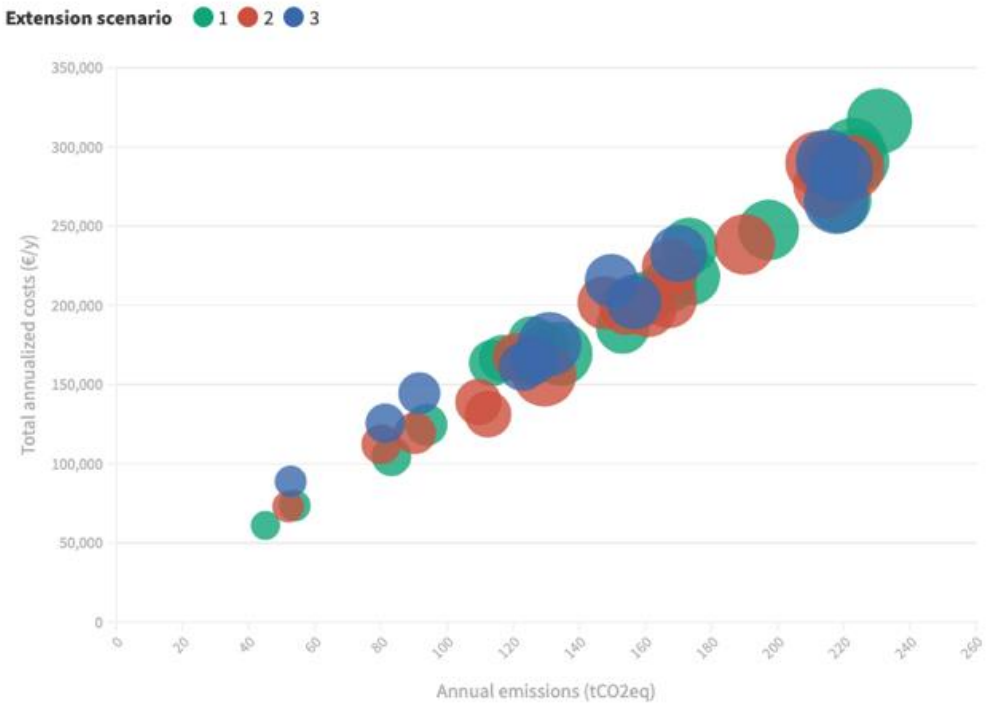

(a)

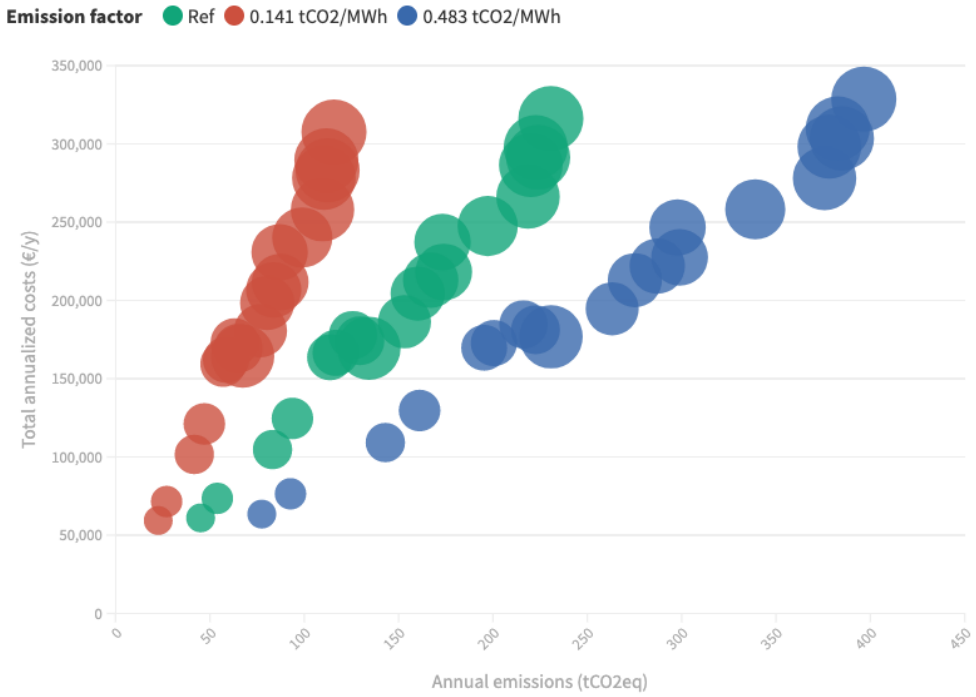

(b)

Figure 61. Total annualized costs vs. annual emissions. (a) All extension scenarios. The bubble size represents the candidates' peak power (MW). (b) First extension scenario with different electricity emission factors.

5.4 Cooling scenarios

In Figure 62, the NT-DHC system costs are compared with the A/W HPs solution in the first default extension. The orange bars illustrate how the overall cost of both solutions increases as cooling penetration increases. In both the 2020 and 2050 scenarios, it is observed that the former is less costly than the latter. It is possible to see from Figure 63 that due to a higher cooling penetration, the NT-DHC solution has a higher advantage when compared to traditional gas boilers combined with conventional cooling units. Figure 64 shows that a different transition pathway results from the cooling scenario of 2050 as compared to the transition pathway obtained in Figure 56. Due to the cumulative cooling sales under these cooling conditions, clusters 2 and 13 combined result in a more attractive investment option than cluster 12 alone in the second iteration.

It can be concluded that the NT-DHC solution in general benefits from a greater cooling penetration. Nevertheless, this factor alone does not justify investing in low heat density areas. Those areas are best suited to A/W HPs, as shown in the previous scenarios.

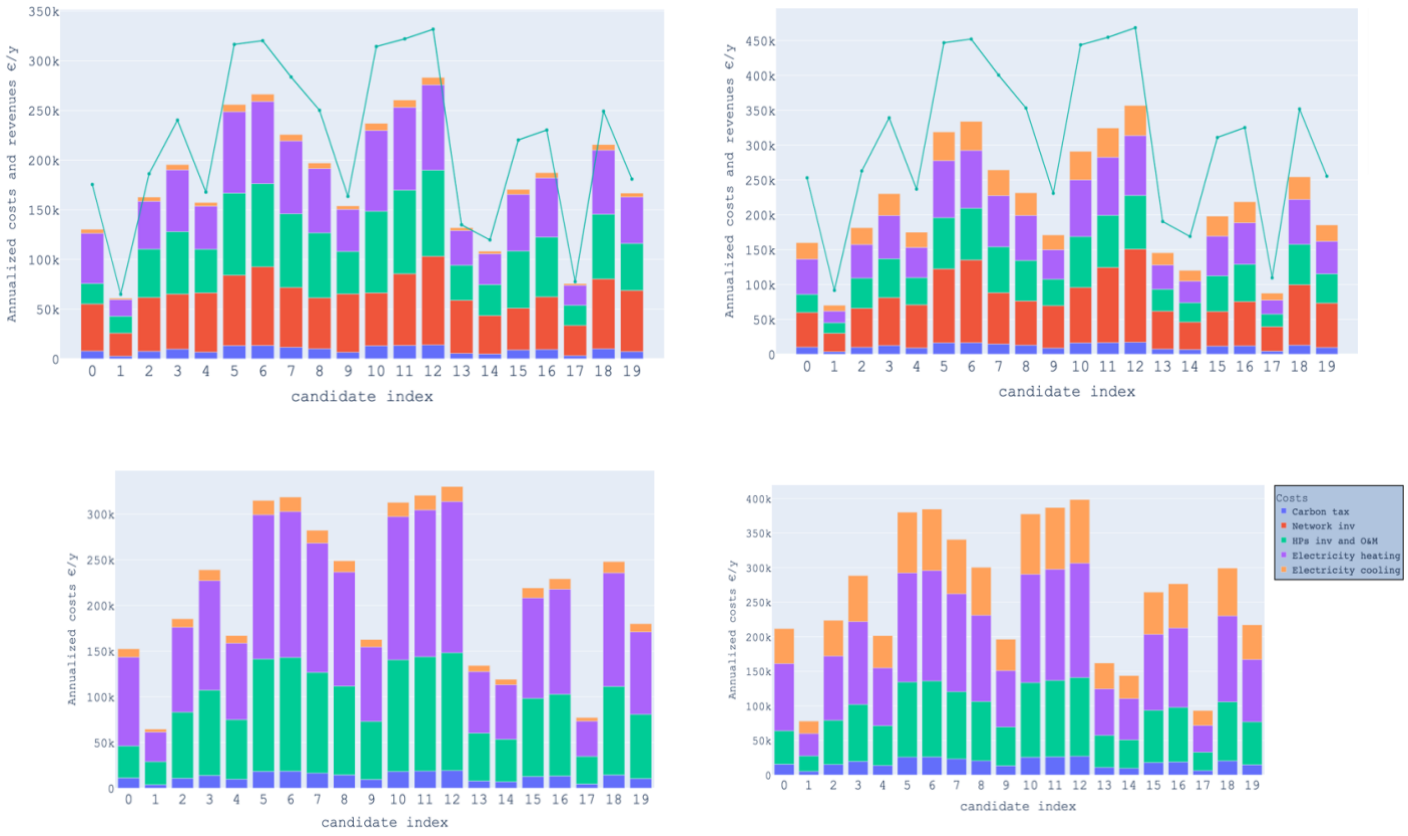

(a) (b)

Figure 62. Cooling scenarios. NT-DHC costs are shown at the top, while A/W HPs costs are shown at the bottom. (a) 2020 scenario (b) 2050 scenario

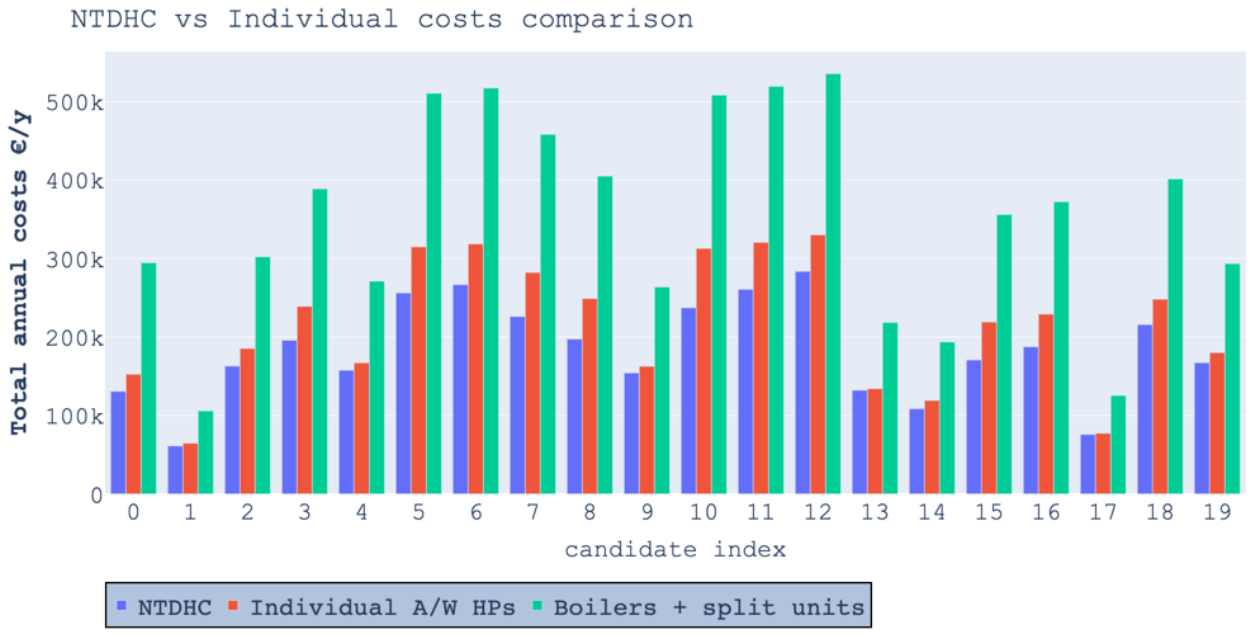

(a)

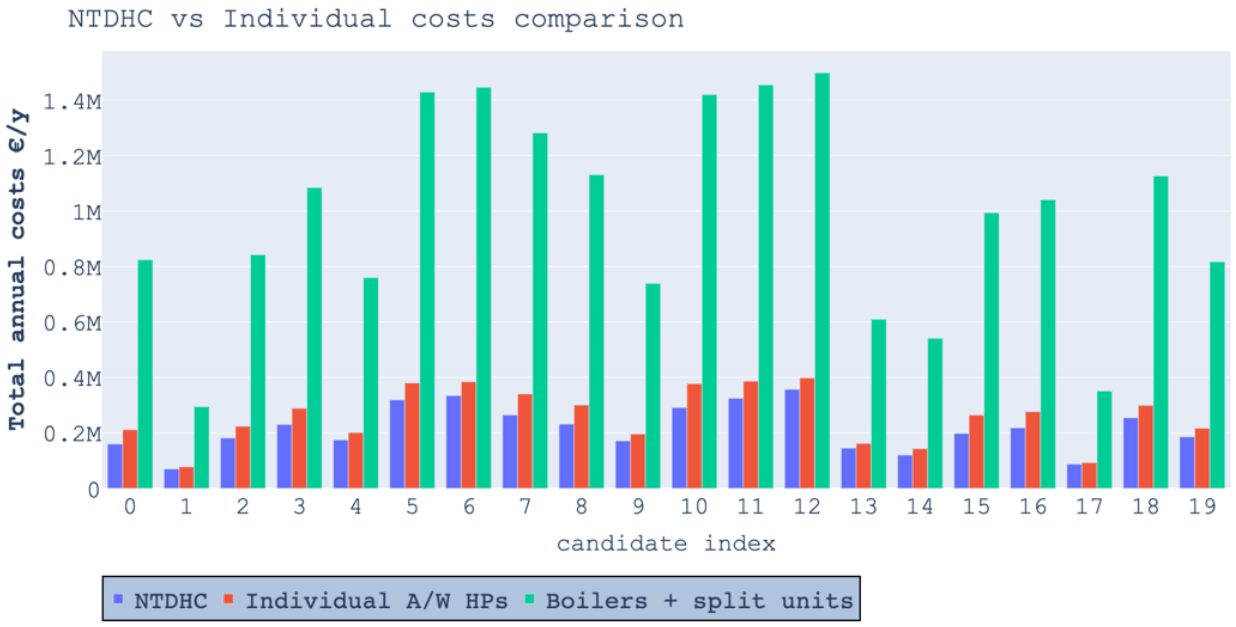

(b)

Figure 63. Comparison of the NT-DHC solution vs. individual H&C under different cooling penetration scenarios (a) 2020 scenario (b) 2050 scenario

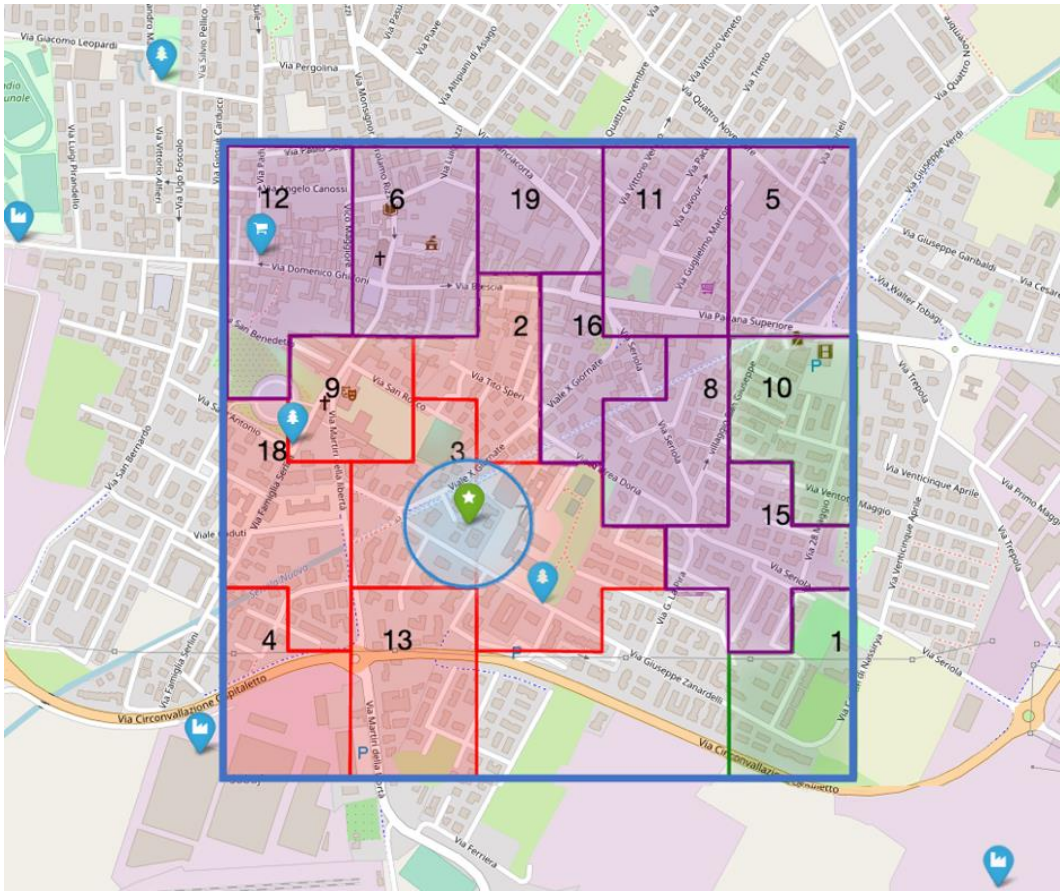

Figure 64. Final extension covering 95.47 % of the FU in the cooling scenario 2050.

6

Conclusions and further work

This study presents a methodology for analyzing scenarios and identifying spatial expansions of a novel type of district heating network. The application to a case study has been conducted to evaluate the system's competitiveness against conventional heating and cooling systems. In this chapter, the motivations of this dissertation and the goals it aimed to achieve are summarized, along with the main contributions and results, followed by future research and perspectives.

Motivations and objectives

NT-DHC is one of the most recent types of DH networks, and therefore it is important to study their applications with tools and models. As of today, the ability to model NT-DHC systems and create master plans is very limited even for traditional high-temperature networks (TDH). Techno-economic assessments (TEAs) in the DHC sector are typically focused on optimizing existing systems. Instead, this project offers an approach to TEA in areas where DH is not present, or the conditions are limited for the development of TDH.

This dissertation aimed to develop a reliable methodology for assessing NT-DHC systems' technical, economic, and environmental performance. Specifically, the following objectives were proposed:

- *To develop a new methodology for the techno-economic scenario analysis of NT-DHC systems and validate it on a case study.*
- *To apply an optimization model to identify transition pathways for the network extension and its application to the case study.*

Main contributions and results

Chapter 2: Model methodology

In this chapter, it is presented in detail a new methodology for the TEA of NT-DHC systems and the identification of future spatial expansion scenarios to neighboring areas. The model simulations are executed with an hourly resolution, allows the integration of multiple WH sources, thermal availability, and temperature. The network control allows the implementation of specific operation strategies based on sources' merit order. A knapsack approach is proposed for solving the optimal expansion problem of a NT-DHC system. A mathematical formulation of the 0-1 knapsack problem in the DHC context is provided. The computational advantages are discussed and its limitations.

As a result, this comprehensive methodology extends the State of the Art by modeling the performance of a network system based on decentralized HP substations, as well as incorporating economic factors that are not considered in DH physical models and optimizing the selection of the best system extension.

Chapter 3: Verification and calibration

The chapter focuses on the core DH model validation and calibration. It is built on the lumped approach of the Excel tool developed during the FLEXYNETS project. In an initial stage, a parametric analysis was carried out in a theoretical FU in a Mediterranean climate to assess the performance of a NT-DHC system using different shares of WH. The results show economic advantages of the network solution with an important role of cooling.

The case study of the NT-DHC network in Ospitaletto, Italy is presented. The lumped model and the physical model (also called "detailed") are described, and the main technical results are compared. It was concluded that the models provided results in reasonable agreement: a 15% difference in the overall electricity consumed by the HPs. According to the approximate and detailed models, the estimated thermal losses to the ground were 46% and 40%, respectively, due to uninsulated pipes. According to both models, the pumping consumptions were 2% of the total thermal energy delivered at the HPs' evaporators. Electric consumption of decentralized HPs, heat absorbed by the HPs from the network, and average COP are all closely linked.

Finally, the computational performance of both models was also reported. The lumped model can be executed immediately, while the detailed model takes about 30 min to solve the whole network (about 50 vertices) for an entire year with an hourly time step. The difference between the two types of models is evident: whereas intermediate approximation levels can be chosen, a detailed model is impractical

for parametric analysis or optimization.

The second part of the chapter discusses the calibration of an upgraded lumped model with experimental data: the characteristics described in Table 2 had been implemented in Python.

The network relies on source temperatures between 15 and 25 °C and exhibits an SPF of 3.11. Large parts of the network pipes are not insulated, resulting in thermal losses of about 30%. Electric pumping consumptions are of the order of 4 % of the users' thermal consumptions. The lumped model provides proper order of magnitudes for these values even using simplified default estimates. However, for a good agreement (a few percent of the difference in the most important indicators), two simple phenomenological coefficients must be calibrated.

Based on this analysis, it was concluded that a lumped approach seems appropriate for such a simple network (most deviations can be explained by physical details unrelated to individual differences). A lumped model offers a quick tool for scenario analysis, a needed application for this innovative NT-DHC network strongly coupling electrical and thermal consumptions.

Chapters 4 and 5: Model application and results

Despite the broadness of the proposed method, the approach was applied to the Ospitaletto case study for simplicity. The essential inputs required for a default simulation are presented in Chapter 4: sources and heat density data, techno-economic and environmental parameters, as well as assumptions. A sensitivity analysis is carried out to answer the research questions presented in subsection 1.4. The results from Chapter 5 highlight the following:

Is it feasible to expand a NT-DHC network efficiently using available waste heat sources?

The results of applying the model to the case study indicate that NT-DHC systems can be feasibly expanded based on the current WH availability in the city, and are more suitable in dense urban areas, whereas A/W HP systems may be more competitive in low-heat density areas. Nevertheless, in the case of Ospitaletto, despite having low building heat density compared to larger cities, it is still possible to identify feasible scenarios. This opens the opportunity to many other cases.

Which conditions (technical, economic, environmental) make the NT-DHC solution more competitive than individual solutions?

Since the NT-DHC solution has network costs (and not explicitly quantified administrative costs) that individual solutions lack, its competitiveness largely depends on favorable conditions leading to lower

operating costs. In this regard, the HPs in the network solution must perform at their highest level. By selecting waste heat sources at a 30-40°C temperature range, the SCOP of the NT-DHC solution can be enhanced over A/W HPs.
The electricity market affects the competitiveness of H&C solutions. To reduce the risks and vulnerability of global markets, it is imperative to create mechanisms to decouple from these effects. This can be accomplished by diversifying the sources of electricity production and investing in local RES.

Is it possible to identify optimal expansion strategies, minimizing the overall costs and emissions (through carbon taxes)?

The optimal expansion strategy is highly susceptible to the selected boundary conditions. It was observed from the application of the method to the case study that the expansion strategy changes drastically when varying the order in which the WH sources become available. The tool allows for a detailed analysis of the boundary conditions that make the NT-DHC solution competitive against individual H&C technologies, as well as the assessment of different business models and the exploration of the break-even points.

Future research and perspectives

Future research could apply this methodology to other locations with higher heat density zones or other climatic conditions (with more significant cooling requirements). Despite that the focus of this research was the study of NT-DHC technology, it is worth investigating under which conditions (besides the source availability) it is proven to be an advantage over 4GDH (where the HPs are located at the sources rather than the user substations and the network temperature remains high). Finally, this framework could be refined further to study the effects of introducing different kinds of storages and, therefore, analyze the system's resilience to sources' fluctuations. (e.g., shutdown of industrial plants supplying WH) and maximize low-grade heat recovery.
The presented model has the potential impact in the DHC sector of reducing the energy demand risks, providing more certainty by identifying the zones where to expand a network to be competitive. This tool is expected to be used for pre-feasibility studies and preliminary design of a new type of DHC network, contributing to a deeper understanding of the opportunities and constraints of a system of this kind from a techno-economic standpoint.

Bibliography

[1] "AR5 Synthesis Report: Climate Change 2014 — IPCC." https://www.ipcc.ch/report/ar5/syr/

[2] "Data & Statistics," *IEA*. https://www.iea.org/data-and-statistics/data-browser

[3] M. Isaac and D. Vuuren, "Modeling global residential sector energy demand for heating and air conditioning in the context of climate change," *Energy Policy*, vol. 37, pp. 507–521, Feb. 2009.

[4] "Low-Temperature District Heating Implementation Guidebook. IEA DHC Report, 2021," p. 206.

[5] S. Werner, "District Heating and Cooling," Elsevier, 2013.

[6] "FLEXYNETS project (EU H2020, GA No. 649820)." http://www.flexynets.eu

[7] H. Lund *et al.*, "4th Generation District Heating (4GDH)," *Energy*, vol. 68, pp. 1–11, Apr. 2014.

[8] S. Buffa, M. Cozzini, M. D'Antoni, M. Baratieri, and R. Fedrizzi, "5th generation district heating and cooling systems: A review of existing cases in Europe," *Renew. Sustain. Energy Rev.*, vol. 104, pp. 504–522, Apr. 2019, doi: 10.1016/j.rser.2018.12.059.

[9] S. Boesten, W. Ivens, S. C. Dekker, and H. Eijdems, "5th generation district heating and cooling systems as a solution for renewable urban thermal energy supply," in *Advances in Geosciences*, Sep. 2019, vol. 49, pp. 129–136. doi: 10.5194/adgeo-49-129-2019.

[10] H. Lund *et al.*, "Perspectives on fourth and fifth generation district heating," *Energy*, vol. 227, p. 120520, Jul. 2021, doi: 10.1016/j.energy.2021.120520.

[11] "D2Grids." https://www.nweurope.eu/projects/project-search/d2grids-increasing-the-share-of-renewable-energy-by-accelerating-the-roll-out-of-demand-driven-smart-grids-delivering-low-temperature-heating-and-cooling-to-nwe-cities/ (accessed Sep. 29, 2020).

[12] "Life4heatrecovery project." http://www.life4heatrecovery.eu/en/

[13] "Rewardheat project." https://www.rewardheat.eu/en/

[14] "Reuseheat project," *ReUseHeat*. https://www.reuseheat.eu/

[15] "W.E. District," *Wedistrict*. https://www.wedistrict.eu/

[16] "Home - Upgrade DH." https://www.upgrade-dh.eu/en/home/

[17] "COOL, low temperature district heating (LTHD) Lund & Høje-Taastrup - COOL DH." http://www.cooldh.eu/

[18] W. Ma, S. Fang, G. Liu, and R. Zhou, "Modeling of district load forecasting for distributed energy system," *Appl. Energy*, vol. 204, pp. 181–205, Oct. 2017.

[19] "Trnsys18." http://trnsys.de/en/trnsys18

[20] "HOMER - Hybrid Renewable and Distributed Generation System Design Software." https://www.homerenergy.com/

[21] "Welcome to ESP-r." https://www.esru.strath.ac.uk//Courseware/ESP-r/tour/

[22] "TERMIS Simulation Modes | TERMIS." http://7t.dk/products/termis/Product-Information/termis-simulation-modes.aspx

[23] "energyPRO - A leading software module for complex projectsEMD International." https://www.emd-international.com/energypro/modules/

[24] "Comsof Heat - District Heating Network Planning & Design Software," *Comsof Heat*. https://comsof.com/heat/

[25] "EnergyPLAN," *EnergyPLAN*. https://www.energyplan.eu/

[26] "LEAP." https://leap.sei.org/default.asp

[27] "Crystal City," *Artelys*. https://www.artelys.com/crystal/city/

[28] "METIS." https://energy.ec.europa.eu/data-and-analysis/energy-modelling/metis_en (accessed Mar. 29, 2022).

[29] S. Nielsen, K. Hansen, R. Lund, and D. Moreno, "Unconventional Excess Heat Sources for District

Heating in a National Energy System Context," *Energies*, vol. 13, no. 19, Art. no. 19, Jan. 2020, doi: 10.3390/en13195068.
[30] H. Dorotić, K. Čuljak, J. Miškić, T. Pukšec, and N. Duić, "Technical and Economic Assessment of Supermarket and Power Substation Waste Heat Integration into Existing District Heating Systems," *Energies*, vol. 15, no. 5, Art. no. 5, Jan. 2022, doi: 10.3390/en15051666.
[31] M. Bilardo, F. Sandrone, G. Zanzottera, and E. Fabrizio, "Modelling a fifth-generation bidirectional low temperature district heating and cooling (5GDHC) network for nearly Zero Energy District (nZED)," *Energy Rep.*, vol. 7, pp. 8390–8405, Nov. 2021, doi: 10.1016/j.egyr.2021.04.054.
[32] "Dublin Region Energy Master Plan | Energy Efficiency Agency Dublin | Codema." https://www.codema.ie/projects/local-projects/dublin-region-energy-master-plan/ (accessed Mar. 25, 2022).
[33] A. Manzella, "General Introduction to Geothermal Energy," in *Geothermal Energy and Society*, A. Manzella, A. Allansdottir, and A. Pellizzone, Eds. Cham: Springer International Publishing, 2019, pp. 1–18. doi: 10.1007/978-3-319-78286-7_1.
[34] B. Sanner, "Shallow geothermal energy." GHC Bulletin, 2001.
[35] A. Mustafa Omer, "Ground-source heat pumps systems and applications," *Renew. Sustain. Energy Rev.*, vol. 12, no. 2, pp. 344–371, Feb. 2008, doi: 10.1016/j.rser.2006.10.003.
[36] P. L. Younger, "Ground-Coupled Heating-Cooling Systems in Urban Areas: How Sustainable Are They?," *Bull. Sci. Technol. Soc.*, vol. 28, no. 2, pp. 174–182, Apr. 2008, doi: 10.1177/0270467607313963.
[37] D. Banks, *An introduction to thermogeology: ground source heating and cooling*. John Wiley & Sons, 2012.
[38] "ReUseHeat Handbook," *ReUseHeat*, Apr. 04, 2022. https://www.reuseheat.eu/reuseheat-handbook/ (accessed Apr. 07, 2022).
[39] A. M. Jodeiri, M. J. Goldsworthy, S. Buffa, and M. Cozzini, "Role of sustainable heat sources in transition towards fourth generation district heating – A review," *Renew. Sustain. Energy Rev.*, vol. 158, p. 112156, Apr. 2022, doi: 10.1016/j.rser.2022.112156.
[40] M. Andrés, M. Regidor, A. Macía, A. Vasallo, and K. Lygnerud, "Assessment methodology for urban excess heat recovery solutions in energy-efficient District Heating Networks," *Energy Procedia*, vol. 149, pp. 39–48, Sep. 2018, doi: 10.1016/j.egypro.2018.08.167.
[41] M. Wahlroos, M. Pärssinen, S. Rinne, S. Syri, and J. Manner, "Future views on waste heat utilization – Case of data centers in Northern Europe," *Renew. Sustain. Energy Rev.*, vol. 82, pp. 1749–1764, Feb. 2018, doi: 10.1016/j.rser.2017.10.058.
[42] F. Bühler, S. Petrović, K. Karlsson, and B. Elmegaard, "Industrial excess heat for district heating in Denmark," *Appl. Energy*, vol. 205, pp. 991–1001, Nov. 2017, doi: 10.1016/j.apenergy.2017.08.032.
[43] F. Bühler, S. Petrović, T. Ommen, F. M. Holm, H. Pieper, and B. Elmegaard, "Identification and Evaluation of Cases for Excess Heat Utilisation Using GIS," *Energies*, vol. 11, no. 4, p. 762, Apr. 2018, doi: 10.3390/en11040762.
[44] M. D. A. Albert, K. O. Bennett, C. A. Adams, and J. G. Gluyas, "Waste heat mapping: A UK study," *Renew. Sustain. Energy Rev.*, vol. 160, p. 112230, May 2022, doi: 10.1016/j.rser.2022.112230.
[45] R. C. McKenna and J. B. Norman, "Spatial modelling of industrial heat loads and recovery potentials in the UK," *Energy Policy*, vol. 38, no. 10, pp. 5878–5891, Oct. 2010, doi: 10.1016/j.enpol.2010.05.042.
[46] S. Broberg, S. Backlund, M. Karlsson, and P. Thollander, "Industrial excess heat deliveries to Swedish district heating networks: Drop it like it's hot," *Energy Policy*, vol. 51, pp. 332–339, Dec. 2012, doi: 10.1016/j.enpol.2012.08.031.
[47] J. Pelda, F. Stelter, and S. Holler, "Potential of integrating industrial waste heat and solar thermal energy into district heating networks in Germany," *Energy*, vol. 203, p. 117812, Jul. 2020, doi: 10.1016/j.energy.2020.117812.

[48] L. Miró, S. Brueckner, R. McKenna, and L. F. Cabeza, “Methodologies to estimate industrial waste heat potential by transferring key figures: A case study for Spain,” *Appl. Energy*, vol. 169, pp. 866–873, May 2016, doi: 10.1016/j.apenergy.2016.02.089.

[49] A. Dénarié *et al.*, “Assessment of waste and renewable heat recovery in DH through GIS mapping: The national potential in Italy,” *Smart Energy*, vol. 1, p. 100008, Feb. 2021, doi: 10.1016/j.segy.2021.100008.

[50] G. Spirito, A. Dénarié, V. F. Cirillo, F. Casella, J. Famiglietti, and M. Motta, “Energy mapping and district heating as effective tools to decarbonize a city: Analysis of a case study in Northern Italy,” *Energy Rep.*, vol. 7, pp. 254–262, Oct. 2021, doi: 10.1016/j.egyr.2021.08.147.

[51] J. Pelda, R. Geyer, C. Sinclair, R. Stollnberger, E. Gebetsroither-Geringer, and S. Holler, “MEMPHIS - Methodology to Evaluate and Map the Potential of Waste Heat from Industry, Service Sector and Sewage Water by Using Internationally Available Open Data,” IEA DHC, 2019. [Online]. Available: https://www.iea-dhc.org/the-research/annexes/annex-xii/annex-xii-project-02

[52] S. Frederiksen and S. Werner, *District Heating and Cooling*. Studentlitteratur, 2013.

[53] “Residential heating with wood and coal: health impacts and policy options in Europe and North America,” World Health Organization, Denmark, 2015. [Online]. Available: https://www.euro.who.int/en/health-topics/environment-and-health/air-quality/publications/2015/residential-heating-with-wood-and-coal-health-impacts-and-policy-options-in-europe-and-north-america

[54] B. Koffi, A. Cerutti, M. Duerr, A. Iancu, A. Kona, and G. Janssens-Maenhout, “Covenant of Mayor Default Emission Factors for the Member States of the European Union. Joint Research Centre (JRC) of the European Commission.” 2017.

[55] M. A. Drupp, F. Nesje, and R. C. Schmidt, “Pricing Carbon,” Social Science Research Network, Rochester, NY, SSRN Scholarly Paper 4054113, 2022. doi: 10.2139/ssrn.4054113.

[56] E. Asen, “Carbon Taxes in Europe,” *Tax Foundation*, Jun. 03, 2021. https://taxfoundation.org/carbon-taxes-in-europe-2021/ (accessed Feb. 17, 2022).

[57] “The EU’s Carbon Border Tax Will Redefine Global Value Chains,” *BCG Global*, Oct. 07, 2021. https://www.bcg.com/publications/2021/eu-carbon-border-tax (accessed Mar. 02, 2022).

[58] M. Cozzini, S. Calixto, S. Buffa, and R. Fedrizzi, “Reti di teleriscaldamento e teleraffrescamento basate su pompe di calore decentralizzate,” *AICARR J.*, vol. 60.

[59] M. Cozzini, M. D’Antoni, S. Buffa, R. Fedrizzi, and F. Bava, “District Heating and Cooling Networks Based on Decentralized Heat Pumps: Energy Efficiency and Reversibility at Affordable Costs”.

[60] “Hotmaps Project - The open source mapping and planning tool for heating and cooling,” *Hotmaps Project*. https://www.hotmaps-project.eu/

[61] F. Pedregosa *et al.*, “Scikit-learn: Machine Learning in Python,” *J. Mach. Learn. Res.*, vol. 12, no. 85, pp. 2825–2830, 2011.

[62] U. Persson and S. Werner, “Effective Width : The Relative Demand for District Heating Pipe Lengths in City Areas,” 2010, pp. 128–131.

[63] O. A. Sianaki, O. Hussain, and A. R. Tabesh, “A Knapsack problem approach for achieving efficient energy consumption in smart grid for endusers’ life style,” in *2010 IEEE Conference on Innovative Technologies for an Efficient and Reliable Electricity Supply*, Sep. 2010, pp. 159–164. doi: 10.1109/CITRES.2010.5619873.

[64] B. Göblyös and M. Réger, “Mathematical model for the optimal distribution of district heat sources,” in *2016 IEEE 14th International Symposium on Applied Machine Intelligence and Informatics (SAMI)*, Jan. 2016, pp. 121–124. doi: 10.1109/SAMI.2016.7422993.

[65] B. Göblyös and M. Réger, “Determining the priority of heat sources used in district heating,” in *2015 IEEE 13th International Symposium on Intelligent Systems and Informatics (SISY)*, Sep. 2015, pp. 319–322. doi: 10.1109/SISY.2015.7325402.

[66] M. Cozzini, R. Fedrizzi, S. Calixto, and G. Manzolini, “Modelling of an Existing Neutral Temperature District Heating Network: Detailed and Approximated Approaches,” presented at the Sustainable Development of Energy, Waterand Environment Systems, Cologne, Germany, 2020. [Online]. Available: https://www.cologne2020.sdewes.org/programme
[67] S. Calixto, M. Cozzini, and G. Manzolini, “Modelling of an Existing Neutral Temperature District Heating Network: Detailed and Approximate Approaches,” *Energies*, vol. 14, no. 2, Art. no. 2, Jan. 2021.
[68] S. Calixto, C. Köseoğlu, M. Cozzini, and G. Manzolini, “Monitoring and aggregate modelling of an existing neutral temperature district heating network,” presented at the The 17th International Symposium on District Heating and Cooling, Nottingham Trent University, Nottingham, United Kingdom, Sep. 2021.
[69] S. Calixto, C. Köseoğlu, M. Cozzini, and G. Manzolini, “Monitoring and aggregate modelling of an existing neutral temperature district heating network,” *Energy Rep.*, vol. 7, pp. 140–149, Oct. 2021.
[70] “Hotmaps Project.” https://www.hotmaps-project.eu/ (accessed Dec. 11, 2019).
[71] S. Pezzutto *et al.*, “D2.3 WP2 Report – Open Data Set for the EU28,” p. 158.
[72] “TABULA WebTool.” https://webtool.building-typology.eu/#bm (accessed Mar. 25, 2022).
[73] B. A. Fricke, “Waste Heat Recapture from Supermarket Refrigeration Systems,” ORNL/TM-2011/239, 1028753, Nov. 2011. doi: 10.2172/1028753.
[74] D. Verma and M. Meil, “A Comparison of Spectral Clustering Algorithms,” p. 19.
[75] L. D. D. Harvey, “Using modified multiple heating-degree-day (HDD) and cooling-degree-day (CDD) indices to estimate building heating and cooling loads,” *Energy Build.*, vol. 229, p. 110475, Dec. 2020, doi: 10.1016/j.enbuild.2020.110475.
[76] J. Spinoni, J. Vogt, and P. Barbosa, “European degree-day climatologies and trends for the period 1951–2011,” *Int. J. Climatol.*, vol. 35, no. 1, pp. 25–36, 2015.
[77] Dipasquale Chiara, R. Fedrizzi, A. Bellini, and M. D’Antoni, “D6.3b Performance of the Studied Systemic Renovation Packages – Single Family Houses.” iNSPiRe project, 2015.
[78] iNSPiRe project, “iNSPiRe project website,” *iNSPiRe*. https://inspire-fp7.eu/ (accessed Mar. 25, 2022).
[79] K. Vajen and U. Kassel, “DHWcalc: PROGRAM TO GENERATE DOMESTIC HOT WATER PROFILES WITH STATISTICAL MEANS FOR USER DEFINED CONDITIONS.”
[80] Euro Heat & Power, “EcoHeatCool project. WP2 The European Cool Market,” Jun. 25, 2013. https://web.archive.org/web/20130625225232/http://www.euroheat.org/Files/Filer/ecoheatcool/documents/Ecoheatcool_WP1_Web.pdf (accessed Mar. 23, 2022).
[81] I. N. Belova, A. S. Ginzburg, and L. A. Krivenok, “Heating seasons length and degree days trends in Russian cities during last half century,” *Energy Procedia*, vol. 149, pp. 373–379, Sep. 2018, doi: 10.1016/j.egypro.2018.08.201.
[82] Y. Shi, D.-F. Zhang, Y. Xu, and B.-T. Zhou, “Changes of heating and cooling degree days over China in response to global warming of 1.5 °C, 2 °C, 3 °C and 4 °C,” *Adv. Clim. Change Res.*, vol. 9, no. 3, pp. 192–200, Sep. 2018, doi: 10.1016/j.accre.2018.06.003.
[83] A. D’Amico, G. Ciulla, D. Panno, and S. Ferrari, “Building energy demand assessment through heating degree days: The importance of a climatic dataset,” *Appl. Energy*, vol. 242, pp. 1285–1306, May 2019, doi: 10.1016/j.apenergy.2019.03.167.
[84] O. Büyükalaca, H. Bulut, and T. Yılmaz, “Analysis of variable-base heating and cooling degree-days for Turkey,” *Appl. Energy*, vol. 69, no. 4, pp. 269–283, Aug. 2001, doi: 10.1016/S0306-2619(01)00017-4.
[85] A. Matzarakis and C. Balafoutis, “Heating degree-days over Greece as an index of energy consumption,” *Int. J. Climatol.*, vol. 24, no. 14, pp. 1817–1828, 2004, doi: 10.1002/joc.1107.
[86] I. Yildiz and B. Sosaoglu, “Spatial distributions of heating, cooling, and industrial degree-days in Turkey,” *Theor. Appl. Climatol.*, vol. 90, no. 3, pp. 249–261, Nov. 2007, doi: 10.1007/s00704-006-0281-1.

[87] K. Papakostas, T. Mavromatis, and N. Kyriakis, “Impact of the ambient temperature rise on the energy consumption for heating and cooling in residential buildings of Greece,” *Renew. Energy*, vol. 35, no. 7, pp. 1376–1379, Jul. 2010, doi: 10.1016/j.renene.2009.11.012.
[88] Dipasquale Chiara, R. Fedrizzi, A. Bellini, and M. D’Antoni, “D2.1c Simulation Results of Reference Buildings. Development of Systemic Packages for Deep Energy Renovation of Residential and Tertiary Buildings including Envelope and Systems.” iNSPiRe project, 2014.
[89] G. Borghi, “Analysis of the Urban Heat Island effect in Ospitaletto and of the mitigation potential provided by waste heat recovery measures,” Trento University, Italy, 2020.
[90] M. Nichat, “Landmark based shortest path detection by using Dijkestra Algorithm and Haversine Formula,” *Int. J. Eng. Res. Appl. ISSN 2248-9622 Vol 3 Issue 3 May-Jun 2013 Pp162*, May 2013.
[91] H. Li and S. Svendsen, “District Heating Network Design and Configuration Optimization with Genetic Algorithm,” *J. Sustain. Dev. Energy Water Environ. Syst.*, vol. [1], no. [4], p. [291]-[303], Dec. 2013.
[92] M. Vesterlund, A. Toffolo, and J. Dahl, “Simulation and analysis of a meshed district heating network,” *Energy Convers. Manag.*, vol. 122, pp. 63–73, Aug. 2016, doi: 10.1016/j.enconman.2016.05.060.
[93] A. Dénarié, S. Macchi, F. Fattori, G. Spirito, M. Motta, and U. Persson, “A validated method to assess the network length and the heat distribution costs of potential district heating systems in Italy,” *Int. J. Sustain. Energy Plan. Manag.*, vol. 31, pp. 59–78, May 2021, doi: 10.5278/ijsepm.6322.
[94] F. Bava, “FLEXYNETS D6.11, Pre-design support tool.”
[95] L. Sánchez-García, H. Averfalk, and U. Persson, “Further investigations on the Effective Width for district heating systems,” *Energy Rep.*, vol. 7, pp. 351–358, Oct. 2021, doi: 10.1016/j.egyr.2021.08.096.
[96] F. M. White, *Fluid Mechanics*. McGraw-Hill Series in Mechanical Engineering.
[97] E. Eckert and R. M. Drake, “Heat and mass transfer, 1959,” *McGraw-Hill*, vol. 2, pp. 2–1.
[98] W. Grassi, *Heat pumps: fundamentals and applications*. Springer, 2017.
[99] M. Cozzini and F. Bava, “D3.2 Integration of substations into DHC networks.” FLEXYNETS project, 2018.
[100] B. Welsch, L. Göllner-Völker, D. O. Schulte, K. Bär, I. Sass, and L. Schebek, “Environmental and economic assessment of borehole thermal energy storage in district heating systems,” *Appl. Energy*, vol. 216, pp. 73–90, Apr. 2018, doi: 10.1016/j.apenergy.2018.02.011.
[101] R. Geyer, J. Krail, B. Leitner, R.-R. Schmidt, and P. Leoni, “Energy-economic assessment of reduced district heating system temperatures,” *Smart Energy*, vol. 2, p. 100011, May 2021, doi: 10.1016/j.segy.2021.100011.
[102] P. Yu, D. Dempsey, and R. Archer, “Techno-Economic feasibility of enhanced geothermal systems (EGS) with partially bridging Multi-Stage fractures for district heating applications,” *Energy Convers. Manag.*, vol. 257, p. 115405, Apr. 2022, doi: 10.1016/j.enconman.2022.115405.
[103] Euroheat, “TEMPO Project - Crowdfunding As A Novel Financial Tool For District Heating Projects.” https://www.euroheat.org/resource/tempo-project-crowdfunding-as-a-novel-financial-tool-for-district-heating-projects.html (accessed Apr. 11, 2022).
[104] “Technology Data for Individual Heating Plants,” *Energistyrelsen*. https://ens.dk/en/our-services/projections-and-models/technology-data/technology-data-individual-heating-plants
[105] G. B. Mathews, “On the Partition of Numbers,” *Proc. Lond. Math. Soc.*, vol. s1-28, no. 1, pp. 486–490, Nov. 1896, doi: 10.1112/plms/s1-28.1.486.
[106] M. Assi and R. A. Haraty, “A Survey of the Knapsack Problem,” in *2018 International Arab Conference on Information Technology (ACIT)*, Nov. 2018, pp. 1–6.
[107] R. Bellman, “On the Theory of Dynamic Programming,” *Proc. Natl. Acad. Sci. U. S. A.*, vol. 38, no. 8, pp. 716–719, Aug. 1952.
[108] H. Maya and S. Dipti, “Different approaches to solve the 0/1 knapsack problem.,” presented at the The Midwest Instruction and Computing Symposium, 2005.
[109] G. Steve, “Data Stuctures and Algorithms. Lecture 8: Dynamic Programming,” Fall 2004.

https://cse.unl.edu/~goddard/Courses/CSCE310J/Lectures.html
[110] F. B. P. Maurera, “The Algorithms - Python.” [Online]. Available: https://github.com/fernandobperezm/Python/blob/2ec3750885b71a84969252ad978f046632bbeadf/dynamic_programming/knapsack.py
[111] S. Velut and H. Tummescheit, “Implementation of a transmission line model for fast simulation of fluid flow dynamics,” in *Proceedings of the 8th International Modelica Conference; March 20th-22nd; Technical Univeristy; Dresden; Germany*, 2011, no. 063, pp. 446–453.
[112] B. van der Heijde *et al.*, “Dynamic equation-based thermo-hydraulic pipe model for district heating and cooling systems,” *Energy Convers. Manag.*, vol. 151, pp. 158–169, Nov. 2017, doi: 10.1016/j.enconman.2017.08.072.
[113] “European Residual Mix | AIB.” https://www.aib-net.org/facts/european-residual-mix (accessed Nov. 06, 2020).
[114] “Database - Eurostat.” https://ec.europa.eu/eurostat/web/main/data/database
[115] ISPRA, “Fattori di emissione atmosferica di gas a effetto serra nel settore elettrico nazionale e nei principali Paesi Europei,” 2019. https://www.isprambiente.gov.it/it/pubblicazioni/rapporti/fattori-di-emissione-atmosferica-di-gas-a-effetto-serra-nel-settore-elettrico-nazionale-e-nei-principali-paesi-europei

Appendix

A.1 Spectral Clustering algorithm application to the Aalborg University case.

N=2

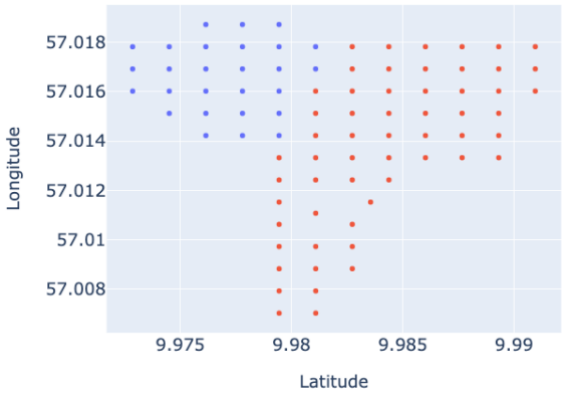

N=4

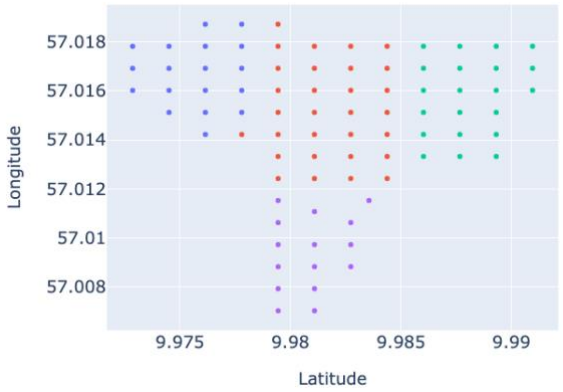

N=6

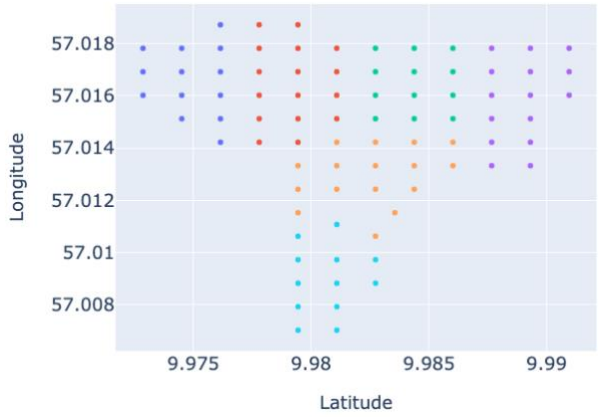

N=8

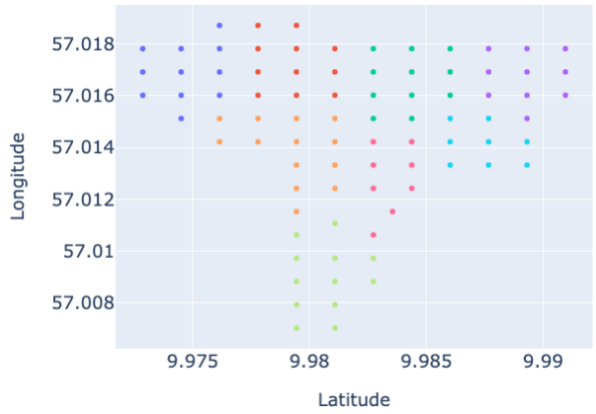

N=10

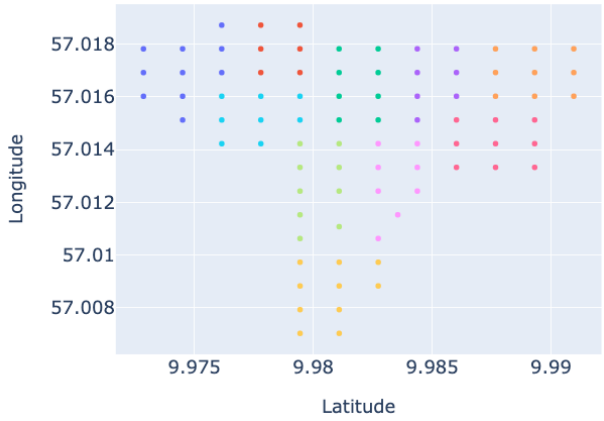

N=12

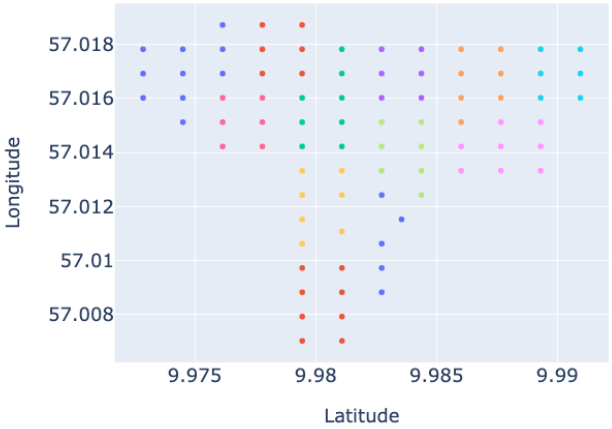

A.2 Network costs

Table 19. Network composition and scaling factors

Pipe category	Length [%]	Scaling factor
Cat.1	43%	0,025
Cat.2	24%	0,043
Cat.3	18%	0,109
Cat.4	8%	0,244
Cat.5	4%	0,665
Cat.6	3%	1,0

Table 20. Piping costs data from different diameters and insulation classes (FLEXYNETS tool).

Pipe [mm] Di	diameter DN	Max speed [m/s]	Piping costs [€/m]			Installation costs [€/m]	
			SERIES 1	SERIES 2	SERIES 3	Existing district	New district
26,90	20	1,00	19,45	24,03	28,60	44,84	24,08
33,70	25	1,00	24,82	30,23	35,65	57,62	32,45
42,40	32	1,00	31,68	38,17	44,67	87,50	49,10
48,30	40	1,00	38,53	44,73	50,93	98,20	55,05
60,30	50	1,50	46,67	54,14	61,60	137,18	76,80
76,10	65	1,50	53,07	68,12	83,16	181,15	101,36
88,90	80	1,50	68,53	79,60	90,67	218,48	122,25
114,30	100	1,50	90,27	104,84	119,40	297,27	167,16
129,16	125	1,50	105,87	121,60	137,33	355,30	199,89
144,40	150	1,50	147,27	171,04	194,80	416,82	235,39
204,21	200	2,00	273,00	317,04	361,07	526,58	299,11
223,70	250	2,00	358,07	411,17	464,27	628,34	359,75
270,92	300	2,50	451,80	501,97	552,13	694,59	400,96
281,49	350	2,75	498,07	567,03	636,00	742,27	431,42
406,40	400	3,00	544,33	632,10	719,87	787,23	462,14
457,00	450,00	3,00	617,43	716,98	816,54	826,94	490,32
508,00	500,00	3,00	690,53	801,87	913,20	874,81	526,98
609,60	600,00	3,00	904,59	1068,71	1232,82	966,45	607,57
711,20	700,00	3,00	1185,01	1424,66	1664,31	1038,51	677,86
812,80	800,00	3,00	1552,36	1899,59	2246,82	1125,65	763,15

A.3 Individual solutions cost data

Table 21. Factors used to estimate investment and O&M costs of each individual technology. Gas boiler cost data, apartment reference building, year 2020.

Country	lifetime	η_{tech}	$k1_{inv}$	$k2_{inv}$	$k1_{fixed_{OM}}$	$k2_{fixed_{OM}}$
Austria	25	1.02	718	-0.428	76	-0.64
Belgium	25	1.02	801	-0.428	75	-0.64
Bulgaria	25	1.02	550	-0.428	44	-0.64
Croatia	25	1.02	644	-0.428	56	-0.64
Cyprus	25	1.02	802	-0.428	62	-0.64
Czech Republic	25	1.02	623	-0.428	53	-0.64
Denmark	25	1.02	877	-0.428	85	-0.64
Estonia	25	1.02	646	-0.428	61	-0.64
Finland	25	1.02	815	-0.428	78	-0.64
France	25	1.02	797	-0.428	71	-0.64
Germany	25	1.02	753	-0.428	69	-0.64
Greece	25	1.02	637	-0.428	63	-0.64
Hungary	25	1.02	581	-0.428	48	-0.64
Ireland	25	1.02	738	-0.428	70	-0.64
Italy	25	1.02	777	-0.428	74	-0.64
Latvia	25	1.02	587	-0.428	58	-0.64
Lithuania	25	1.02	622	-0.428	56	-0.64
Luxembourg	25	1.02	812	-0.428	78	-0.64
Malta	25	1.02	888	-0.428	72	-0.64
Netherlands	25	1.02	762	-0.428	75	-0.64
Poland	25	1.02	513	-0.428	44	-0.64
Portugal	25	1.02	779	-0.428	65	-0.64
Romania	25	1.02	605	-0.428	48	-0.64
Slovakia	25	1.02	630	-0.428	56	-0.64
Slovenia	25	1.02	690	-0.428	62	-0.64
Spain	25	1.02	727	-0.428	69	-0.64
Sweden	25	1.02	887	-0.428	83	-0.64
United Kingdom	25	1.02	741	-0.428	72	-0.64

A.4 Knapsack problem/dynamic programming/Python script [110]

```
"""
    Given weights and values of n items, put these items in a knapsack of
     capacity W to get the maximum total value in the knapsack.
    Note that only the integer weights 0-1 knapsack problem is solvable
     using dynamic programming.
    """


    def MF_knapsack(i, wt, val, j):
        """
        This code involves the concept of memory functions. Here we solve the subproblems
        which are needed unlike the below example
        F is a 2D array with -1s filled up
        """
        global F  # a global dp table for knapsack
        if F[i][j] < 0:
            if j < wt[i - 1]:
                val = MF_knapsack(i - 1, wt, val, j)
            else:
                val = max(
                    MF_knapsack(i - 1, wt, val, j),
                    MF_knapsack(i - 1, wt, val, j - wt[i - 1]) + val[i - 1],
                )
            F[i][j] = val
        return F[i][j]


    def knapsack(W, wt, val, n):
        dp = [[0 for i in range(W + 1)] for j in range(n + 1)]

        for i in range(1, n + 1):
            for w in range(1, W + 1):
                if wt[i - 1] <= w:
                    dp[i][w] = max(val[i - 1] + dp[i - 1][w - wt[i - 1]], dp[i - 1][w])
                else:
                    dp[i][w] = dp[i - 1][w]
```

```
    return dp[n][W], dp


def knapsack_with_example_solution(W: int, wt: list, val: list):
    """
    Solves the integer weights knapsack problem returns one of
    the several possible optimal subsets.
    Parameters
    ---------
    W: int, the total maximum weight for the given knapsack problem.
    wt: list, the vector of weights for all items where wt[i] is the weight
    of the i-th item.
    val: list, the vector of values for all items where val[i] is the value
    of the i-th item
    Returns
    -------
    optimal_val: float, the optimal value for the given knapsack problem
    example_optional_set: set, the indices of one of the optimal subsets
    which gave rise to the optimal value.
    Examples
    -------
    >>> knapsack_with_example_solution(10, [1, 3, 5, 2], [10, 20, 100, 22])
    (142, {2, 3, 4})
    >>> knapsack_with_example_solution(6, [4, 3, 2, 3], [3, 2, 4, 4])
    (8, {3, 4})
    >>> knapsack_with_example_solution(6, [4, 3, 2, 3], [3, 2, 4])
    Traceback (most recent call last):
        ...
    ValueError: The number of weights must be the same as the number of values.
    But got 4 weights and 3 values
    """
    if not (isinstance(wt, (list, tuple)) and isinstance(val, (list, tuple))):
        raise ValueError(
            "Both the weights and values vectors must be either lists or tuples"
        )

    num_items = len(wt)
    if num_items != len(val):
        raise ValueError(
            "The number of weights must be the "
```

```
            "same as the number of values.\nBut "
            f"got {num_items} weights and {len(val)} values"
        )
    for i in range(num_items):
        if not isinstance(wt[i], int):
            raise TypeError(
                "All weights must be integers but "
                f"got weight of type {type(wt[i])} at index {i}"
            )

    optimal_val, dp_table = knapsack(W, wt, val, num_items)
    example_optional_set = set()
    _construct_solution(dp_table, wt, num_items, W, example_optional_set)

    return optimal_val, example_optional_set


def _construct_solution(dp: list, wt: list, i: int, j: int, optimal_set: set):
    """
    Recursively reconstructs one of the optimal subsets given
    a filled DP table and the vector of weights
    Parameters
    ---------
    dp: list of list, the table of a solved integer weight dynamic programming problem
    wt: list or tuple, the vector of weights of the items
    i: int, the index of the  item under consideration
    j: int, the current possible maximum weight
    optimal_set: set, the optimal subset so far. This gets modified by the function.
    Returns
    -------
    None
    """
    # for the current item i at a maximum weight j to be part of an optimal subset,
    # the optimal value at (i, j) must be greater than the optimal value at (i-1, j).
    # where i - 1 means considering only the previous items at the given maximum weight
    if i > 0 and j > 0:
        if dp[i - 1][j] == dp[i][j]:
            _construct_solution(dp, wt, i - 1, j, optimal_set)
        else:
            optimal_set.add(i)
```

```
            _construct_solution(dp, wt, i - 1, j - wt[i - 1], optimal_set)


if __name__ == "__main__":
    """
    Adding test case for knapsack
    """
    val = [3, 2, 4, 4]
    wt = [4, 3, 2, 3]
    n = 4
    w = 6
    F = [[0] * (w + 1)] + [[0] + [-1 for i in range(w + 1)] for j in range(n + 1)]
    optimal_solution, _ = knapsack(w, wt, val, n)
    print(optimal_solution)
    print(MF_knapsack(n, wt, val, w))  # switched the n and w

    # testing the dynamic programming problem with example
    # the optimal subset for the above example are items 3 and 4
    optimal_solution, optimal_subset = knapsack_with_example_solution(w, wt, val)
    assert optimal_solution == 8
    assert optimal_subset == {3, 4}
    print("optimal_value = ", optimal_solution)
    print("An optimal subset corresponding to the optimal value", optimal_subset)
```